3-2021

The Effect of Amino Acids and Molar Peroxide Ratio on the Oxidation of 2,4 Dinitroanisole in an Ultraviolet Light Emitting Diode/H_2O_2 Advanced Oxidation Process

Jeffry P. Hart

THE EFFECT OF AMINO ACIDS AND MOLAR PEROXIDE RATIO ON THE OXIDATION OF 2,4 DINITROANISOLE IN AN ULTRAVIOLET LIGHT EMITTING DIODE/H2O2 ADVANCED OXIDATION PROCESS

THESIS

Jeffry P. Hart, Major, USMC

AFIT-ENV-MS-21-M-232

DEPARTMENT OF THE AIR FORCE
AIR UNIVERSITY

AIR FORCE INSTITUTE OF TECHNOLOGY

Wright-Patterson Air Force Base, Ohio

AFIT-ENV-MS-21-M-232

THE EFFECT OF AMINO ACIDS AND MOLAR PEROXIDE RATIO ON THE OXIDATION OF 2,4 DINITROANISOLE IN AN ULTRAVIOLET LIGHT EMITTING DIODE/H_2O_2 ADVANCED OXIDATION PROCESS

THESIS

Presented to the Faculty

Department of Systems Engineering & Management

Graduate School of Engineering and Management

Air Force Institute of Technology

Air University

Air Education and Training Command

In Partial Fulfillment of the Requirements for the

Degree of Master of Science

Jeffry P. Hart, BS

Major, USMC

March 2021

AFIT-ENV-MS-21-M-232

THE EFFECT OF AMINO ACIDS AND MOLAR PEROXIDE RATIO ON THE OXIDATION OF 2,4 DINITROANISOLE IN AN ULTRAVIOLET LIGHT EMITTING DIODE/H2O2 ADVANCED OXIDATION PROCESS

Jeffry P. Hart, BS

Major, USMC

Committee Membership:

Dr. W. F. Harper, PhD
Chair

LtCol. J. E. Stubbs
Member

Dr. A. C. Burdsall, PhD
Member

Abstract

2,4 Dinitroanisole (DNAN) is an organic insensitive munition that is a likely candidate to replace trinitrotoluene (TNT) for a variety of purposes. The manufacturing and use of DNAN poses several environmental hazards that may cause human and environmental health problems. Safe and efficient treatment of wastewater and drinking water is required for water for military and civilian operations. Advanced Oxidation Processes (AOPs) are a promising method that have the potential to reduce a variety of persistent chemicals, however, the performance of these systems may be degraded by co-contaminants in the influent. In this contribution, DNAN, with casamino acids as a co-contaminant, was oxidized with Ultraviolet (UV) Light Emitting Diodes (LEDs) with hydrogen peroxide (H_2O_2) in an AOP in a laboratory.

The UV/H_2O_2 AOP was capable of degrading DNAN with casamino acids present, from a relative concentration (C/C_0) of 1.0 – 0.63 over a molar peroxide ratio (H_2O_2:DNAN) range of 50:1 to 1000:1. An increase in the degradation rate of DNAN was observed with increased concentrations of H_2O_2. The pseudo first order rate constant for DNAN removal was typically greatest at 250:1 and 500:1. The presence of casamino acids had minimal effects on the effectiveness of the AOP, possibly due to light screening.

Potential byproducts were identified using mass spectrometry chromatograms and Nitrobenzene +CN is a potential byproduct of DNAN degradation.

Acknowledgments

I would like to express my sincere appreciation to my thesis advisor, Dr. Willie Harper Jr., for his guidance and support throughout the course of this thesis effort. I would also like to thank Dr. Daniel Felker and Dr. Adam Burdsall for their guidance and wisdom in navigating the complexities of this work inside the laboratory. Finally, I would like to thank my wife and children for their unwavering support throughout this endeavor.

Jeffry P. Hart

Table of Contents

Page

List of Figures

Page

List of Tables

Page

List of Equations

Page

THE EFFECT OF AMINO ACIDS AND MOLAR PEROXIDE RATIO ON THE OXIDATION OF 2,4 DINITROANISOLE IN AN ULTRAVIOLET LIGHT EMITTING DIODE/H_2O_2 ADVANCED OXIDATION PROCESS

I. Introduction

1.1 Chapter Overview

This chapter identifies the problem, background, and investigative questions for using an UV LED AOP in a water treatment process. Additionally, it includes a brief discussion of the methodology for the experiments. Finally, this section defines the assumptions and limitations of this study.

1.2 General Issue

The purpose of this thesis is to increase understanding for using UV LEDs in a water treatment system utilizing an AOP. This research attempts to optimize the molar peroxide ratio for the AOP of DNAN with casamino acid as a co-contaminant in an UV LED reactor as well as suggest possible byproduct structures.

Treating water has long been a task the military has undertaken to ensure clean and safe water is available for use (Mitchell & Ensley, 2019). The military needs water treatment capabilities that can operate in austere environments and that are capable of removing traditional pollutants, as well as pollutants found on a battlefield such as munitions constituents and chemical weapon byproducts (Duckworth et al., 2015). The Department of Defense (DoD) has a responsibility to meet National Pollutant Discharge Elimination System (NPDES) permit requirements at its wastewater treatment plants (US EPA, 2010). Wastewater treatment standards may become more stringent over time. As

such, munitions constituents and other chemicals in wastewater may require advanced treatment methods in order to ensure effluents are safe for discharge.

This research used use a UV LED/H_2O_2 based AOP. There are several scholarly works using UV LED AOPs, however, the overall research conducted is still limited and warrants further investigation (Duckworth et al., 2015; Scott et al., 2017; Stubbs, 2017). Additionally, there is little research that targets the effects of co-contaminants, such as casamino acids, in the treatment process. Specifically, research has shown that background chemicals such as nitrates and carbonates may interfere with the destruction of the target contaminant (Stocking, Rodriguez, & Browne, 2000). These background chemicals and other co-contaminants that are not the primary target of AOPs have the potential to create regulated byproducts that may be as toxic or more toxic than those present before treatment started (Munter, 2001; Stocking et al., 2000). Thus, it is important to understand and predict byproducts created by the AOP.

UV/H_2O_2-based AOPs expose H_2O_2 to UV LED light inside a reactor which transforms into hydroxyl radicals that can quickly and non-selectively react with any organic pollutants and their byproducts (Crittenden, Trussell, Hand, Howe, & Tchobanoglous, 2014; Scott et al., 2017). These hydroxyl radicals can attack organic pollutants by: (1) hydrogen abstraction (i.e. removal of a hydrogen atom from a saturated hydrocarbon), (2) hydroxylation (i.e. adding the hydroxyl group to an unsaturated hydrocarbon), or (3) oxidation without transfer of atoms (Buxton, Greenstock, Helman, W, & Ross, 1988; Scott et al., 2017; Stubbs, 2017).

1.3 Problem Statement

The Air Force Institute of Technology (AFIT), in collaboration with the Environmental Protection Agency (EPA), is studying the use of UV LEDs for improving water treatment procedures. UV LED AOPs are relatively new, however, they provide many benefits over traditional mercury lamp-based AOPs and have demonstrated efficient and reliable operation in several experiments (Duckworth et al., 2015; Scott et al., 2017; Stewart, 2016; Stubbs, 2017). While promising, further study and analysis is warranted to fully understand the operational limits and conditions required for properly treating water.

1.4 Research Objectives/Questions

This research has two main questions: 1.) What molar peroxide ratios best effect the degradation of DNAN in a UV LED/H_2O_2 AOP? 2.) What effect do casamino acids have on the degradation of DNAN in a UV LED/H_2O_2 AOP?

- Determine the effect of amino acids and molar peroxide ratios on the oxidation of DNAN in an UV LED/H_2O_2 AOP.
- Propose associated byproducts from oxidation of DNAN in an UV LED/H_2O_2 AOP.

1.5 Investigative Questions

How do molar peroxide ratios affect the reaction? Several studies have shown there is a relationship between molar stoichiometry and associated degradation of contaminants (Scott et al., 2017; Stewart, Miller, Kempisty, Stubbs, & Harper, 2018; Stubbs, 2017; Su et al., 2019). Literature suggests increasing H_2O_2 may improve

degradation rates, however, too much H_2O_2 can reduce degradation rates because it will act as a scavenger for OH· (Su et al., 2019; Yang et al., 2018). Additionally, the hypothesis for this research question is that molar peroxide ratio has a has a significant effect on the degradation of DNAN.

How does the presence of casamino acids effect the degradation of DNAN? Previous research by Hoigne (1998) demonstrated that nearly all dissolved organic compounds in water create a detrimental effect on the degradation of target compounds by removing •OH. Thus, it is prudent to suggest that casamino acids will impact the degradation process. The hypothesis for this research question is that casamino acids have a detrimental effect on the degradation of DNAN in an UV LED/H_2O_2 AOP.

1.6 Methodology

To answer the investigative questions, a series of AOP experiments were conducted at AFIT. The AOP experiment consisted of five different molar ratios of DNAN and H_2O_2 while the duty cycle (DC) remained constant at 100% and powered by 12.50v and 0.10 amperes. Casamino acid was added as a co-contaminant to determine what effect, if any, it had on DNAN removal. For each experiment, a solution of DNAN casamino acid, and H_2O_2 flowed from the source flask, through biocompatible tubing, through a reactor where it was exposed to UV LEDs, and then flowed out of the reactor where samples were collected. Effluent that was not collected for sampling flowed into a waste beaker for disposal.

Reactor effluent samples were collected, filtered, well mixed, and processed in a High-Performance Liquid Chromatography (HPLC) to produce chromatograms.

Chromatograms were used to analyze the effect of H_2O_2:DNAN molar peroxide ratios on DNAN degradation. Mass spectrophotometry (MS) was also conducted and used for proposing potential effluent byproduct structures.

Two control experiments were conducted for this research. The first control was conducted without H_2O_2, which prevented a complete AOP from occurring and resulted in negligible DNAN degradation. A second control was conducted, also without H_2O_2 but with casamino acids well mixed into the solution to determine if the casamino acids and DNAN interact.

Results were statistically analyzed with Anaconda ® and JMP ® software to conduct a one-way Analysis of Variance (ANOVA) and *t*-Test. MathWorks ® MATLAB 2020 software was used for curve fitting of the data.

1.7 Assumptions/Limitations

The limitations of this research are:

1. The dual LED method and low flow rates used in this experiment is not likely to be replicated on a full-sized water treatment system due to scaling issues. While appropriate at the experimental level, methods will likely need to be up-scaled and modified in order to replicate effects on a high-volume system.

2. Casamino acid levels in the laboratory setting are assumed to remain consistent because it was well mixed in the solution beaker. If future water treatment system tests are to occur at a larger scale it is important to understand the effects and likely concentrations of co-contaminants and understand that they may change throughout the treatment process, potentially altering degradation efficiency.

II. Literature Review

2.1 Chapter Overview

This chapter reviews relevant literature and its application to the AOP process. Specifically, the literature is used to analyze operating parameters in a UV LED H_20_2 AOP. Relevant areas of research include UV light, AOPs, and previous work with DNAN and co-contaminants.

2.2 Background

The DoD has a non-negotiable requirement for access to clean and safe water for all its operations (Mitchell & Ensley, 2019). The DoD is responsible for the manufacturing and use of insensitive munitions which have the potential to cause contamination to wastewater and drinking water systems. As such, the DoD and civilian systems must be prepared to protect against and treat a variety of contaminants that may enter wastewater and drinking water systems.

2.3 Advanced Oxidation Processes

AOPs were first proposed in the 1980s and use strong hydroxyl (OH·) or sulfate radicals ($SO_4\cdot^-$) as major oxidizers to treat wastewater (Deng & Zhao, 2015). AOPs form strong oxidants and these react with organic contaminants in water (Stocking et al., 2000). These methods were further used to treat several types of wastewaters because the strong oxidants were capable of removing recalcitrant organic pollutants as well as certain inorganic pollutants, or to increase the biodegradability of wastewater as a pretreatment prior to being subject to a follow-on biological treatment (Deng & Zhao, 2015). AOPs are not commonly employed for inactivation of pathogens because the

radical half-life is too short and the detention times are prohibitive (Deng & Zhao, 2015). OH· is non-selective and will rapidly react with numerous species at rate constants of $10^8 – 10^{10}$ M^{-1} s^{-1} (Deng & Zhao, 2015). Since the OH· has such a short lifetime, they are produced *in situ* through different methods, including irradiation with an UV light (Deng & Zhao, 2015; Huang, Dong, & Tang, 1993).

Scott et al. (2017) researched the effect of UV LEDs and H_2O_2 in an AOP to degrade Brilliant Blue dye and tartrazine. Their research demonstrated the potential of using UV LED AOP treatment methods for contaminated water and identified several factors that may influence their performance, including mixing, DC, and operating time (Scott et al., 2017). Their research highlights the need for further understanding AOPs because they are effective at destroying toxic pollutants in water. Specifically, their study chose UV light for the AOP process in place of the larger mercury-based fluorescent lamps. While mercury-based fluorescent lamps were the leading source of UV light for water treatment, they are large, fragile, and potentially hazardous due to high voltage and mercury contained in the system (Scott et al., 2017). UV LEDs offer many benefits over conventional mercury lamps because of their small size, durability, and lack of hazardous materials (Scott et al., 2017). Scott et al. (2017) notes, however, that UV LEDs have yet to prove themselves as a full replacement for conventional mercury lamps and require further testing and evaluation. Additionally, Scott et al. (2017) also researched the effect of DC, which periodically pulsed the UV LED, in order to determine optimum conditions for reducing brilliant blue dye and tartrazine. A flow through reactor with 250 nm LEDs was utilized, with a peak output at 247 nm because peroxide absorbs light energy well within this range (Beers & Sizer, 1951; Scott et al., 2017). DCs of 5, 10, 20, 30 and 100%

were used and those with higher DCs, particularly those at 100%, yielded higher reduction of brilliant blue, whereas lower DCs, removed only very small amounts of the brilliant blue (Scott et al., 2017). Tartrazine removal was conducted using similar DCs of 5, 10, 20, 30, 50, 70, and 100%. Conversely, tartrazine was only reduced by 17% at 100% DC for over 300 minutes, 13% at 70% DC, and continually decreased with lower DC (Scott et al., 2017). Tartrazine and brilliant blue experiments were conducted in duplicate, and showed that brilliant blue is more receptive to UV AOP than tartrazine (Scott et al., 2017).

During this study the data points for degradation of tartrazine and brilliant blue oscillated above and below the R^2 value best fit lines (Scott et al., 2017). These oscillations can be attributed to non-ideal mixing conditions, multiple flow paths within a reactor, as well as variations in the radiation intensity (Scott et al., 2017; Wols, Hofman, Uijttewaal, Rietveld, & van Dijk, 2010). If the continuously stirred tank reactor (CSTR) conditions are not ideal, each particle may receive greatly different UV doses, and lead to instability in the effluent concentration (Scott et al., 2017). Tartrazine experiments were repeated while mechanically stirring the UV LED reactor which showed an 8% improvement in TAR removal at 300 minutes and 100% DC. The methods researched by Scott et al. (2017) are of importance to future AOP processes, particularly the effect of DC and mixing within the reactor.

Scott et al. (2017) also observed the effect of staining and found it had a minimal impact because tartrazine and brilliant blue are anionic dyes and were not expected to adsorb to the negatively charged quartz LED lenses. These results differed from Duckworth et al. (2015), who used methylene blue in their study and observed LED

power degradation due to staining (Scott et al., 2017). Interestingly, Scott et al. (2017) observed steadily declining normalized apparent first-order rate constants and attributed this behavior to heat buildup in the LEDs which led to their degradation. This can be attributed to both the heat during the "on" condition as well as cycling the LED on and off (Scott et al., 2017). DC was positively correlated with first-order rate constants for tartrazine and brilliant blue, but was negatively correlated with the normalized first-order rate constants k_s/DC which demonstrates pollutant removal was more efficient at lower DCs (Scott et al., 2017). Scott et al. (2017) demonstrated the potential to treat contaminated water with UV LEDs and highlight the need for more research of mixing DC, operating time, as well as understanding the impacts of staining and chemical structure of contaminants on the AOP.

Duckworth et al. (2015) used an UV LED H_2O_2 AOP to degrade methylene blue. Radical production is hypothesized to be proportional to optical power of the LEDs, regardless of pulse rate (Duckworth et al., 2015). McDonald et al. (2000), however, offer that optical power may not be proportional to the inactivation of organisms in the presence of an oxidizing agent. In the experiment conducted by Duckworth et al. (2015), they investigated the rate of radical production from hydrogen peroxide, as indicated by the degradation of methylene blue, as a function of DC with pulsed UV LEDs. The UV LED AOP used a flow through electro-polished 316 L stainless steel reactor with 240 nm LEDs was used in which 5 mM hydrogen peroxide and 0.01 mM methylene blue were exposed to UV light, permitting the creation of hydroxyl radicals to destroy target contaminants (Duckworth et al., 2015). Experiments were conducted using various DCs and their results showed first-order degradation kinetics for methylene blue at all DCs

(Duckworth et al., 2015). Interestingly, the adjusted first-order degradation rate constant for methylene blue was significantly higher for the 5 and 10% DCs (Duckworth et al., 2015). Duckworth et al. (2015) state this increased degradation could be because the short UV pulses more effectively produce hydroxyl radicals, however, they could also be caused by peroxide limitations or scavenging of hydroxyl radicals by MB byproducts. Hydroxyl radical production may also not be accurately measured if the hydroxyl radicals are scavenged by the methylene blue byproducts (Duckworth et al., 2015). Additionally, LED surfaces were fouled during the experiment by methylene blue adsorption which complicated the data analysis process (Duckworth et al., 2015). The adsorption of chemicals onto LED surfaces must be dealt with in large scale applications, as it creates the likelihood of decreased degradation that may require additional chemicals or increased exposure time within a reactor, both of which will cause delays and may increase costs associated with water treatment.

Stewart et al. (2018) researched the effects of UV LEDs in a H_2O_2 AOP reactor to reduce tartrazine under different pH and DC conditions. The objective of their work was to determine what effect pH and DC had on the oxidation of tartrazine in a UV/H_2O_2-based AOP. Alternative water treatment methods such as AOPs have the potential to remove harmful contaminants from water because AOPs use radicals to rapidly and non-selectively oxidize several electron-rich organic pollutants (Crittenden et al., 2014; Scott et al., 2017). Stewart et al. (2018) also used pulsing UV LEDs to extend the life of the UV LED, and found that DC was positively correlated with oxidation efficiency and pH was negatively correlated with oxidation efficiency and was typically greatest at pH 6.

Stewart et al. (2018) expanded upon previous research of Scott (2017), and sought to identify byproducts associated with UV LED AOPs. After processed through the AOP, byproducts in the effluent were analyzed using High Performance Liquid Chromatography Mass Spectrometry (HPLC-MS) (Stewart et al., 2018). Additionally, first order rate constants were determined from the non-steady state solution for the effluent tartrazine concentration (Stewart et al., 2018). Each experiment was conducted with approximately 25 mM H_2O_2 and .05 mM tartrazine processed in a stainless steel cylindrical reactor with seven 245 nm LEDs in the end plate of the reactor (Stewart et al., 2018). The UV LED DC was controlled via computer at rates of 5, 10, 20, 30, 50, 70, and 100% (Stewart et al., 2018). The LEDs made physical contact with the solution in the reactor and the tartrazine and H_2O_2 solution was pumped through the reactor at approximately 0.7 mL per minute (Stewart et al., 2018). Improving on the method of Scott et al. (2017), Stewart (2018) mechanically mixed the solution within the reactor with a magnetic stir bar. For pH 6 and 7, tartrazine degradation increased as DC increased from 0 to 100% (Stewart et al., 2018). There was a notable exception at pH 7, where the 50% DC narrowly exceeded the degradation of the 70% DC (Stewart et al., 2018). Lower levels of tartrazine degradation occurred for pH of 8 and 9, and both exhibited their highest relative degradation levels at the 50% DC instead of the 100% DC (Stewart et al., 2018). Interestingly, while increasing pH negatively impacted tartrazine oxidation, the computational data showed that tartrazine reactivity did not increase with pH (Stewart et al., 2018). This may be attributed to hydroxyl radicals being scavenged by bicarbonate ions (Buxton et al., 1988; Stewart et al., 2018).

Additionally, Stewart et al. (2018) found that while the relative contribution of DC to tartrazine degradation was 57%, and pH was 19%, the interaction of DC and pH resulted in a 24% contribution to degradation. Stewart et al. (2018) found that it was difficult to degrade tartrazine in a UV/H_2O_2 AOP, and assert this is due to the strong absorbance of tartrazine in the UV spectrum, resulting in nondestructive radiative transfer and fluorescence which reduces the available UV energy for cleaving the O-O bond and produce hydroxyl radicals. Four byproduct structures were proposed, including two that demonstrate tartrazine rings were cleaved (Stewart et al., 2018). Stewart et al. (2018) suggested future studies use stronger LEDs and focus on improving reactor mechanics including materials (stainless steel vs. Teflon), UV arrangement, and hydraulic residence time distribution.

Tran et al. (2014) used pulsed LEDs in the UV range to inactivate *Bacillus globigii*. This was done using pulsed UV LEDs instead of continuous UV LEDs to reduce the power consumption and increase LED bulb operational life (Tran et al., 2014). LED bulbs are more capable of conducting pulsed operations because they don't require a warm-up time which allows them to be rapidly turned on and off (Tran et al., 2014). While the research conducted was not specific to AOPs, its findings are applicable to future work with AOPs. Specifically, it was found that kinetic profiles for continuous UV LEDs reached 6-log inactivation than pulsed UV LED, however the pulsed required less fluence (Tran et al., 2014). Additionally, pulsed UV LED inactivation rate constants were higher than continuous UV LEDs, indicating that the high energy bursts associated with pulsing UV LEDs were more effective at causing cellular damage (Tran et al., 2014). LED bulb life is increased by pulsing in part because bulbs do not reach critical

temperature thresholds (Lenk & Lenk, 2017; Tran et al., 2014). The disinfection apparatus was mounted atop a shaker table with a n orbital motion of 115-120 rpm (Tran et al., 2014). It is worth considering the results of using a shaker table compared to a CSTR, and how each may be scaled up to meet future water treatment systems. Specifically, Tran et al. (2014) noticed tailing in *Bacillus globigii* spore disinfection over time and partially attributed this to crevices in the test apparatus. This observation should directly translate to UV H_2O_2 AOPs as it also requires influent to be exposed to UV LED and any crevices may cause improper mixing and exposure to UV LEDs. By running UV LEDs in a pulsing configuration, there is potential to increase operational life of the bulbs, thus reducing maintenance or increasing replacement intervals in future water treatment systems.

Stubbs (2017) conducted a study to "evaluate the effect of reaction stoichiometry, molecular structure, and optical output power on the UV LED/H_2O_2 process". His work used a bench-scale UV LED H_2O_2 AOP to degrade 6 dye and 5 achromatic organic compounds (Stubbs, 2017). His research found a linear relationship between input drive current, optical output power, and the apparent first order degradation rate constant (Stubbs, 2017). Additionally, the drive current and degradation exhibited a linear relationship (Stubbs, 2017). He found that the ideal ratio for moles peroxide to moles of a test compound were at or near 500:1 for the majority of the dyes (Stubbs, 2017). Interestingly, erythrosine B exhibited the best results in the 2500:1-3000:1 range and this is most likely attributed to its relatively high molar absorptivity ratio (Stubbs, 2017).

Additionally, Stubbs (2017) highlights further benefits of using UV LEDs in an AOP as compared to traditional mercury lamps. Specifically, while UV LEDs may have

output power in the milliwatt (mW) range, they can be arranged more effectively and be adjusted to output specific wavelengths, whereas the large and more powerful mercury lamps can reach significantly higher outputs in the kilowatt (kW) range (Stubbs, 2017). Furthermore, UV LEDs may have other benefits beyond more flexible arrangements, they offer selective output wavelengths, while low pressure lamps are limited to a single 254 nm wavelength and medium pressure lamps emit between 200 and 320 nm (Stubbs, 2017). The comparison of mercury lamps to LED is important as the reactor must provide adequate exposure to UV light to cleave the O-O bond in the H_2O_2 molecule (Stubbs, 2017). Because the UV LEDs produce significantly less optical output power than their mercury-based equivalent, design of a UV LED AOP reactor needs careful consideration in order to reach the desired energy per unit time of the UV LEDs as well as the solution's residence time in the reactor. Proper mixing and UV fluence are also critical to the effectiveness of hydroxyl radicals as oxidants (Stubbs, 2017; US EPA, 1999). His work also emphasizes the importance of selecting the correct starting molar ratios of H_2O_2 to dyes, as too low a level of H_2O_2 may limit the generation of hydroxyl radicals, whereas too much H_2O_2 appears to scavenge hydroxyl radicals (Muruganandham & Swaminathan, 2004; Oancea & Meltzer, 2014; Sharma, 2015; Stubbs, 2017). Stubbs' (2017) work is applicable to future research as well as water treatment systems. Specifically, his study of the effect of different dyes and achromatic compounds and their degradation in a UV LED AOP emphasize the importance of design and the ability of a large-scale UV LED AOP to reduce a variety of chemicals in a water treatment train.

UV AOPs can leave a variety of byproducts compounds in the effluent after treatment (Stewart et al., 2018). Chang and Young (2000) studied Methyl *tert*-butyl ether

(MTBE) degradation kinetics in UV/H_2O_2 AOP with H_2O_2:MTBE molar ratios of 15:1, 7:1, and 4:1. Over 99.9% of MTBE was removed after 75 minutes at each peroxide (Chang & Young, 2000). Of interest, the AOP process resulted in a *tert*-butyl formate (TBF) byproduct (Chang & Young, 2000). After 1-hour of treatment, there was 35 times as much TBF as the remaining MTBE (Chang & Young, 2000). Chang and Young (2000) suggest that other byproducts, such as formaldehyde or acetone, were likely formed, however they may have gone undetected because they were not purgeable or they were too small or volatile to appear in the analytical results. The resulting byproducts reported by Stewart (2016), Stubbs (2017), and Chang and Young (2000) are important to future water treatment processes, as some byproducts have the potential to be damaging to human health and may require further treatment prior to being safe to enter wastewater effluent.

Terracciano et al. (2018) used a UV/H2O2 AOP to treat water contaminated with the insensitive munition 3-nitro-1,2,4-trizole-5-one (NTO). The reactor was able to successfully remove NTO, sourced either from actual chemical plants or created synthetically, from the water (pH=3.0 ± 0.1) when using a hydrogen peroxide concentration of at least 1500 mg L^{-1} (Terracciano et al., 2018). The organic carbon in the NTO ring was completely converted to inorganic carbon (CO_2) and produced nitrate and ammonium ions as the primary byproducts (Terracciano et al., 2018).

Furthermore, implementing AOPs can be a difficult process, as their mechanisms are not as well understood when compared to air stripping and sorption because of the complex physical and chemical reactions that are occurring in oxidation processes (Stocking et al., 2000). Additionally, because their effectiveness is mainly determined by

the quality of the contaminated water, they may not be practical or affordable in many cases (Stocking et al., 2000). Because oxidation processes react non-selectively and are prone to interference, they may result in increased costs due to extra chemicals or power required to properly degrade target contaminants. Background chemicals that are not the primary target of AOPs can result in other regulated by-products that essentially cause water to become worse off than when treatment started (Stocking et al., 2000). Other background chemicals such as nitrates and carbonates may interfere with the destruction of the target contaminant (Stocking et al., 2000). Thus, it is important for future research and water treatment applications to ensure that not only is the AOP process understood for the target pollutant, but to know how a variety of other co-contaminants and background chemicals will impact the process.

2.4 2,4-dinitroanisole

Nitroaromatic compounds are associated with industrial chemical processes, including explosives production (Li, Shea, & Comfort, 1998). Production of TNT and dinitrotoluene (DNT) may produce over 30 nitroaromatic compounds (Levsen, Preiss, & Berger-Preiss, 1995; Li et al., 1998). Li et al. (1998) found that more than 95% of TNT in aqueous extracts of contaminated soil was mineralized when exposed to UV/Fenton oxidation. Furthermore, Li et al. (1998) highlight that AOPs using highly reactive intermediates, such as hydroxyl radicals, have shown promising results for remediating wastewater contaminated with aromatic compounds (Ho, 1986; Li, Comfort, & Shea, 1997). Because TNT and DNAN are both nitroaromatic compounds and share similar

chemical structures, AOPs with hydroxyl radicals are a promising source for their chemical remediation in wastewater

DNAN is a potential replacement for TNT. DNAN is less sensitive to inadvertent detonation than TNT, has an increased detonation temperature, yet still provides similar desirable properties to TNT which makes for an easier manufacturing process (Hawari et al., 2015; Platten III, 2011). While DNAN has been manufactured since at least the 1950s, it has not been widely produced (Platten III, 2011). The U.S. Army is currently evaluating the use of DNAN, and if accepted as an alternative to TNT, its manufacturing rate will likely increase dramatically and may end up in waste streams at the Load, Assemble, and Pack (LAP) plants (Platten III, 2011). Additionally, if DNAN replaces TNT, it will likely be used worldwide for training and combat purposes. TNT detonation often leaves chemical residue around the blast site which has the potential to leach into the ground and water. Without proper treatment, DNAN has the potential to pass through water treatment trains intact. DNAN, given similar properties to TNT, may have similar negative effects on the environment. Studies have indicated that DNAN has deleterious effects on organisms such as bacteria, algae, earthworms, and plants (Dodard et al., 2013; Yang et al., 2018). DNAN's known toxic effects, future mass production, and its potential for introduction into associated waste streams and training environments create a need for an increased understanding of the environmental fate and transport as well as potential remediation techniques.

2.4.1 Advanced Oxidation of 2,4-dinitroanisole

Environmental transformation of DNAN can occur naturally by photolysis, although these processes generally exhibit slow rates of degradation of DNAN (Yang et al., 2018). These degradation rates, while slow, have the potential to be combined with advanced processes to further reduce DNAN. Because DNAN slowly transforms, and has a high potential to end up in waste streams at LAP plants, degradation methods using an AOP have a strong potential to appreciably reduce DNAN in wastewater.

Noss and Chyrek (1984) studied the effects of UV radiation and H_2O_2 on TNT and a variety of other chemicals commonly found in manufacturing plants. Their study found that pH had a minimal effect on the degradation of chemicals (Noss & Chyrek, 1984). It was noted that UV alone, at 253.7 nm, effectively degraded all compounds, including TNT, RDX, and HMX, when they were treated together (Noss & Chyrek, 1984). Interestingly, among all the munitions tested in the presence of UV radiation alone, only TNT persisted when treated individually (Noss & Chyrek, 1984). This is important, as understanding waste plant effluent composition may impact treatment plans. When TNT absorbs UV light, it inhibits the radical production necessary for its degradation (Noss & Chyrek, 1984). Noss and Chyrek (1984) found ideal concentrations of H_2O_2 to be less than 0.1% when combined with UV radiation which produced first-order reaction rate constants of 0.038 $-k_{min}^{-1}$ with 0.01% H_2O_2.

Yang et al. (2018) investigated the degradation of DNAN in water by UV-based AOPs, including UV/H_2O_2 and UV/persulfate (UV/PS). The UV/H_2O_2 reactor used low pressure mercury lamps which predominantly emitted light at 254 nm (Yang et al., 2018). Both methods were able to degrade DNAN, however, UV/PS appeared to be a more

efficient process than UV/H_2O_2, particularly when high levels of peroxide were applied (Yang et al., 2018). Additionally, Yang et al. (2018) tested pH levels of 3.03, 7.10, and 10.08 found that it had a negligible impact on DNAN degradation. The data from the UV/H_2O_2 AOP process demonstrated an increase in DNAN degradation when H_2O_2 concentration was elevated from 2 to 5 mM but exhibited a detrimental effect at high levels (e.g. 10mM) (Yang et al., 2018). This is likely attributed to the scavenging effect of H_2O_2 and self-recombination of HO· (Yang et al., 2018). The rate constants for the UV/H_2O_2 were not available at the time of publishing this report. The UV/PS was also capable of degrading DNAN, but the process did not inhibit DNAN degradation with increased levels of PS (Yang et al., 2018). Specifically, the UV/PS reactor achieved pseudo-first-order rate constants of 0.0014 to 0.0189 min^{-1}, with 10 mM yielding the best performance (Yang et al., 2018). Yang (2018) attributes this to the lower rate of self-recombination of SO_4^{2-}% and how it reacts with PS. This suggests that UV/PS may be a more efficient system for DNAN degradation when compared to UV/H_2O_2 (Yang et al., 2018). Photolysis of the naturally occurring photoinducer NO_3^- can also create reactive species, including HO·, nitrogen dioxide radical (NO2), and peroxynitrite anion (ONOO−), that may react with DNAN and mitigate the photoinducing effects of NO3− and effectively degrade DNAN (Yang et al., 2018).

Su et al. (2019) conducted photocatalyzed H2O2 oxidation experiments to study the effect of initial pH and H2O2 dosage on the kinetics of DNAN decomposition. The results show that DNAN degradation followed zero-order kinetics in a 250 ppm DNAN solution with UV light and 1500-4500 ppm H2O2 and a pH between 4-7 (Su et al., 2019). When H2O2 was increased to 750ppm, DNAN degradation increased to pseudo-first

order kinetics, indicating DNAN is easily reduced by UV/H2O2 treatment (Su et al., 2019). Su et al (2019) concluded that 1500 ppm H2O2 and an initial pH of 7 were optimal conditions for treating 250 ppm of a DNAN solution and resulted in DNAN reduction from 250 to 1 ppm in 3 hours. Total organic carbon (TOC) and total carbon (TC) concentrations were reduced slowly, indicating the formation of other organic compounds during the treatment process (Su et al., 2019). These intermediates were oxidized to CO_2, and they found that most of the DNAN could be oxidized to CO_2 and nitrate (Su et al., 2019). While Su et al. (2019) found that the H_2O_2 AOP was a good candidate for DNAN reduction, there is research to be done, specifically on how well this system maintains efficiency over time as well as how it reacts in the presence of co-contaminants, specifically, naturally occurring photoinducers as they have the potential to inhibit system efficiency and degradation of target organisms. Additionally, it is worth considering the application of the system on a large scale and whether the time required for proper degradation is feasible in a conventional water treatment system.

Conventional biological treatment does not effectively treat wastewater containing nitroaromatic compounds such as DNAN (Shen et al., 2013). Shen et al. (2013) used a combined zero-valent iron (ZVI) reduction and Fenton oxidation process to evaluate the pretreatment of 2,4-dinitroanisole (DNAN) in wastewater. The combined process uses ZVI as a reductive stage to convert nitroaromatic compounds in DNAN into chemical species that are more susceptible to the subsequent Fenton oxidation process (Shen et al., 2013). Using this method, nearly all nitroaromatic compounds were removed with an 8-hour empty bed processing time (Shen et al., 2013). Since this treatment process uses a two-stage method, it may be beneficial when treating water with co-

contaminants that may inhibit other AOPs. Because the ZVI can convert nitroaromatic compounds like DNAN to compounds that are more susceptible to the following Fenton oxidation, it may lead to enhanced DNAN degradation during the oxidation process and overall efficiency in the combined system.

Gallucci (2016) studied the effects of different LED designs in a variety of reactor conditions. His work demonstrated that UV LED H2O2 AOP was capable of a 2-Log reduction of *E. coli* (Gallucci, 2016). More importantly, his work optimized conditions with a medium thickness Teflon walled reactor with high power UV LEDs that could be used for future research (Gallucci, 2016). This study uses a reactor designed by Gallucci and used by Stubbs (Gallucci, 2016; Stubbs, 2017). Much of the work in this study is a continuation of the work of Scott, Stewart, and Stubbs (Scott et al., 2017; Stewart, 2016; Stubbs, 2017).

2.5 Soluble Microbial Products and Co-Contaminants

Effluents from wastewater treatment systems are known to contain a variety of soluble organic compounds, including residual degradable and hard-biodegradable influent substrate, as well as complex organic compounds which are categorized as Soluble Microbial Products (SMPs) (Azami, Sarrafzadeh, & Mehrnia, 2012). SMPs have been identified as containing humic acids, proteins, antibiotics, and amino acids (Azami et al., 2012). SMPs in wastewater effluents vary depending on the method of treatment. Utilization-associated products (UAPs) in SMP were found to be carbonaceous compounds with a molecular weight less than 290kDa (Ni, Rittmann, & Yu, 2011). Secondary effluent from three wastewater treatment facilities showed protein

concentrations of less than 10 mg/L (Westgate, 2009). SMPs also have a significant effect on the physico-chemical properties of microbial aggregates in secondary wastewater sludge (Sheng, Yu, & Li, 2010; Zhang et al., 2017). Additionally, SMPs can increase membrane fouling and cause flux decline in wastewater reclamation and reuse systems (Jarusutthirak & Amy, 2006). Specifically, reverse osmosis, nanofiltration, and ultrafiltration fouling is caused by SMPs forming a cake or gel layer due to steric exclusion (Jarusutthirak & Amy, 2006). Because SMPs can cause fouling of filters, it is possible that over time they will foul UV lights in an AOP. More importantly, because the AOP used in this experiment has the potential to be used in wastewater treatment, it is critical to understand the effects of SMPs on the performance of the reactor.

Yang et al. (2018) also researched the effects of naturally occurring photoinducers, including Suwannee River fulvic acid (SRFA) and nitrate (NO3-) in a UV/PS system and found they inhibited the reduction of DNAN. DNAN degradation was likely inhibited because the SRFA caused radical scavenging, light screening effects, and reductive conversion of intermediate radicals (Yang et al., 2018). Additionally, "High concentration of NO3− mitigated the inhibitory effect, presumably due to the reactive nitrogen species (RNS) generated by NO3− photolysis" (Yang et al., 2018). Furthermore, Yang et al. (2018) propose that SRFA's strong absorbance at 254 nm may inhibit PS decomposition upon UV radiation to produce SO4·-.

There is a gap in understanding how photoinducing co-contaminants react and influence DNAN degradation in an UV/H2O2 AOP. While Yang et al. (2018) did not research the effects of naturally occurring photoinducers in the UV/ H_2O_2 process, it is likely they have an inhibitory effect, possibly due to blocking UV light within a reactor.

Assuming wastewater from DNAN production and municipal wastewater will have other co-contaminants, further research should be conducted using an UV/H_2O_2 AOP with likely co-contaminants to determine the efficacy of the system when exposed to various concentrations of co-contaminants.

2.6 Wastewater Treatment at DoD facilities in Continental United States

DoD wastewater facilities in the Continental United States (CONUS) must comply with the parameters of National Pollution Discharge Elimination System (NPDES) permits (US EPA, 2010, p. 1–5). Conventional wastewater facilities can be expected to produce effluent that complies with NPDES permits. This effluent, however, may cause complications with subsequent advanced treatment methods, particularly AOPs which may be degraded my naturally occurring photoinducers (Yang et al., 2018).

Barry (2012) characterized domestic wastewater treatment processes at DoD installations located in the Continental United States. Of the 86 military water treatment facilities studied, approximately 63% used an activated sludge process, 17% used advanced treatment, 15% primary treatment only, 6% settling ponds, and 1% used septic tanks (Barry, 2012). Those systems with advanced sludge processes would produce effluent containing SMPs. Because naturally occurring photoinducers can degrade the DNAN in an AOP (Yang et al., 2018), it is important that the DoD understand not only the characterization of its wastewater byproducts, but its selected treatment method in order to produce safe water that meets NPDES permit requirements.

III. Methodology

3.1 General Operating Parameters

AOP experiments were conducted in a Teflon UV LED reactor with an internal volume of approximately 35 ml, a flow rate of 2 ml/min, and a residence time of approximately 17.5 minutes (Stubbs, 2017). Solution flowed through a Masterflex L/S® Model 77200-50 peristaltic pump and Masterflex L/S® PharMed® BPT 14 precision pump tubing (Cole-Parmer Instrument Co, Vernon Hills, Illinois). The pump was set to 7.8 rpm which resulted in a 2 mL/min flow rate for all experiments. A 0.5-inch PTFE coated stir bar was placed inside the reactor to create a CFSTR and the reactor was placed horizontally on a Fisher Scientific 14-511-2 magnetic stir plate (Thermo Fisher Scientific, Waltham, Massachusetts). Figures 1-3 depict the reactor used in this experiment. The BPT tubing entered the reactor where the solution was exposed to light from two UV-CLEAN LEDs (Sensor Electronic Technology Inc, Columbia, South Caroline) emitting at 264 nm, and each light consisting of nine diodes receiving 100mA. The LEDs were powered by a circuit board with 12 LUXdrive™ model 4006 DynaOhm™ 20mA semiconductor resistors (LEDdynamics, Randolph, Vermont). The circuit board was controlled by a Keysight E3620A series bench power supply. After passing through the reactor, effluent exited in PTFE tubing and was used for grab sampling or directed into a waste beaker.

3.2 AOP Experiment

In order to answer the first research question, the independent variable, molar peroxide ratio, was adjusted and expected to greatly influence the observed first order

rate constants (k_s). The solutions for the AOP experiments were comprised of DNAN (CAS 119-27-7 Alfa Aesar ®), reverse osmosis, purified, deionized water (DI Water, AFIT ENV Lab), casamino acids (MP Biomedicals Cat No. 3060-012, Solon, OH), and Hydrogen Peroxide (30% in water, Fisher Scientific, Pittsburgh, PA). Molar peroxide ratios H2O2:DNAN were adjusted to 50:1, 100:1, 250:1, 500:1, and 1000:1.

DNAN solutions were prepared three days prior to experiments to ensure thorough mixing. The 250 ml solution consisted of 10mg/L DNAN in a 250ml Type A volumetric flask. DNAN was measured using a Mettler-Toledo XP26 Precision Balance (Mettler-Toledo, LLC, Columbus, Ohio). A 1.0-inch PTFE stir bar was placed inside the volumetric flask, the flask was capped, covered in foil, and placed on a Thermo Scientific Model SP88857100 stir plate (Thermo Fisher Scientific, Waltham, Massachusetts) set to 850 rpm for three days.

On the day of the experiment, a casamino acid solution was prepared, that when added to the DNAN solution, produced a casamino acid concentration of 1 mg/L. To prepare the casamino acid solution, 250 mg of casamino acid powder was mixed with reverse osmosis, purified, deionized water in a 100 ml volumetric flask. A 0.5-inch PTFE stir bar was placed inside the volumetric flask, hand mixed for 20 minutes, then mixed on a Thermo Scientific Model SP88857100 stir plate (Thermo Fisher Scientific, Waltham, Massachusetts) for one-hour. Upon thorough mixing of the casamino acid solution, an appropriate volume was added to the DNAN solution to create a concentration of 1 mg/L of casamino acids in the DNAN solution.

H_2O_2 was then added (volume dependent on target molar ratio) to the DNAN and casamino acid solution and hand mixed for five minutes, then placed back on the stir

plate for 20 minutes. After thorough mixing, a sample of approximately 8 ml was drawn from the solution in a 10 ml luer lock syringe (Henke Sass Wolf, Tuttlingen, Germany) to be analyzed by a SevinMulti pH Meter (Mettler-Toledo, LLC, Columbus, Ohio). It is important to note the pH of the solution varied throughout the experiments, from 5.18 to 7.09, and was only measured after a complete DNAN-Casamino Acid-H_2O_2 solution was well mixed. The variations in pH are likely due to storage conditions as well as maintenance conducted on the water purification system. Standards were then created for a calibration curve. Standards were made from the prepared DNAN solution and DI water to create a blank, 10, 20, 40, 60, 80, and 100% DNAN solution. DNAN presence was detected and quantified via HPLC chromatogram analysis. DNAN appears at 1.098 min residence time and increased proportionately with increased ratios in standards.

3.2.1 *AOP Experiments Description*

For each experiment, the reactor was placed on a Fisher Scientific stir plate 14-511-2 magnetic stir plate (Thermo Fisher Scientific, Waltham, Massachusetts) which was started once fluid entered the reactor. Approximately 45 ml of DNAN solution was added to the influent lines, reactor, and effluent lines via a 60 ml Luer-Lok syringe (Becton, Dickinson, Franklin Lakes, New Jersey) in order to remove any air from the system. The pump was started and the DNAN flowed at 2.0 ml/min through the reactor with the UV LEDs turned off for 60 minutes of control sampling. Samples were taken at 10, 20, 30, 40, 50 and 60 minutes. Each 1.5 ml sample was collected in a 10 ml syringe, and filtered with a Millex ® Hydrophobic Flouropore ™ PTFE filter with 0.2 um membrane (MilliporeSigma, Burlington, Massachusetts) into a 2.0 ml amber screw top vial (Agilent

Technologies, Santa Clara, California). All samples were well mixed for 30 seconds on a SBV1000 Vortex Mixer (Southwest Science, Hamilton Township, New Jersey). After 60 minutes elapsed, the circuit board was turned on, applying 100mA and 12.50v to the UV LEDs. The DNAN solution was then ran through the reactor for 60 minutes, with samples taken at 5, 10, 15, 20, 25, 35, 45, and 60 minutes. Samples were collected and prepared in the same manner as the previous step, and prepared for analysis in the HPLC.

3.2.2 *H_2O_2 Control Experiments*

There may be interaction between the DNAN and casamino acids. An experiment was conducted without H_2O_2 but with casamino acids present. A control was conducted for 60 minutes with UV LEDs turned off (samples taken at 0, 10, 20, 30, 40, 50, & 60 min), followed by 60 minutes with UV LEDs turned on (samples taken at 5, 10, 15, 20, 25, 35, 45, & 60 min). The k_s was expected to be near zero. A second control was conducted, in similar fashion to the one previously described, however, casamino acids were not added. The k_s was also expected to be near zero.

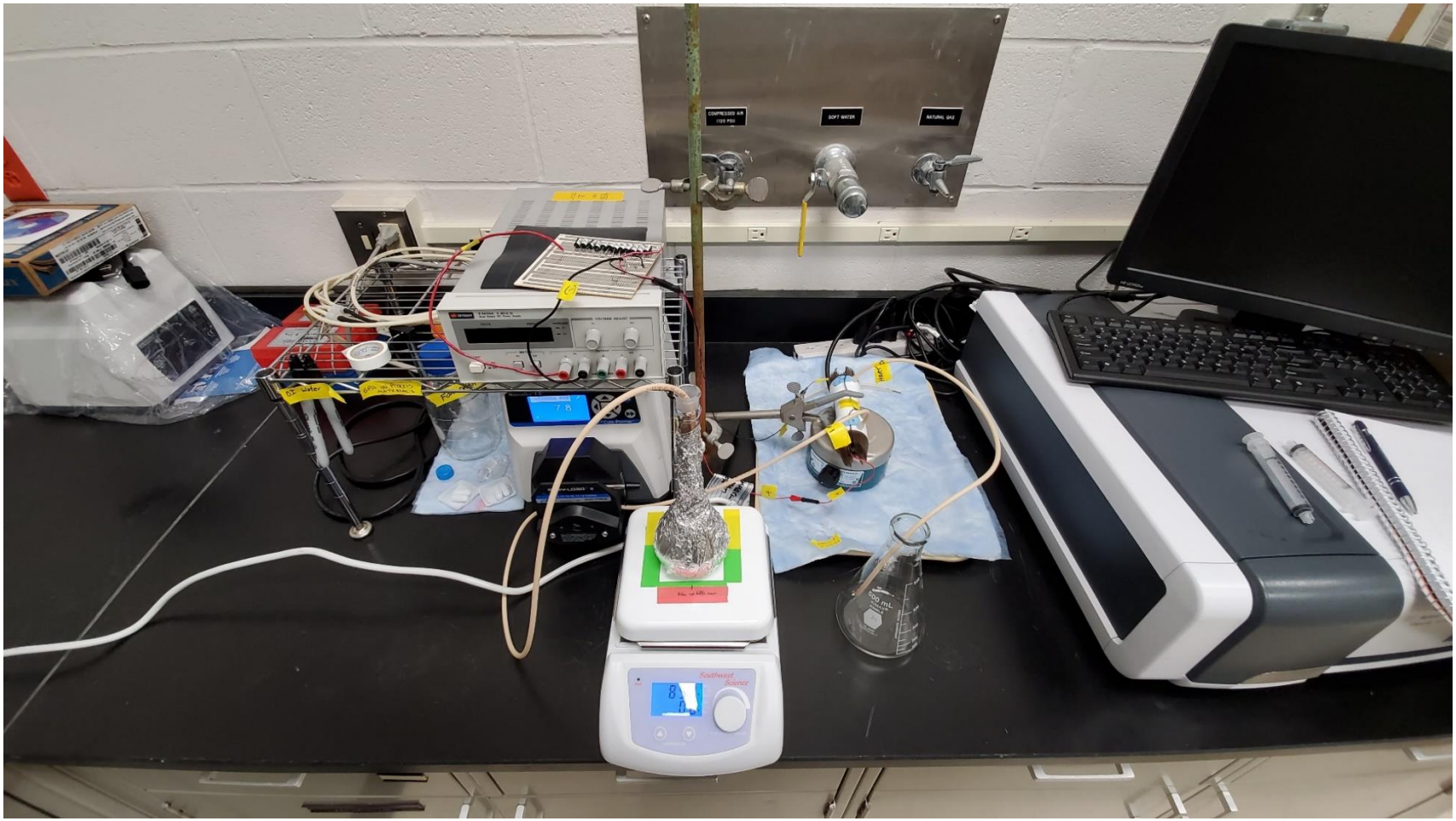

Figure 1: AOP Experimental Setup

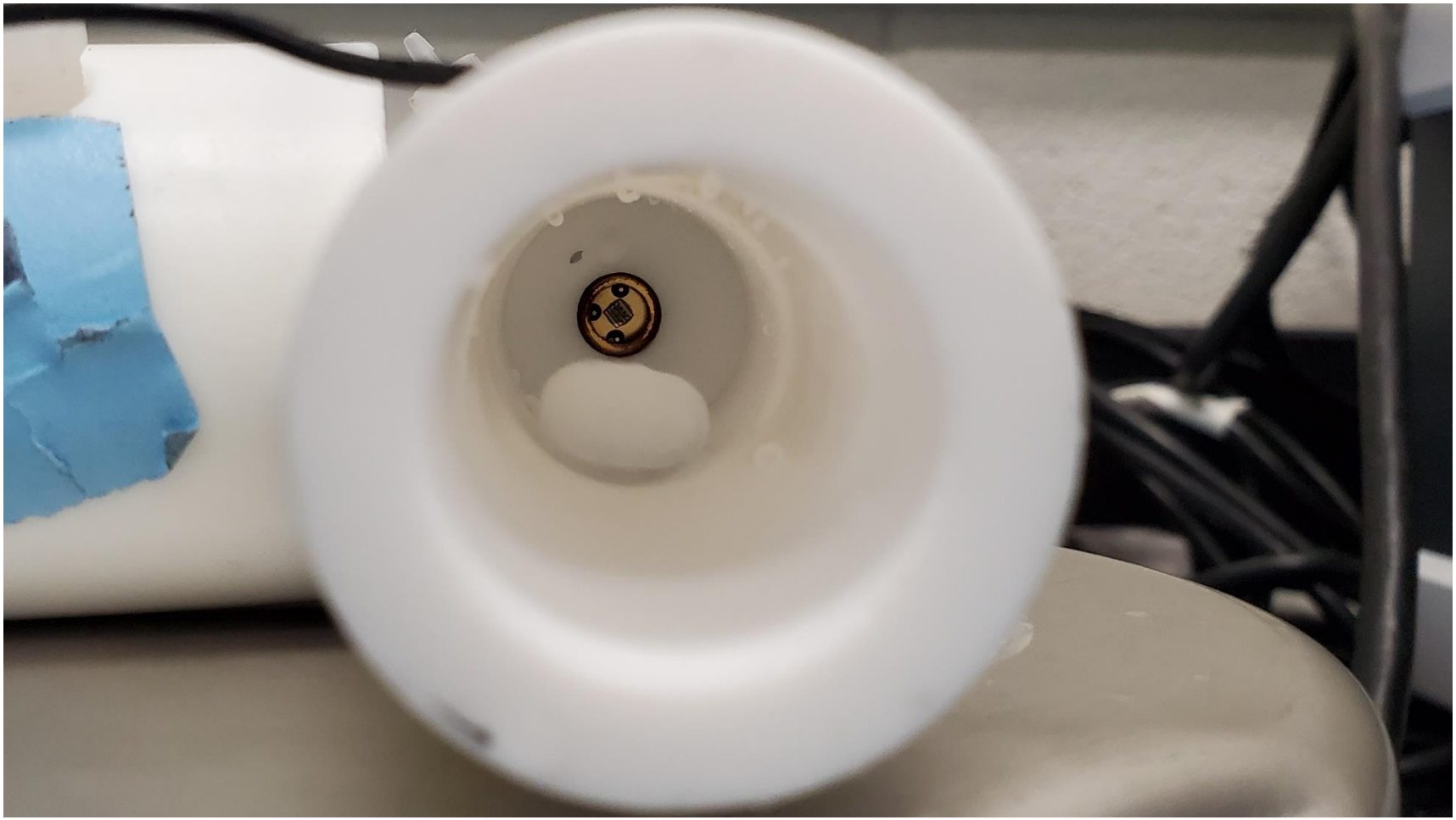

Figure 2: Internal View of Reactor LED and Stir Bar

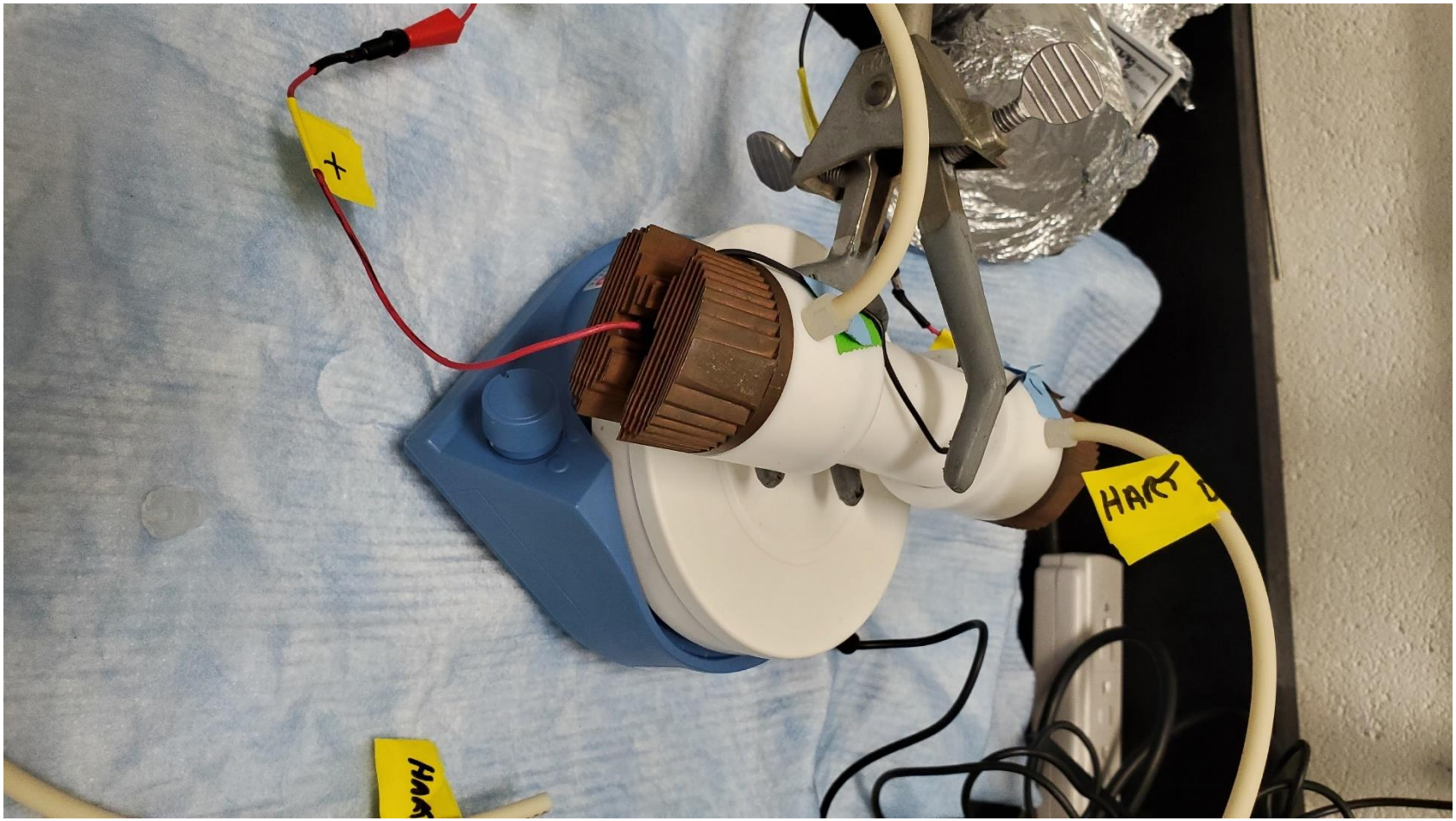

Figure 3: AOP Reactor Power Input, Influent and Effluent Lines, and Heat Sinks

3.3 HPLC and Mass Spectroscopy Analysis

Samples were analyzed in an Agilent Technologies 1260 Infinity HPLC coupled with a 6130 Quadrupole LC/MS (Agilent Technologies, Santa Clara, California). Treated DNAN was separated by a 1.8 µm, 2.1x50 mm, C18 column (Model: 82770-902, SN: USWEY 12941, Agilent Technologies, Santa Clara, California). Acetonitrile and water (1% formic acid) constituted the mobile phase. The HPLC quaternary pump flow was set to 0.6 ml/min with a solvent composition of 50% water, 10% formic acid, and 40% acetonitrile. Chromatogram peaks were integrated using Agilent Technologies ChemStation software.

MS spectra was used to suggest possible byproduct structures. After processing each experiment in the HPLC, they were analyzed by mass spectrometry. Chromatogram peaks were integrated using Agilent Technologies ChemStation software. Atomic mass units and retention times were used to propose possible byproduct structures. See Appendix F for chromatograms.

3.4 Statistical Analysis

Data for all experiments was entered into Microsoft Excel to show the change in effluent DNAN concentration (C/C_0) over time as measured by the HPLC. Curve-fitting was conducted with MATLAB R2020 in order to retrieve the observed pseudo first-order rate constants associated with DNAN removal. See Appendix D for MATLAB code. The mathematical basis of the curve fit was non-steady state solution for a CFSTR with first order reaction:

Equation 1: CFSTR with 1st order reaction

$$C(t)/Cin = [(1 + (\tau k)(\exp[(1/\tau + k)(-1)t])] / (\tau k + 1)$$

Where C(t) is concentration at time t
Cin is initial concentration
τ is average reactor residence time
t is time
k is apparent first-order reaction rate constant

3.4.1 Analysis of Variance

A Kruskal-Wallis H-Test was conducted using JMP® and Python ® software to determine if there are statistically significant differences between treatments (k_s values). The Kruskal-Wallis H-Test is a non-parametric technique that compares the means of the groups, categorized here as k_s by molar ratio. Additionally, the Kruskal-Wallis H-Test requires no assumptions about population probability distributions (Sincich, Mcclave, & Benson, 2018). H_0 for this test is that the populations medians are equal. H_a for this test is that at least two of the population medians are not equal. This test will indicate whether the population medians are different, however, it will not indicate which populations medians are different. For that, the Two-Sample *t*-Statistic is used.

3.4.2 Two Sample t-Statistic

In order to determine which treatment is differs at a statistically significant level, a t-test was performed. The t-test is useful when the sampled populations are only approximately normally distributed, which may be the case with only three samples per molar ratio. Additionally, when sample sizes are equal, the assumption of equal population variance can be relaxed and the test statistic will still produce an approximate Student's t-distribution (Sincich et al., 2018, p. 463). The t-test will use approximate

small-sample procedures to compare molar ratios to determine if there is a statistically significant difference. With this test, *t* is based on 2(n-1) degrees of freedom.

Equation 2: t-Test for Small Samples When $\sigma_1^2 \neq \sigma_2^2$

Confidence Interval: $(\bar{x}_1\text{-}\bar{x}_2) \pm = t_{\alpha/2}\sqrt{(s_1^2 + s_2^2) / n}$

Test Statistic for H_0: $t = \frac{(\overline{x_1} - \overline{x_2})}{\sqrt{(s_1^2 + s_2^2)/n}}$

Where $\bar{x}$ is the sample mean
$t_{\alpha/2}$ is Student's t-value
s_1^2 is the sample variance
n is number of samples

IV. Analysis and Results

4.1 The Effect of Molar Peroxide Ratio on DNAN Degradation

Figure 4 shows the effect of 50:1 H_2O_2 to DNAN ratio on the relative concentration of DNAN. The x-axis shows time elapsed, and the y-axis shows relative concentration of DNAN (C/C_0). For trial one, over the course of a 60-minute experiment, the relative concentration of DNAN (C/C_0) decreased to 0.899, 0.891, 0.837, 0.828, 0.816, 0.805, 0.812, and 0.814. Trial two decreased to 0.909, 0.870, 0.849, 0.834, 0.826, 0.821, 0.821, and 0.811. Trial three decreased to 0.902, 0.866, 0.848, 0.816, 0.817, 0.807, 0.808, and 0.803. The k_s (min^{-1}) for trials 1-3 were 0.015, 0.015, and 0.016, respectively. The mean k_s (min^{-1}) for 50:1 trials was 0.0153 and is displayed with the other molar ratios in Figure 10. With a low relative concentration of H_2O_2, the overall degradation of DNAN was less than subsequent experiments. A possible explanation for lower performance than subsequent molar ratios may be a lack of hydroxyl radical production due to decreased presence of H_2O_2.

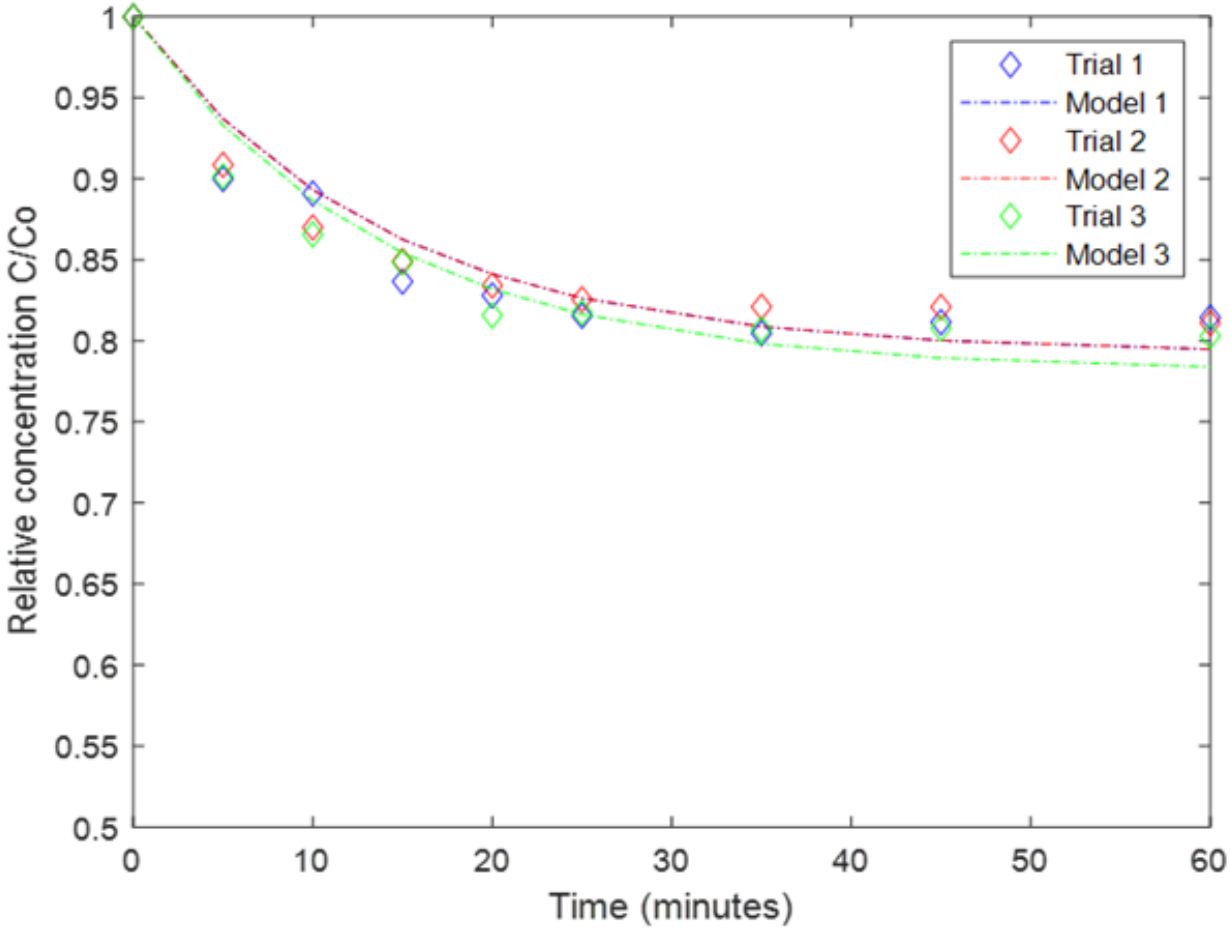

Figure 4: The Effect of 50:1 H2O2 to DNAN on the Removal of DNAN

Figure 5 shows the effect of 100:1 H2O2 to DNAN ratio on the relative concentration of DNAN. The x-axis shows time elapsed, and the y-axis shows relative concentration of DNAN (C/C_0). For trial one, over the course of a 60-minute experiment, the relative concentration of DNAN (C/C0) decreased to 0.894, 0.827, 0.786, 0.775, 0.753, 0.732, 0.732, and 0.719. Trial two decreased 0.920, 0.854, 0.822, 0.791, 0.765, 0.755, 0.750, 0.744. Trial three decreased to 0.919, 0.856, 0.825, 0.804, 0.782, 0.765, 0.759, 0.729. The k_s (min^{-1}) for trials 1-3 were 0.023, 0.02, and 0.02, respectively. The mean k_s (min^{-1}) for 100:1 trials was 0.021 and is displayed with the other molar ratios in Figure 10. The data was as expected, with increased degradation compared to the 50:1 trial.

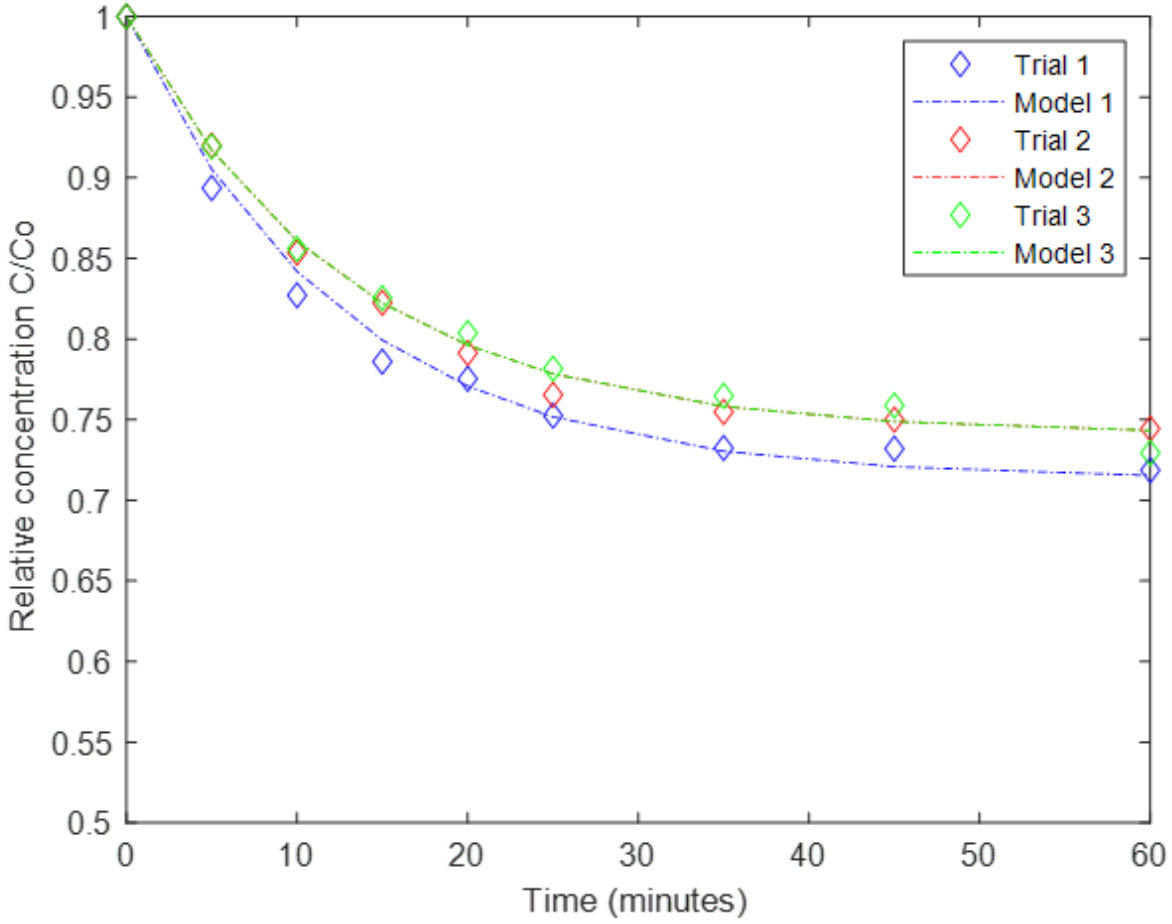

Figure 5: The Effect of 100:1 H2O2 to DNAN on the Removal of DNAN

Figure 6 shows the effect of 250:1 H_2O_2 to DNAN ratio on the relative concentration of DNAN. The x-axis shows time elapsed, and the y-axis shows relative concentration of DNAN (C/C_0). For trial one, over the course of a 60-minute experiment, the relative concentration of DNAN (C/C0) decreased to 0.846, 0.795, 0.770, 0.731, 0.715, 0.710, 0.701, and 0.686. Trial two decreased to 0.832, 0.786, 0.730, 0.719, 0.709, 0.695, 0.691, and 0.691. Trial three decreased to 0.845, 0.806, 0.763, 0.737, 0.736, 0.728, 0.729, and 0.715. The k_s (min^{-1}) for trials 1-3 were 0.027, 0.029, and 0.025, respectively. The mean k_s (min^{-1}) for 250:1 trials was 0.027 and is displayed with the other molar ratios in Figure 10.

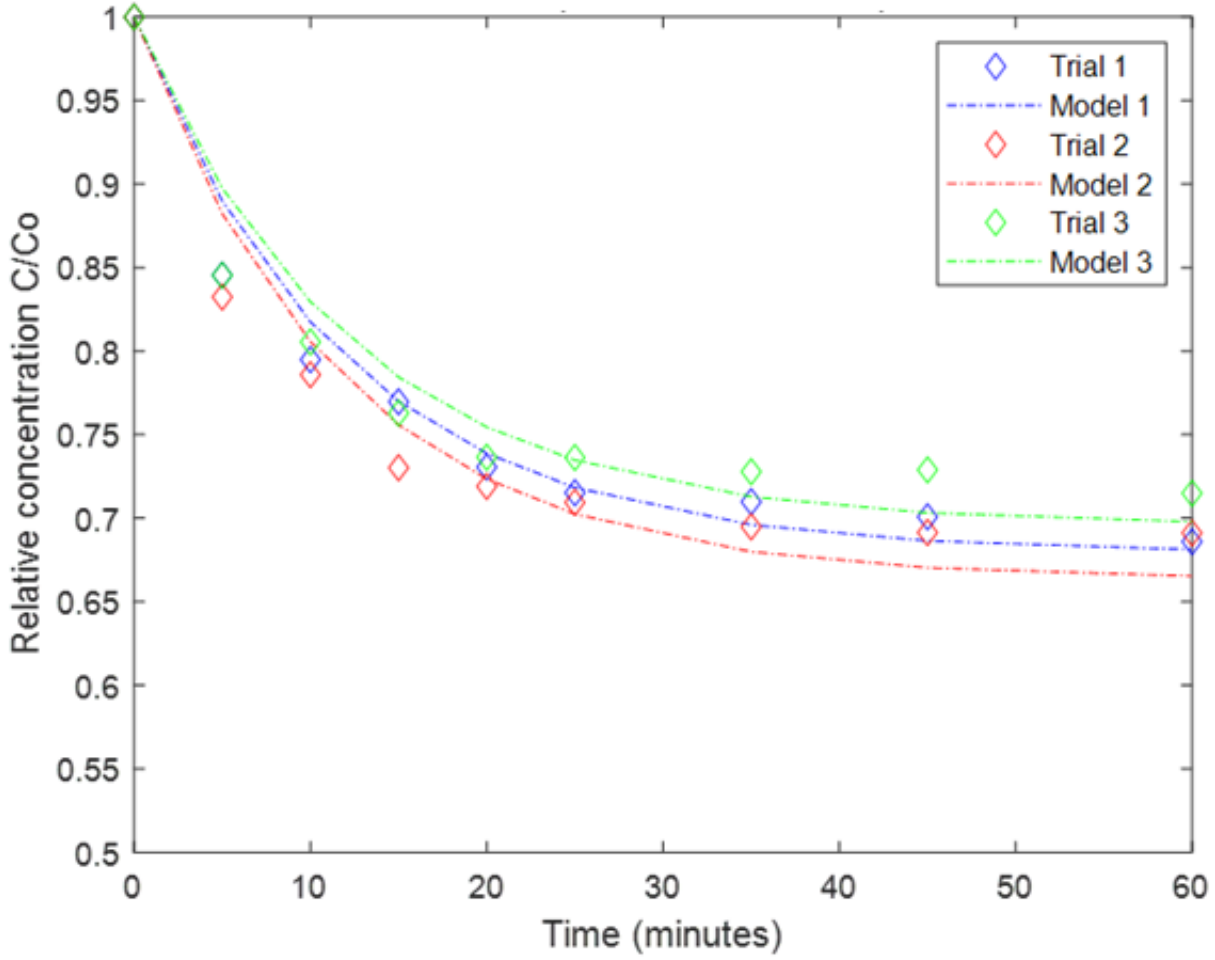

Figure 6. The Effect of 250:1 H2O2 to DNAN on the Removal of DNAN

Figure 7 shows the effect of 500:1 H_2O_2 to DNAN ratio on the relative concentration of DNAN. The x-axis shows time elapsed, and the y-axis shows relative concentration of DNAN (C/C_0). For trial one, over the course of a 60-minute experiment, the relative concentration of DNAN (C/C0) decreased to 0.861, 0.814, 0.756, 0.743, 0.721, 0.691, 0.685, and 0.629. Trial two decreased to 0.866, 0.767, 0.757, 0.711, 0.706, 0.699, 0.690, and 0.683. Trial three decreased to 0.848, 0.775, 0.754, 0.730, 0.715, 0.714, 0.693, and 0.688. The k_s (min^{-1}) for trials 1-3 were 0.029, 0.029, and 0.028, respectively. The mean k_s (min^{-1}) for 500:1 trials was 0.0287 and is displayed with the other molar ratios in Figure 10.

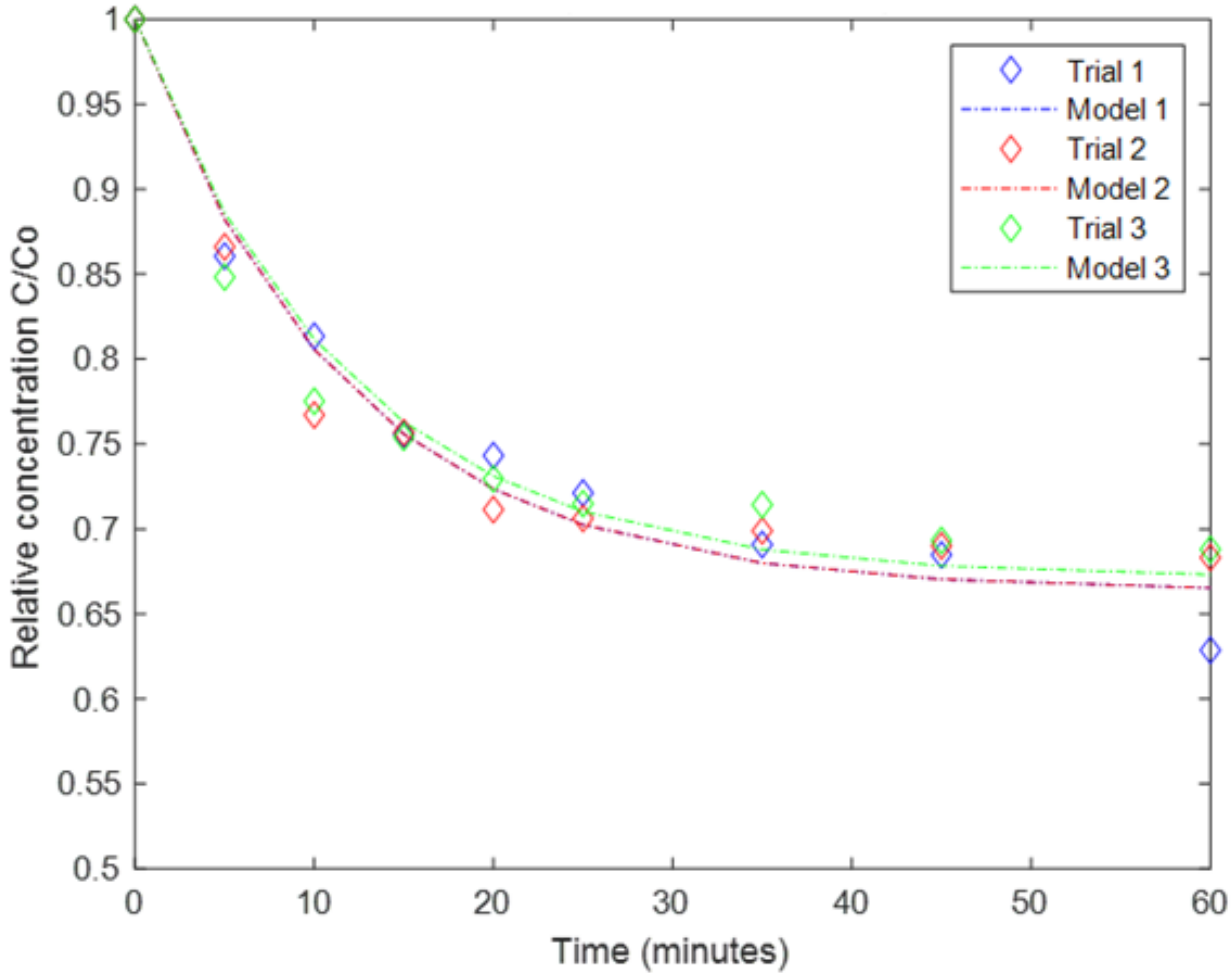

Figure 7. The Effect of 500:1 H2O2 to DNAN on the Removal of DNAN

Figure 8 shows the effect of 1000:1 H_2O_2 to DNAN ratio on the relative concentration of DNAN. The x-axis shows time elapsed, and the y-axis shows relative concentration of DNAN (C/C_0). For trial one, over the course of a 60-minute experiment, the relative concentration of DNAN (C/C0) decreased to 0.841, 0.795, 0.751, 0.735, 0.728, 0.713, 0.722, and 0.714. For this trial, the 45-minute sample of 0.722 relative concentration of DNAN (C/C_0) showed less degradation than the sample drawn at 35 minutes. This is likely attributed to the solution reaching maximum residence time in the reactor and the effluent being influenced by mixing performance inside the reactor. Trial two decreased to 0.831, 0.794, 0.769, 0.756, 0.748, 0.721, 0.709, and 0.706. Trial three decreased to 0.764, 0.706, 0.681, 0.668, 0.653, 0.645, 0.639, 0.626. The k_s (min^{-1}) for trials 1-3 were 0.026, 0.026, and 0.038, respectively. The mean k_s (min^{-1}) for 1000:1 trials was 0.030 and is displayed with the other molar ratios in Figure 10.

Trial three displayed significantly more degradation (10.1% and 8.9% respectively) at the five-minute sampling mark than trial one and two. This is statistically significant and may be attributed to several factors. It is possible that this result, although an outlier, is actually a valid result. It is important, however, to speculate why it could be an anomaly. Because the CFSTR is made of Teflon, it is not possible to observe the internal conditions, specifically whether the stir bar is properly spinning within the reactor. It is possible to hear and feel the stir bar spinning, but it cannot be guaranteed where the stir bar is spinning and whether it is spinning properly. It is possible the stir bar, when exposed to a continuous flow, moved inside the reactor and created sub-optimal mixing conditions. This is plausible because the 0.5-inch stir bar is spinning in a cylindrical reactor laying on its side, as opposed to a flat surface which would allow the

stir bar to move freely without impacting the sides of the reactor. Although mixing conditions may not have been optimal, this may have produced samples with higher degradation than a trial with proper mixing. This is counterintuitive, but is possible because the effluent is a mixture of fresh influent that has just entered the reactor, and fluid that has been in the reactor close to the maximum residence time. If the stir bar were to improperly operate, it is possible that the effluent was more composed of a solution that had achieved peak residence time instead of a properly mixed solution of untreated and treated fluid with a lower average residence time. If the stir bar were to have a temporary unbalance, this could be noticed as a positive or negative spike on the degradation curve which then recovers back to normal parameters. Additionally, increased degradation could have occurred if pump errors caused either a decreased volume in the reactor or increased residence time. With 1000:1 trial number three, there was no spike, just a significantly larger drop at the first sample. This may be indicative of results with actual increased performance compared to trials one and two, or a reactor that did not stir properly for the entire experiment and only appears to have enhanced degradation.

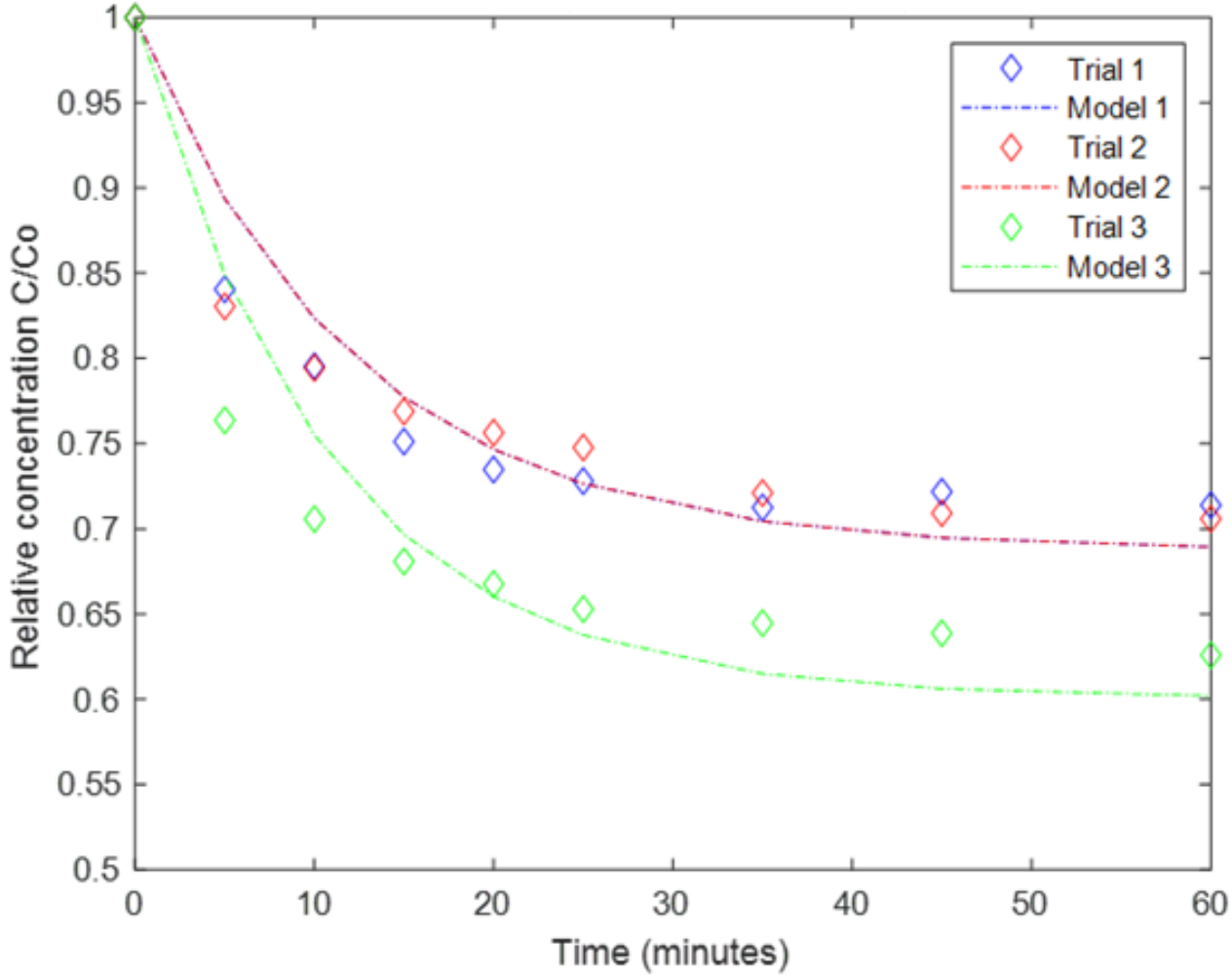

Figure 8. The Effect of 1000:1 H2O2 to DNAN on the Removal of DNAN

Figure 9 shows effect of each molar ratio of H_2O_2 to DNAN (averaged) on the relative concentration of DNAN. The x-axis shows time elapsed, and the y-axis shows relative concentration of DNAN (C/C_0). This depicts the average of each molar ratio to best compare them to each other. By visual analysis, based solely on means, it appears that DNAN degradation increased with an increase in H_2O_2, with 50:1 showing the least overall degradation and 1000:1 with the most degradation. Furthermore, the results show non-linear DNAN reduction under all experimental conditions. This information will be used for further statistical analysis in the next section.

Results depicted in Figure 9 are likely influenced by radical scavengers present in the DNAN solution. The reverse osmosis, purified, deionized water used in the solution limits the types of potential radical scavengers to radical-radical reactions, bicarbonate, and H_2O_2. Among these, radical-radical reactions are the most thermodynamically favorable, followed by bicarbonate, then H_2O_2, with activation energy (Ea) of 8, 14, and 21.2 KJ/mol respectively (Buxton et al., 1988).

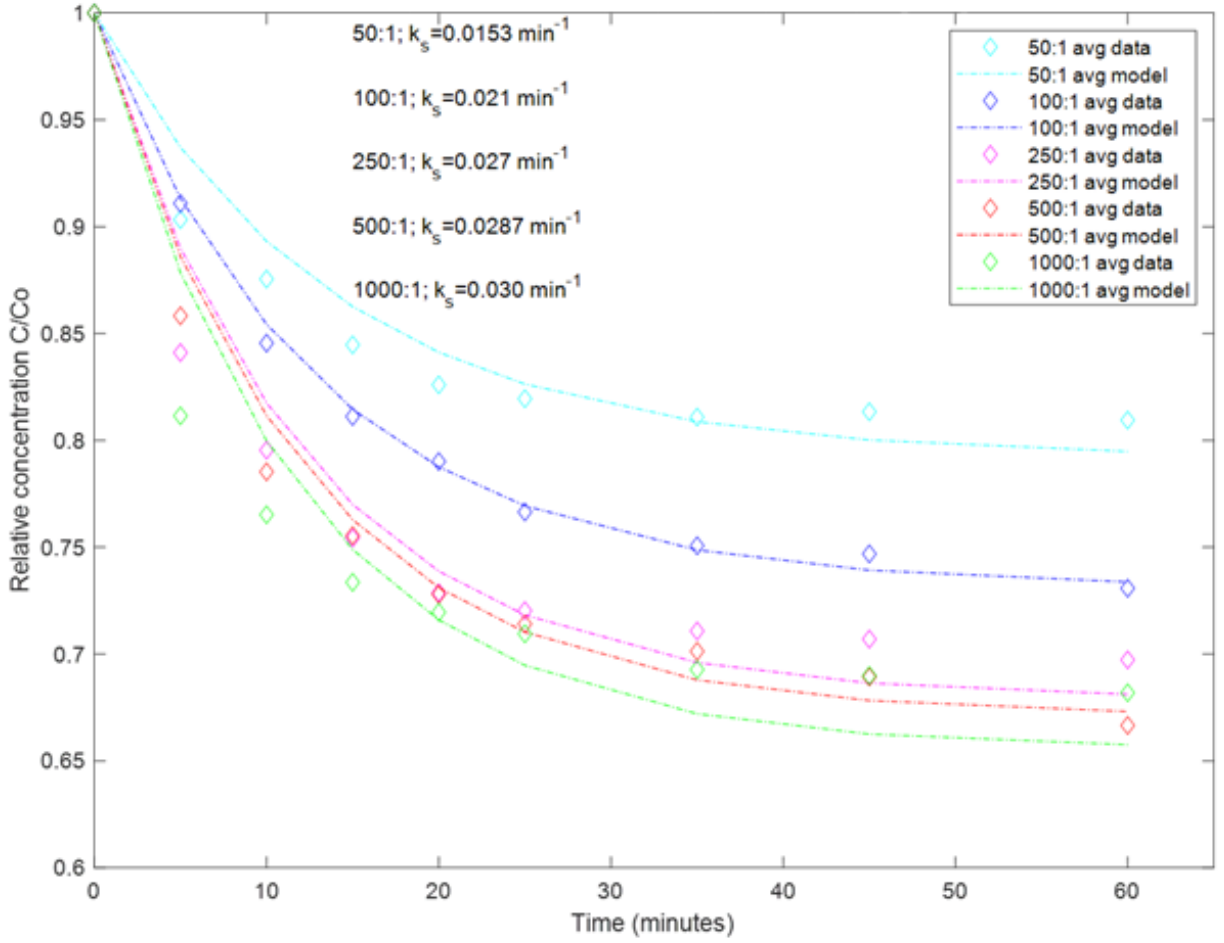

Figure 9. Average DNAN Removal by Molar Ratio

4.2 Statistical Analysis of Pseudo-First Order Rate Constants

Figure 10 shows the results of Welch's ANOVA. The F-Ratio of 144.21 indicates that the means between molar ratios is high and that H_0 (means are equal) will likely be rejected. With an F value of < 0.0001, it is extremely unlikely the differences observed are due to random sampling, thus, the H_0 is rejected. This confirms that there is a statistically significant difference between the five molar ratios.

Welch's Test

Welch Anova testing Means Equal, allowing Std Devs Not Equal

F Ratio	DFNum	DFDen	Prob > F
144.2129	4	4.6829	<.0001*

Figure 10: Welch's ANOVA

Table 1 shows the results of a *t*-test that was performed to determine which treatment is different. The results indicate that four ratio comparisons are different. Specifically, 50:1 is different from 100:1, 250:1, and 500:1. 100:1 is also different from 500:1. In order to determine which molar ratio is "optimum," it is important to define what is desired from the experiment. If 100:1 and 250:1 produce results that are not statistically different, it may be best to use the 100:1 for financial purposes, which would require 2.5x less H_2O_2. Conversely, if 100:1 and 500:1 produce statistically significant different results, it may make most sense to use 500:1 and achieve better overall DNAN degradation. It is important to note, however, that the higher k_s from 1000:1 Trial 3 may be an anomaly. If not treated as an anomaly, then it is not statistically different than 50:1, even though, as shown in Figure 10, 1000:1 achieved greater overall degradation. 50:1

and 1000:1 are not statistically different because of the large degree of variance within the three 1000:1 trials. When all trials are analyzed in this manner, an ideal molar ratio can be selected based on desired criteria. If maximum degradation is a priority, 1000:1 may be best, although the large degree of variance may not always produce the desired results. In that case, 250:1 may be the best ratio of those tested. It produced results only slightly inferior to 500:1, but used half the H_2O_2. If this model were scaled to a large water treatment plant with continuous flow, savings on H_2O_2 could be significant. In order to determine if the k_s of 0.038 is truly and outlier, repeat experiments of the 1000:1 ratio should be conducted.

Table 1. *t*-Test.

Comparison	Margin of error	Lower Bound	Upper Bound	Significant?
50 - 100	0.005	-0.011	-0.001	Y
50 - 250	0.006	-0.017	-0.006	Y
50 - 500	0.002	-0.016	-0.011	Y
50 - 1000	0.019	-0.034	0.005	N
100 - 250	0.007	-0.013	0.001	N
100 - 500	0.005	-0.013	-0.003	Y
100 - 1000	0.020	-0.029	0.011	N
250 - 500	0.006	-0.007	0.004	N
250 - 1000	0.020	-0.023	0.017	N
500 - 1000	0.019	-0.021	0.018	N

If the k_s value of 0.038 for 1000:1 Trial 3 is assumed to be an error due to improper mixing or another reason, the data point could be removed and the data reanalyzed with a *t*-test. This can be evaluated using Dixon's Q-Test as shown in Equation 3, which allows for rejection of outliers. Dixon's Q-Test will work with only three data points, however, if two of those data points are the same, this will result in the rejection of the third data point, as long as it is not the same as the previous two. For instance, values of 0.026, 0.026, and 0.027 would indicate the rejection of 0.027, even

though this is very likely an accurate data point. Thus, this test will not work to exclude 0.038 from the data set.

Equation 3: Dixon's Q-Test

$$Q = \frac{Gap}{Ramge} = \frac{x_2 - x_1}{x_n - x_1}$$

Where x_1 is the smallest (suspect) value,
x_2 is the second smallest value,
x_n is the largest value.

For the purposes of this statistical analysis, the 0.038 data point will be temporarily removed for further analysis. Table 2 shows the results of a *t*-test with 1000:1 k_s of 0.038 removed, leaving only 0.026 and 0.026. When analyzed in this manner, the statistical differences between molar ratios remain similar, except 50:1 now has a statistically significant difference than 1000:1. Once the 0.038 data point is removed from the 1000:1 trials, the average k_s becomes 0.026. Figure 11 shows that when analyzed in MATLAB, 1000:1 achieves less degradation than 250:1 and 500:1, with 500:1 achieving the most degradation, although only slightly greater than 250:1. By this method of analysis, 250:1 would be the optimal of the five molar ratios tested because it uses half the H_2O_2 of 500:1 and achieves similar results.

Table 2: *t*-Test With k_s of .038 Removed as a Data Point

Comparison	Margin of error	Lower Bound	Upper Bound	Significant?
50 - 100	0.005	-0.011	-0.001	Y
50 - 250	0.006	-0.017	-0.006	Y
50 - 500	0.002	-0.016	-0.011	Y
50 - 1000	0.002	-0.012	-0.009	Y
100 - 250	0.007	-0.013	0.001	N
100 - 500	0.005	-0.013	-0.003	Y
100 - 1000	0.005	-0.010	0.000	N
250 - 500	0.006	-0.007	0.004	N
250 - 1000	0.006	-0.005	0.007	N
500 - 1000	0.002	0.001	0.004	N

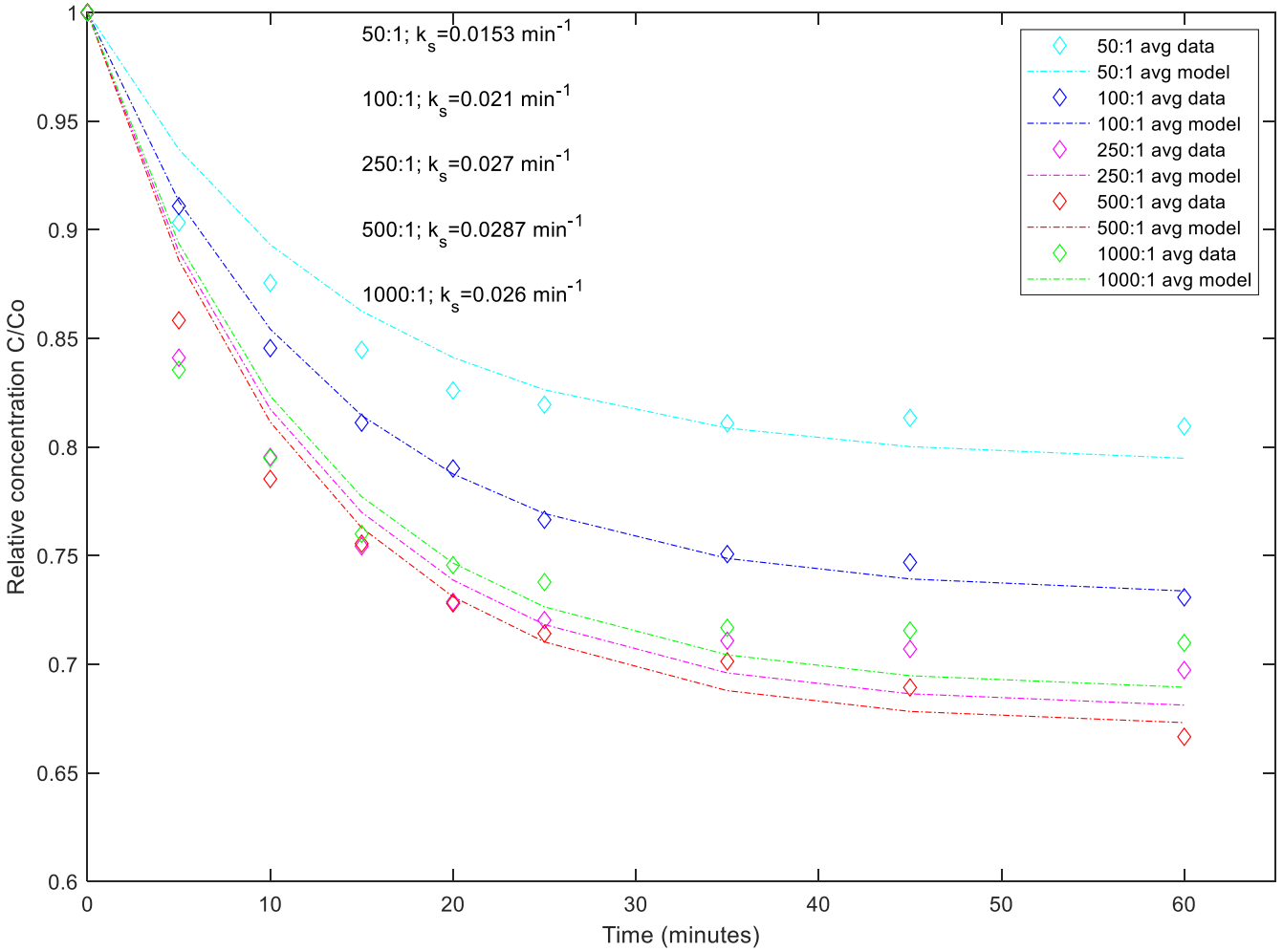

Figure 11: Average DNAN Removal With 1000:1 k_s .038 Removed

A regression analysis, as depicted in Figure 12, was conducted using linear and quadratic models. The blue line depicts a linear analysis which does not fit the data well and has an r^2 value of 0.694. This is expected as previous studies have shown that excess H_2O_2 can increase hydroxyl radical scavenging and thus cause degradation to eventually decrease when a threshold concentration is reached (Su et al., 2019; Yang et al., 2018). The red line depicts a quadratic model with the curve forced through the origin in order to best match the results of near 0.0 k_s (min^{-1}) when there is no H_2O_2 present. This model produces a favorable r^2 value of 0.903, however, a visual analysis makes it clear that this model grossly underestimates k_s values when H_2O_2: DNAN ratios are below 250:1 and overestimates when ratios are above 500:1. The green line represents another quadratic model without forcing the curve through the origin. This model produces an r^2 value of 0.701, however a visual analysis shows that it appears to fit the data better than both the linear model and the quadratic model when forced through the origin. This model produces slight underestimations of k_s when H_2O_2: DNAN ratios are below 250:1 and begins to overestimate when above 500:1. None of the regression models that were analyzed provided a good fit to the data which limits the models use for predicting results. Because of this, further work should be conducted in order to identify a better model that lends itself to accurate predictions across a range of H_2O_2: DNAN ratios.

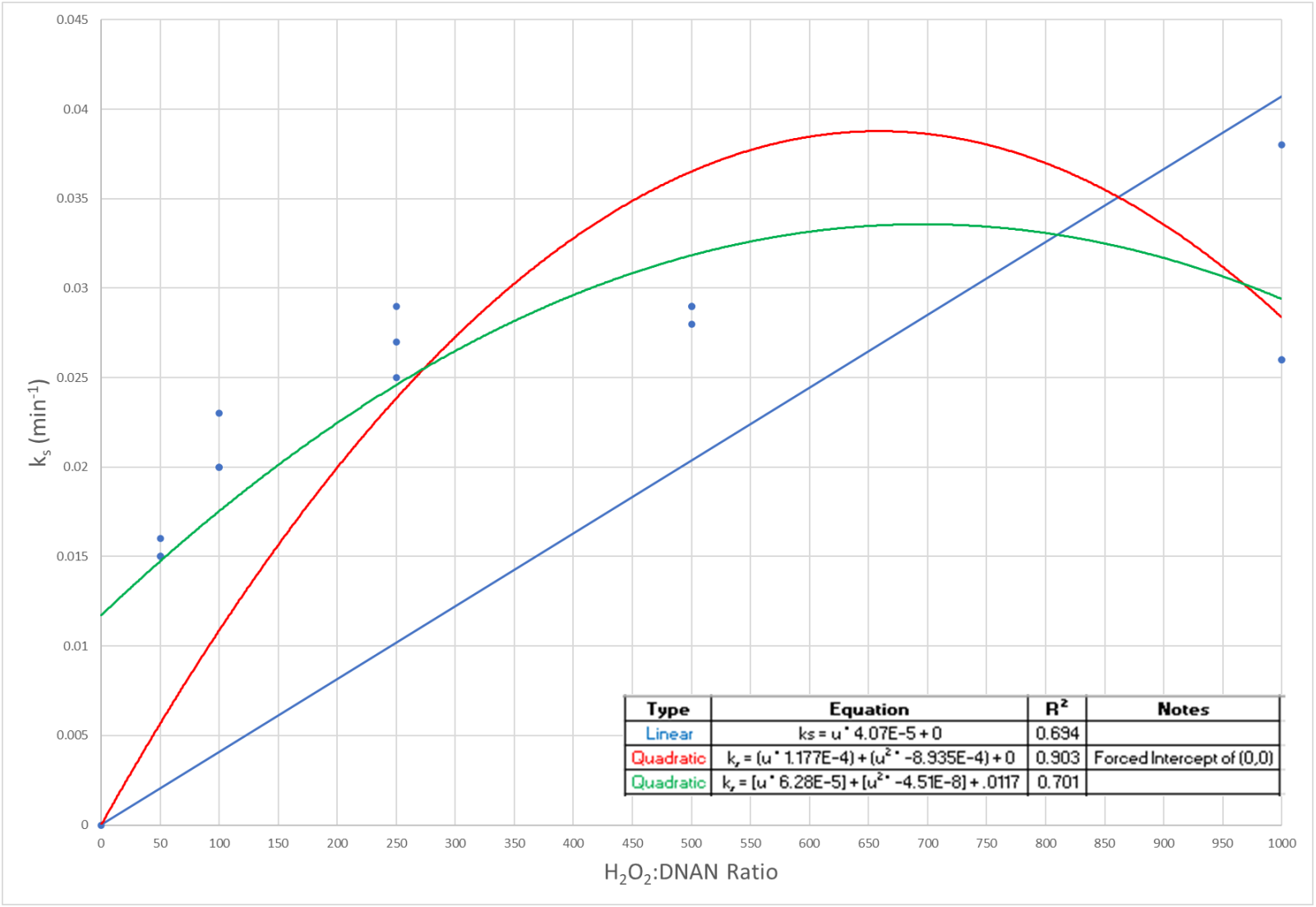

Figure 12: Linear and Quadratic Regression Analysis

4.3 Results Comparison with Related Works

Searcy (2020) conducted similar experiments, with the main exception that he did not include casamino acids as a co-contaminant. The molar ratios and methodology were nearly identical for his experiments. The k_s for 50:1 H_2O_2: DNAN were 0.019, 0.18, and 0.017. The k_s for 100:1 H_2O_2: DNAN were 0.025, 0.022, and 0.023. The k_s for 250:1 H_2O_2: DNAN were 0.032, 0.029. and 0.031. The k_s for 500:1 H_2O_2: DNAN were 0.033, 0.029, and 0.034. The k_s for 1000:1 H_2O_2: DNAN were 0.024, 0.024, and 0.022. The 1000:1 experiment had a trial with a k_s of 0.033 that was rejected. Searcy's average k_s for 50:1, 100:1, 250:1, 500:1, and 1000:1 (after outlier rejection) were 0.018, 0.023, 0.031, 0.032, and 0.023, respectively. The average k_s for Searcy's 50:1, 100:1, 250:1, and 500:1 H_2O_2: DNAN ratios had higher degradation than this experiment. Figure 13 displays Searcy's average DNAN degradation (Searcy, 2020). Searcy's k_s for 1000:1 H_2O_2: DNAN had higher degradation, but only if the 0.038 data point from this experiment is excluded (Searcy, 2020). When analyzed in this manner, the data from Searcy's experiment follows a similar pattern as this study, except Searcy experienced more degradation. The slightly increased degradation reported by Searcy may be attributed to the lack of a co-contaminant in his DNAN solutions. This agrees with previous studies that offer co-contaminants may have an inhibitory effect on UV AOPs (Hoigné, 1998; Yang et al., 2018).

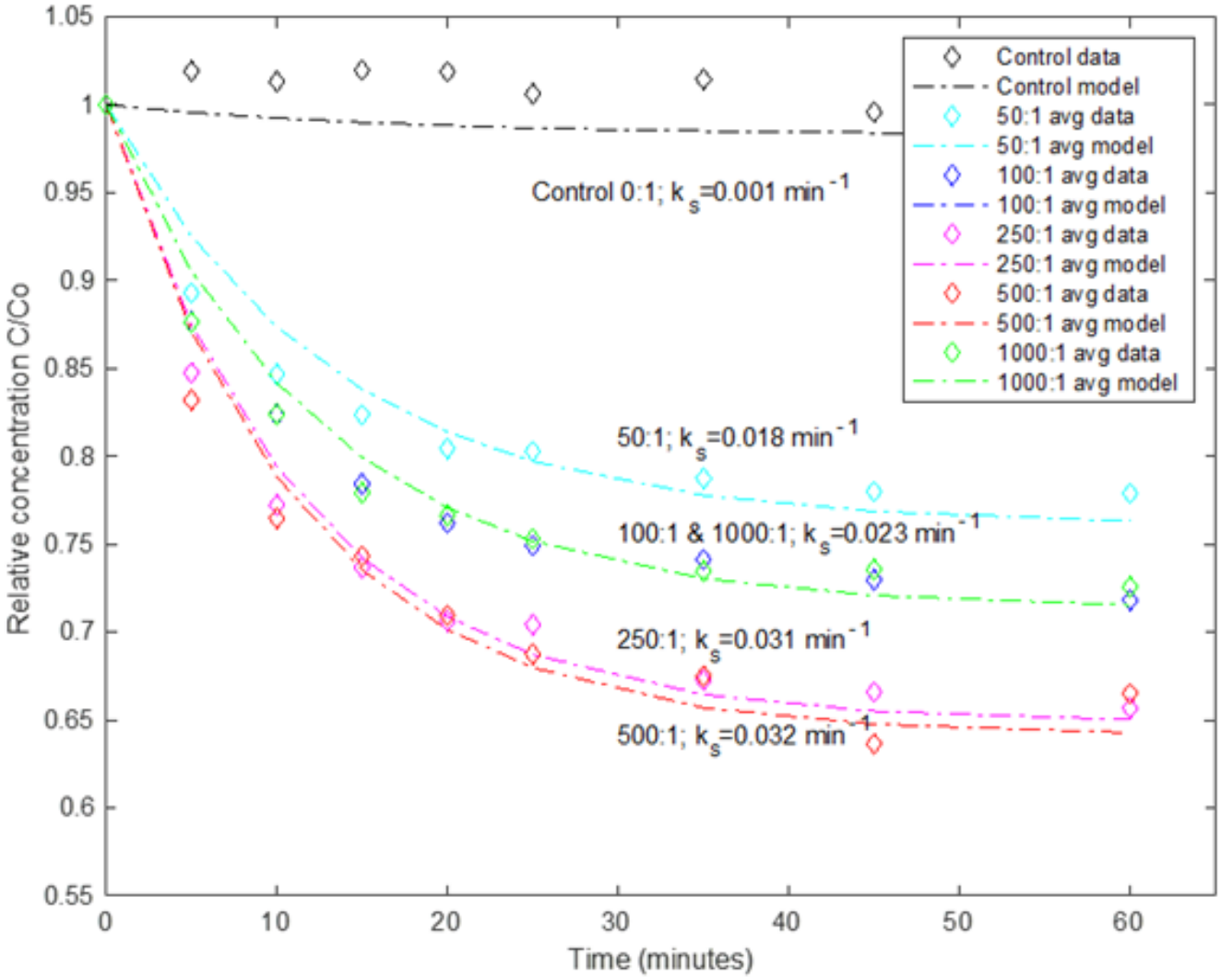

Figure 13: Searcy's Average DNAN Degradation in UV LED AOP (Searcy, 2020)

A statistical comparison of this study and Searcy's work was conducted. The boxplot depicted in Figure 14 indicates that when all experiments are grouped by H_2O_2: DNAN ratios, only one outlier exists, which is the 1000:1 H_2O_2: DNAN ratio experiment from this study with a k_s of 0.038. A simple visual analysis, depicted in Figures 15-18 show that the k_s and C/C_0 values (individual and average) for both studies are similar.

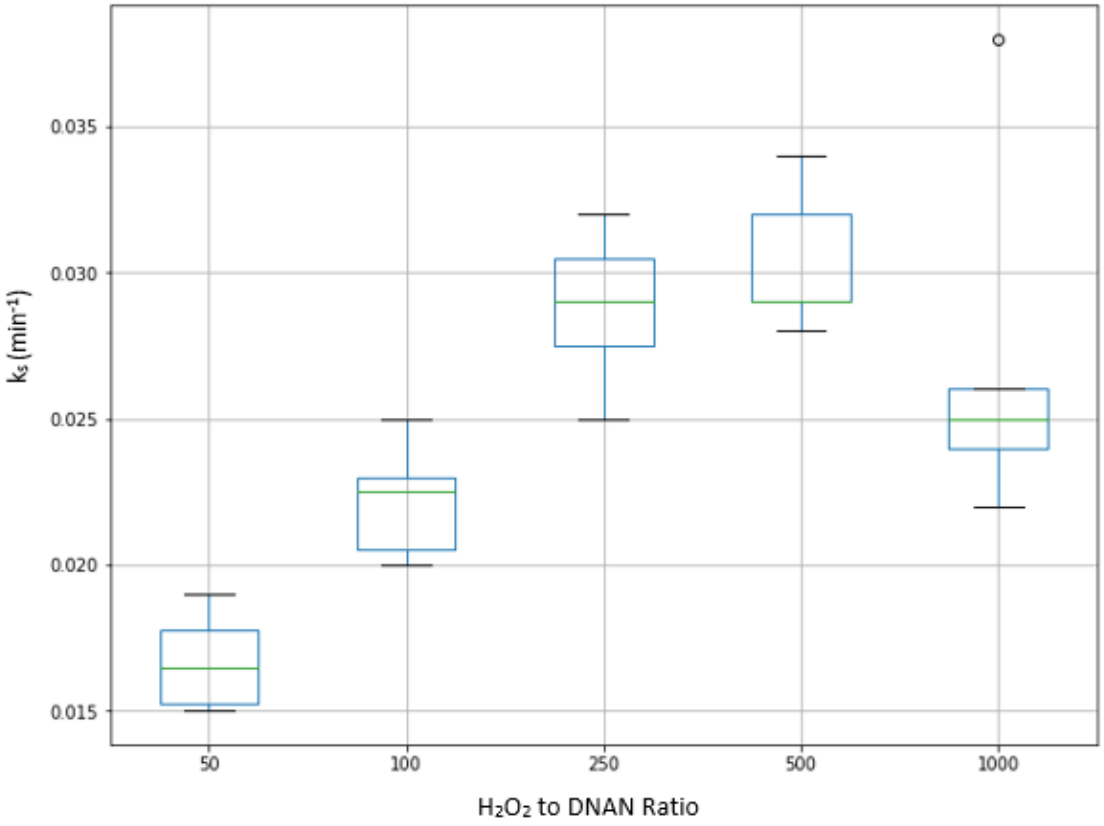

Figure 14: Boxplot of Hart and Searcy k_s Values

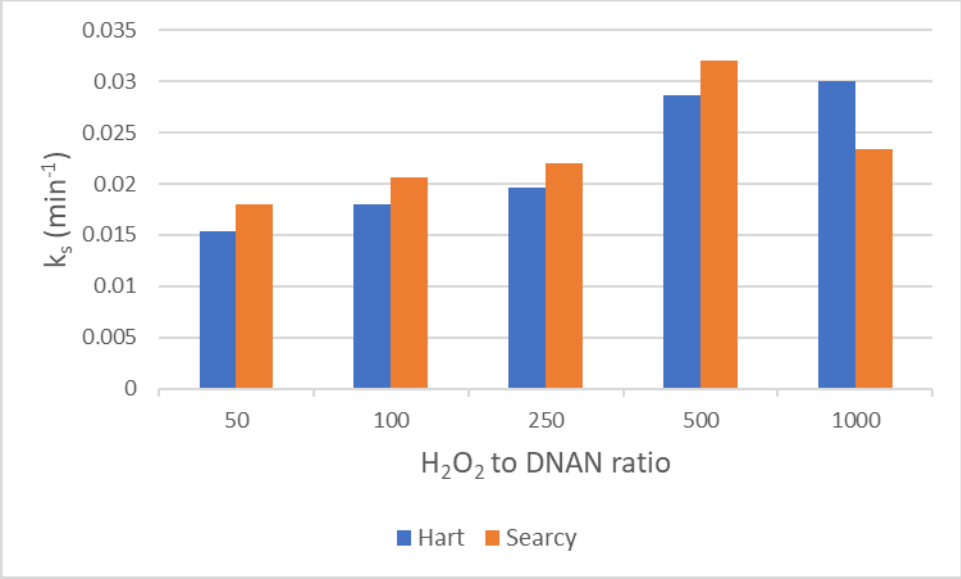

Figure 15: Comparison of Hart and Searcy Average k_s Values

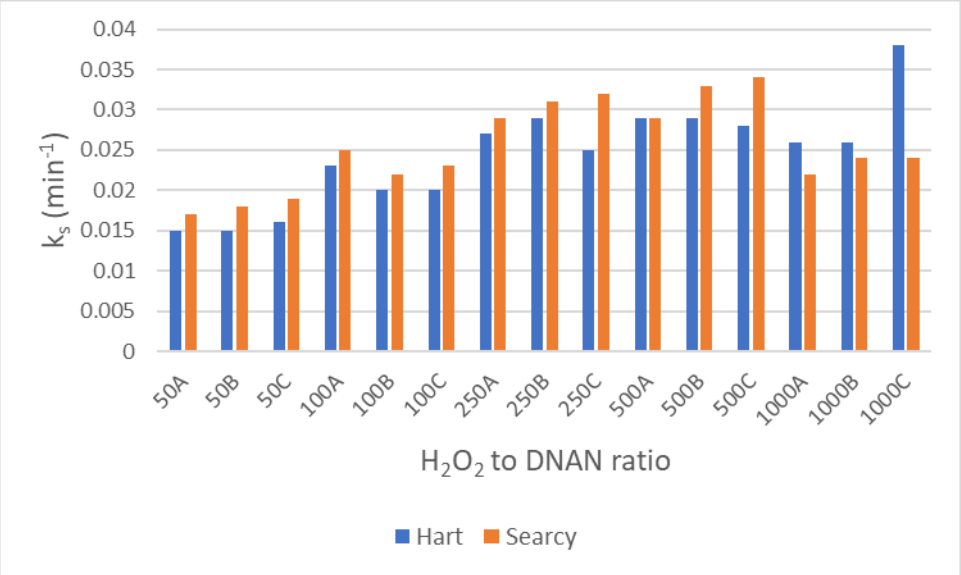

Figure 16: Comparison of Hart and Searcy k_s Values

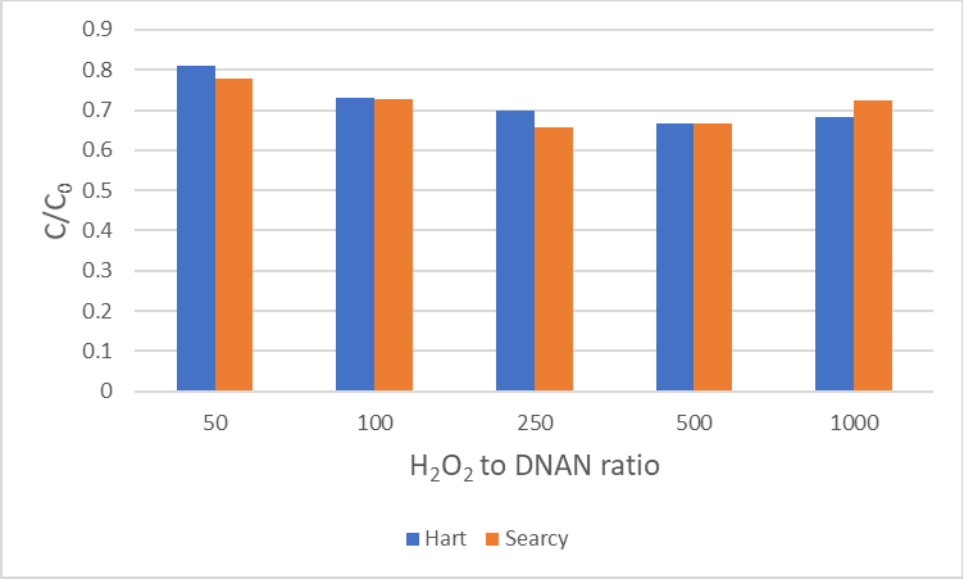

Figure 17: Comparison of Hart and Searcy Average Final C/C_0 Values

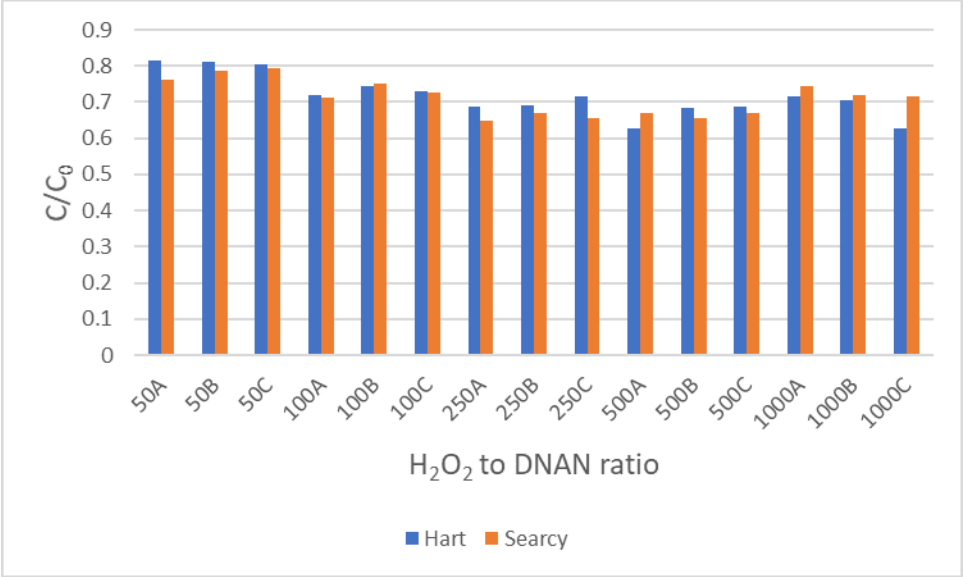

Figure 18: Comparison of Hart and Searcy Final C/C_0 Values

Further analysis was conducted to determine if the presence of casamino acids from this study caused a statistically significant different effect than the k_s values observed by Searcy. In order to do this, the assumption that both experiments were the same needs to be established. It is possible that slight undetected variations in technique occurred, however, the selected methodology, equipment, and procedures were nearly

identical. Thus, it is assumed the experiments were the same except for the use of casamino acids in this study. A one-way ANOVA was conducted for each molar ratio with researcher (Hart or Searcy) as treatments and k_s as the response at a significance level of 0.05 in order to determine if the presence of casamino acids had an effect on k_s values. Table 3 depicts the one-way ANOVA which indicates that only 50:1 H_2O_2: DNAN differed at a statistically significant level. Thus, it appears casamino acids only had a statistically significant effect at the 50:1 H_2O_2: DNAN level. While the majority of experiments conducted in this study had lower k_s values, only one H_2O_2: DNAN ratio was significant. It is plausible that because there is less H_2O_2 available in the 50:1 experiment, that the casamino acids have an increased inhibitory effect on the degradation of DNAN due to radical scavenging or light screening effects. It is also possible that casamino acids have a slight effect at higher ratios (100:1, 250:1, 500:1, and 1000:1), but the effect is not enough to be of statistical significance, perhaps because of its inability to scavenge enough radicals or screen enough light.

Table 3: One-Way ANOVA of Hart and Searcy k_s Values for Each Molar Ratio

Treatment	sum_sq	dd	F	PF(>F)
C(mr50researcher)	0.000011	1	16	0.01613
Residual	0.000003	4	NaN	NaN
C(mr100researcher)	0.000008	1	3.0625	0.15502
Residual	0.000011	4	NaN	NaN
C(mr250researcher)	0.00002	1	6.36842	0.06511
Residual	0.000013	4	NaN	NaN
C(mr500researcher)	0.000017	1	4.54546	0.09998
Residual	0.000015	4	NaN	NaN
C(mr1000researcher)	0.000067	1	2.7027	0.17552
Residual	0.000099	4	NaN	NaN

Yang et al. (2018) reported increased DNAN degradation in a UV/H2O2 AOP when H_2O_2 was increased from 2 mM to 5 mM (50:1 and 125:1 H_2O_2: DNAN ratio), but saw decreased performance when increased to 10 mM (250:1 H_2O_2: DNAN ratio). This report saw increased degradation from 2 mM to 20 mM, with the best results from 10 mM and 20 mM (250:1 and 500:1 H_2O_2:DNAN ratio). While it is a different system, it is important to compare the results of the AOP in this study to those of the UV/PS used by Yang for selecting optimum conditions for future experiments. The UV/PS used by Yang reactor yielded pseudo first-order rate constants up to 0.0189 min^{-1} (Yang et al., 2018). This study achieved higher pseudo-first order rate constants of 0.028 min^{-1}.

Su et al. (2019) reported optimal conditions at 70:1 H_2O_2: DNAN ratio which, when processed in MATLAB ® software, yields a rate constant of .0097 min^{-1}. Su et al. (2019) used a batch reactor vice a CFSTR which may explain the difference in results. Their reactor used an 800 ml solution of DNAN which has significantly higher overall volume than the reactor in this experiment. Additionally, the reactor used by Su et al. (2019) used a single 254 nm LSE Lighting UV Bulb which may account for further differences. It is not known if the bulb used by Su et al. (2019) was an LED or another style.

4.4 Potential Byproducts

Several potential byproducts were detected via mass spectrometry analysis. Mass spectrometry chromatograms (Appendix G) show profiles that were used for potential byproduct identification. Nitrobenzene +CN was a potential byproduct detected during chromatogram analysis for 100:1, 250:1, 500:1, and 1000:1 experiments with a retention

time of 0.371 to 0.382 min and an atomic mass of 146. Potential byproducts with a retention time of 1.164 and an atomic mass of 240 were also detected in 100:1 and 250:1 chromatograms. Potential byproducts with a retention time of 0.376 to 0.377 min and atomic mass of 192 were detected in 250:1 and 1000:1 chromatograms.

4.5 Investigative Questions Answered

The first investigative question asked how molar peroxide ratios affect the degradation of DNAN and the hypothesis proposes that molar peroxide ratio has a has a significant effect on the degradation of DNAN. This hypothesis is supported by the results and analysis of this experiment. Specifically, results show a non-linear removal of DNAN under all experimental conditions with molar peroxide ratios exhibiting a strong influence on reactor performance and degradation of DNAN. This study showed optimal DNAN removal at 250:1 and 500:1 H_2O_2: DNAN ratio with an average pseudo first-order rate constant (k_s) of 0.027 and 0.0287, respectively.

The second investigative question asks how the presence of casamino acids will affect the degradation of DNAN and the associated hypothesis was that casamino acids will impact the degradation process. As demonstrated by Hoigne (1998), nearly all dissolved organic compounds in water create a detrimental effect on the degradation of target compounds. When compared to Searcy's (2020) work, which is very similar to this work except it lacked a co-contaminant, it suggests that Searcy achieved slightly better overall degradation. The presence of casamino acids appear to have a slight inhibitory effect on the degradation of DNAN in this study, however, it was only statistically significant at the 50:1 H_2O_2: DNAN ratio.

V. Conclusions and Recommendations

5.1 Chapter Overview

The chapter provides the results of this study and any conclusions that were determined from the research. The broader significance of this research is also analyzed and recommendations for future research and work are presented.

5.2 Conclusions of Research

The relative concentration of DNAN (C/C_0) was reduced from 1.0 to 0.6259 (maximum value) over the range of selected molar peroxide ratios selected for this study with greatest degradation typically between 250:1 and 500:1 H_2O_2:DNAN ratios. 1000:1 H_2O_2:DNAN ratio had high levels of variance and its results should be treated as such.

Casamino acids as a co-contaminant had slight impacts on DNAN degradation, albeit they were only significant at the 50:1 H_2O_2:DNAN ratio. When compared to Searcy (2020), this study showed similar patterns, albeit with less overall degradation. The reduced k_s values in this study are likely the results of •OH removal by the casamino acids.

Chemical byproduct analysis suggests that Nitrobenzene +CN was created.

5.3 Significance of Research

This study explains the effect of molar peroxide ratios on the pseudo first-order rate constant of DNAN in an UV LED AOP. This research shows that an ideal molar peroxide ratio can be selected for DNAN degradation. Additionally, the impact of SMPs on DNAN degradation in a UV LED AOP was analyzed. This is significant, because

SMPs are commonly found in wastewater secondary effluent, and can negatively influence treatment plans.

The influence of molar peroxide ratios and co-contaminants such as casamino acids are significant findings. Little research has been conducted on the effect of co-contaminants on the degradation of DNAN in an AOP. Additionally, there is limited research on the reduction of DNAN in a UV LED AOP. By studying AOPs and how they are influenced by influent conditions, ideal conditions and parameters can be developed and applied to future water treatment systems.

AOPs that are used to treat water contaminated with DNAN, and possibly other co-contaminants, have the potential to create effluent that contains toxic compounds (Munter, 2001; Stocking et al., 2000). Understanding the mechanisms of degradation and structures of byproducts is important to future water treatment studies. Water treatment plans may need additional treatment beyond the AOP to create effluent that meets the criteria for its desired use.

5.4 Recommendations for Future Research

Future research should consider conducting further experiments to identify the optimal molar peroxide ratios for DNAN degradation and a model that can be used to predict k_s values. Conducting more trials at each ratio would allow for more confidence when conducting statistical analysis. Furthermore, repeat experiments at the 1000:1 H2O2: DNAN ratio should be conducted to determine if the suspected outlier in this study is actually a valid data point. Additionally, future experiments could explore the impacts of higher concentrations of casamino acids on the degradation of DNAN.

Future studies should also focus on the impacts of other co-contaminants, particularly SMPs that are likely to react with hydroxyl radicals such as phenolics or high molecular weight organics, in an UV LED AOP. Specifically, solutions of a variety of co-contaminants commonly found in secondary water treatment effluent may have dramatic effects on the degradation of the target contaminant. Additionally, these co-contaminants may have an effect on long term UV LED performance because of staining or scaling and warrant further research. Future research may also benefit from increasing the scale of the experiment to better simulate actual operating conditions expected with wastewater secondary treatment effluent.

5.5 Summary

Wastewater treatment plays an extremely important role in society and is critical to the safe manufacture of a variety of explosives used by the DoD. UV LED AOPs are a promising approach to treating a variety of chemicals that are present in may wastewater systems. This study demonstrated that a UV LED/H_2O_2 AOP of DNAN is significantly affected by altering the molar peroxide ratio of H_2O_2:DNAN. Additionally, the addition of 1 mg/L casamino acids as a co-contaminant had little effect on DNAN degradation, and was only statistically significant at the 50:1 H_2O_2:DNAN ratio. Future research can be conducted to optimize k_s values in the presence of co-contaminants.

Appendix A: AOP Experiment Schedule

Trial #	H2O2:DNAN	Date	Notes
1	0:1	5/29/2020	Control - No Casamino Acid or H_2O_2
2	100:1	6/5/2020	
3	100:1	6/12/2020	
4	100:1	6/19/2020	
5	500:1	6/26/2020	
6	500:1	7/2/2020	
7	500:1	7/16/2020	
8	1000:1	7/16/2020	
9	1000:1	7/23/2020	
10	1000:1	7/23/2020	Conducted immediately after Trial 9
11	0:1	7/30/2020	Control - Casamino Acids, no H2O2
12	250:1	8/6/2020	
13	250:1	8/6/2020	Conducted immediately after Trial 12
14	250:1	8/13/2020	
15	50:1	8/13/2020	Conducted immediately after Trial 14
16	50:1	8/20/2020	
17	50:1	8/20/2020	Conducted immediately after Trial 16

Appendix B: AOP Experiment Data

Trial	1	2	3	4	5	6	7	8	9	10	11	12	13	14	15	16	17
H_2O_2:DNAN Ratio	0:1	100:1	100:1	100:1	500:1	500:1	500:1	1000:1	1000:1	1000:1	0:1	250:1	250:1	250:1	50:1	50:1	50:1
Experiment Date	5/29/2020	6/5/2020	6/12/2020	6/19/2020	6/26/2020	7/2/2020	7/2/2020	7/16/2020	7/23/2020	7/23/2020	7/30/2020	8/6/2020	8/6/2020	8/13/2020	8/13/2020	8/20/2020	8/20/2020
DNAN Solution Prepared	5/26/2020	6/2/2020	6/9/2020	6/16/2020	6/23/2020	6/29/2020	6/29/2020	7/13/2020	7/20/2020	7/20/2020	7/27/2020	8/3/2020	8/3/2020	8/10/2020	8/10/2020	8/17/2020	8/17/2020
Calculated DNAN Conc (ppm)	10.009	10.016	10.016	10.011	10.001	10.000	10.011	10.009	10.005	10.007	10.004	10.001	10.004	10.001	10.015	10.003	10.001
pH	6.531	6.198	6.745	6.711	7.094	7.079	6.682	6.932	6.238	6.140	6.248	5.177	5.188	5.365	5.232	5.197	5.232
H_2O_2 Vol (µl)	0	128	128	128	638	638	638	1276	1276	1276	0	319	319	319	64	64	64
Avg C_0	9.451	9.583	9.358	9.495	9.607	9.189	9.326	9.301	9.558	9.642	9.568	9.598	9.736	9.547	9.546	9.555	9.646
Control Sample Time (min)	PPM																
0	9.431	9.576	8.292	8.721	9.179	8.799	9.015	9.158	9.131	9.406	9.126	9.203	9.689	9.151	9.322	9.260	9.478
10	-	9.678	9.440	9.590	9.606	9.168	9.227	9.489	9.662	9.639	9.675	9.531	9.686	9.491	9.520	9.554	9.639
20	9.508	9.565	9.528	9.636	9.665	9.676	9.375	9.396	9.700	9.658	9.590	9.559	9.745	9.697	9.583	9.643	9.668
30	-	9.610	9.525	9.557	9.672	9.173	9.484	9.322	9.569	9.617	9.778	9.588	9.639	9.677	9.579	9.680	9.706
40	9.407	9.583	9.526	9.609	9.688	9.012	9.332	9.223	9.648	9.703	9.634	9.714	9.879	9.613	9.637	9.625	9.654
50	-	9.493	9.606	9.657	9.684	9.272	9.474	9.179	9.583	9.711	9.579	9.888	9.807	9.563	9.602	9.532	9.688
60	9.456	9.578	9.588	9.692	9.755	9.220	9.378	9.339	9.615	9.759	9.597	9.703	9.709	9.639	9.582	9.593	9.687
Experiment Sample Time (min)	C/C_0																
5	0.993	0.894	0.920	0.919	0.861	0.866	0.848	0.841	0.831	0.764	1.008	0.846	0.832	0.845	0.900	0.909	0.902
10	0.994	0.827	0.854	0.856	0.814	0.767	0.775	0.795	0.794	0.706	1.011	0.795	0.786	0.806	0.891	0.870	0.866
15	0.988	0.786	0.822	0.825	0.756	0.757	0.754	0.751	0.769	0.681	1.006	0.770	0.730	0.763	0.837	0.849	0.848
20	0.996	0.775	0.791	0.804	0.743	0.711	0.730	0.735	0.756	0.668	1.005	0.731	0.719	0.737	0.828	0.834	0.816
25	0.993	0.752	0.765	0.782	0.721	0.706	0.715	0.728	0.748	0.653	1.003	0.715	0.709	0.736	0.816	0.826	0.817
35	0.992	0.732	0.755	0.765	0.691	0.699	0.714	0.713	0.721	0.645	0.998	0.710	0.695	0.728	0.805	0.821	0.807
45	0.985	0.732	0.750	0.759	0.685	0.690	0.693	0.722	0.709	0.639	1.001	0.701	0.691	0.729	0.812	0.821	0.808
60	0.988	0.719	0.744	0.729	0.629	0.683	0.688	0.714	0.706	0.626	1.007	0.686	0.691	0.715	0.814	0.811	0.803

Data File Name	
DNAN Prepared	5/26/2020
DNAN Conc (mg/L or ppm)	10.0093
pH	6.531
H2O2 Vol (µl)	0
CAS weight (g)	0
CAS Vol (µl)	0
Start Setup	N/A
Start Control	N/A
Stop Experiment	N/A
Ran in HPLC	

Notes
This is the first control experiment. Conducted without H2O2, so we don't expect to see any degradation. There also weren't any Casamino acids, so we may need to conduct another control later with DNAN, CAS, and no H2O2.

Calibration Curve

Concentration (%)	Concentration (ppm)	RT (min)	Area (meas. @ 253 nm)
0.0000	0.0000		0.0
10.0000	1.0009	1.154	77.5
20.0000	2.0019	1.151	149.7
40.0000	4.0037	1.151	299.9
60.0000	6.0056	1.151	441.2
80.0000	8.0074	1.153	594.1
100.0000	10.0093	1.15	747.9
Slope	0.1345		
y-intercept	-0.0992		

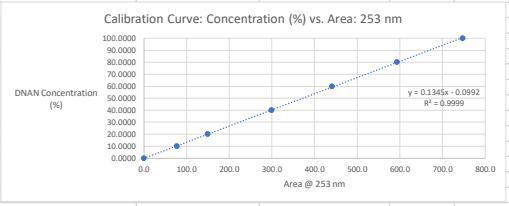

Control # 1: No H2O2, No UV Light

HPLC Type	Sample Time (min)	Concentration (%)	Concentration (ppm)	RT (min)	Area (meas. @ 253 nm)	C_o = Avg Ctrl Conc. (ppm)
C1	0	94.2257	9.4313	1.150	701.3	9.4505
C2	20	94.9923	9.5081	1.151	707.0	
C3	40	93.9836	9.4071	1.148	699.5	
C4	60	94.4678	9.4556	1.151	703.1	

Experiment: No H2O2, With UV Light applied

		DNAN				Byproducts		
HPLC Type	Sample Time (min)	Concentration (%)	Concentration (ppm)	RT (min)	Area (meas. @ 253 nm)	RT (min)	Area (meas. @ 253 nm)	Mass Ratio (C_n / C_o)
C_o (starting Conc)	0		9.4505					1.0000
R1	5	93.7146	9.3802	1.151	697.5			0.9926
R2	10	93.8894	9.3977	1.151	698.8			0.9944
R3	15	93.2573	9.3344	1.153	694.1			0.9877
R4	20	94.0105	9.4098	1.151	699.7			0.9957
R5	25	93.7953	9.3882	1.150	698.1			0.9934
R6	35	93.6877	9.3775	1.153	697.3			0.9923
R7	45	92.9883	9.3075	1.150	692.1			0.9849
R8	60	93.2842	9.3371	1.150	694.3			0.9880

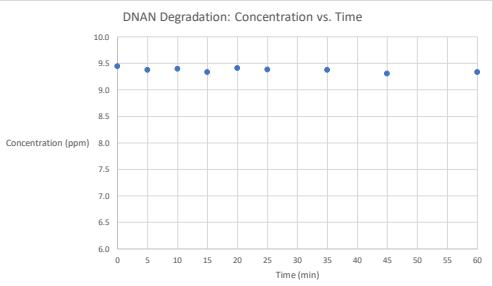

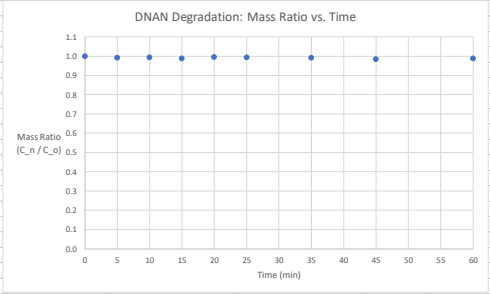

Quality Control Checks: QC 60%

Line	Area	Relative Error (< 10%)
9	445.7	1.0199
17	451.5	2.3345
26	444.7	0.7933

Data File Name			**Notes**							
DNAN Prepared	6/2/2020									
DNAN Conc (mg/L or ppm)	10.016									
pH	6.198									
H2O2 Vol (µl)	128									
CAS weight (g)	0.2556									
CAS Vol (µl)	98									
Start Setup	N/A									
Start Control	N/A									
Stop Experiment	N/A									
Ran in HPLC										

Calibration Curve

		Concentration (%)	Concentration (ppm)	RT (min)	Area (meas. @ 253 nm)
		0.0000	0.0000	0.000	0.0
		10.0000	1.0016	1.112	83.9
		20.0000	2.0032	1.111	154.6
		40.0000	4.0064	1.112	290.4
		60.0000	6.0096	1.109	436.3
		80.0000	8.0128	1.112	581.6
		100.0000	10.0160	1.112	727.1
		Slope	0.1389		
		y-intercept	-0.8294		

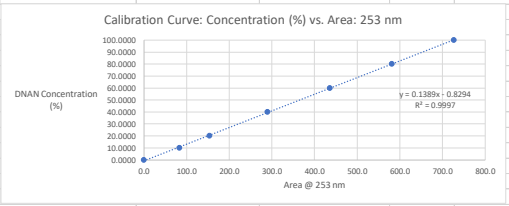

Control Experiment

HPLC Type	Sample Time (min)	Concentration (%)	Concentration (ppm)	RT (min)	Area (meas. @ 253 nm)	C_o = Avg Ctrl Conc. (ppm)
C1	0	95.6089	9.5762	1.110	694.3	9.5831
C2	10	96.6228	9.6777	1.109	701.6	
C3	20	95.4978	9.5651	1.110	693.5	
C4	30	95.9422	9.6096	1.110	696.7	
C5	40	95.6783	9.5831	1.111	694.8	
C6	50	94.7755	9.4927	1.112	688.3	
C7	60	95.6228	9.5776	1.110	694.4	

Experiment: 100:1 (1 of 3)

		DNAN				Byproducts		
HPLC Type	Sample Time (min)	Concentration (%)	Concentration (ppm)	RT (min)	Area (meas. @ 253 nm)	RT (min)	Area (meas. @ 253 nm)	Mass Ratio (C_n / C_o)
C_o (starting Conc)	0		9.5831					1.0000
R1	5	85.4970	8.5634	1.109	621.5			0.8936
R2	10	79.1353	7.9262	1.110	575.7			0.8271
R3	15	75.2045	7.5325	1.110	547.4			0.7860
R4	20	74.1766	7.4295	1.107	540.0			0.7753
R5	25	71.9959	7.2111	1.110	524.3			0.7525
R6	35	70.0791	7.0191	1.108	510.5			0.7324
R7	45	70.0374	7.0149	1.111	510.2			0.7320
R8	60	68.7595	6.8870	1.108	501.0			0.7187

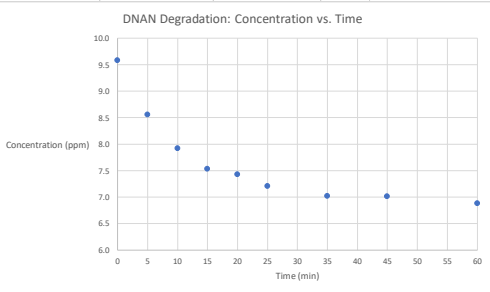

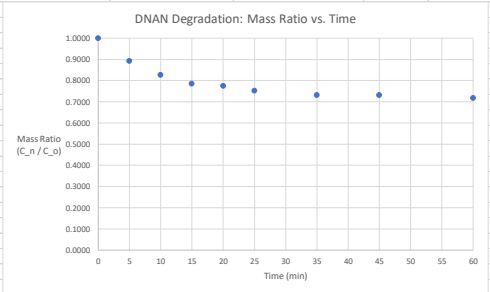

Quality Control Checks: QC 60%

Line	Area	Relative Error (< 10%)
9	438.9	0.5959
17	442.9	1.5127
27	439.6	0.7564

Data File Name			**Notes**							
DNAN Prepared	6/9/2020									
DNAN Conc (mg/L or ppm)	10.016									
pH	6.745									
H2O2 Vol (µl)	128									
CAS weight (g)	0.2529									
CAS Vol (µl)	99									
Start Setup	N/A									
Start Control	N/A									
Stop Experiment	N/A									
Ran in HPLC										

Calibration Curve

		Concentration (%)	Concentration (ppm)	RT (min)	Area (meas. @ 253 nm)
		0.0000	0.0000		0.0
		10.0000	1.0016	1.043	73.7
		20.0000	2.0032	1.047	157.0
		40.0000	4.0064	1.047	302.1
		60.0000	6.0096	1.059	446.7
		80.0000	8.0128	1.076	595.8
		100.0000	10.0160	1.084	747.0
		Slope	0.1344		
		y-intercept	-0.3002		

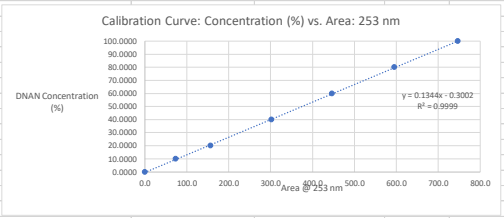

Control Experiment

HPLC Type	Sample Time (min)	Concentration (%)	Concentration (ppm)	RT (min)	Area (meas. @ 253 nm)	C_o = Avg Ctrl Conc. (ppm)
C1	0	82.7859	8.2918	1.094	618.2	9.3578
C2	10	94.2502	9.4401	1.095	703.5	
C3	20	95.1238	9.5276	1.098	710.0	
C4	30	95.0969	9.5249	1.102	709.8	
C5	40	95.1104	9.5263	1.102	709.9	
C6	50	95.9033	9.6057	1.107	715.8	
C7	60	95.7286	9.5882	1.111	714.5	

Experiment: 100:1 (2 of 3)

		DNAN				Byproducts		
HPLC Type	Sample Time (min)	Concentration (%)	Concentration (ppm)	RT (min)	Area (meas. @ 253 nm)	RT (min)	Area (meas. @ 253 nm)	Mass Ratio (C_n / C_o)
C_o (starting Conc)	0		9.3578					1.0000
R1	5	85.9443	8.6082	1.111	641.7			0.9199
R2	10	79.7484	7.9876	1.111	595.6			0.8536
R3	15	76.8320	7.6955	1.112	573.9			0.8224
R4	20	73.9289	7.4047	1.113	552.3			0.7913
R5	25	71.5097	7.1624	1.112	534.3			0.7654
R6	35	70.5152	7.0628	1.112	526.9			0.7548
R7	45	70.0716	7.0184	1.113	523.6			0.7500
R8	60	69.5475	6.9659	1.112	519.7			0.7444

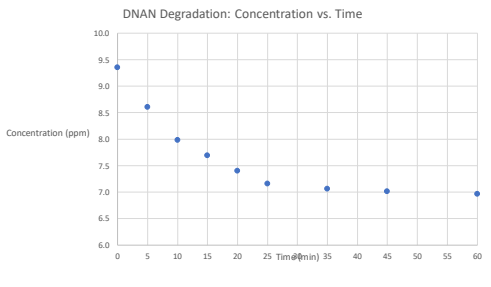

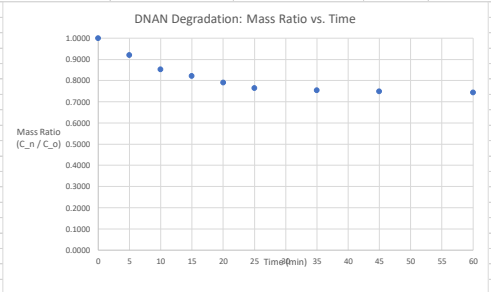

Quality Control Checks: QC 60%

Line	Area	Relative Error (< 10%)
9	443.4	0.7388
17	436.5	2.2834
27	434.6	2.7088

Data File Name	20200619_DNAN_JH
DNAN Prepared	6/16/2020
DNAN Conc (mg/L or ppm)	10.0106
pH	6.711
H2O2 Vol (µl)	128
CAS weight (g)	0.2506
CAS Vol (µl)	100
Start Setup	6:30
Start Control	8:30
Stop Experiment	10:45
Ran in HPLC	11:00

Notes

Calibration Curve

Concentration (%)	Concentration (ppm)	RT (min)	Area (meas. @ 253 nm)
0.0000	0.0000	0.000	0.0
10.0000	1.0011	1.134	74.6
20.0000	2.0021	1.132	150.6
40.0000	4.0042	1.134	305.3
60.0000	6.0064	1.134	445.2
80.0000	8.0085	1.134	586.3
100.0000	10.0106	1.132	737.2
Slope	0.1361		
y-intercept	-0.4251		

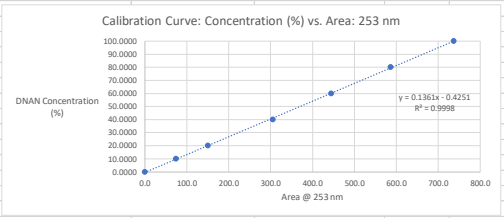

Control Experiment

HPLC Type	Sample Time (min)	Concentration (%)	Concentration (ppm)	RT (min)	Area (meas. @ 253 nm)	C_o = Avg Ctrl Conc. (ppm)
C1	0	87.1144	8.7207	1.137	643.2	9.4945
C2	10	95.7976	9.5899	1.136	707.0	
C3	20	96.2603	9.6362	1.136	710.4	
C4	30	95.4710	9.5572	1.135	704.6	
C5	40	95.9881	9.6090	1.134	708.4	
C6	50	96.4645	9.6567	1.134	711.9	
C7	60	96.8184	9.6921	1.135	714.5	

Experiment: 100:1 (3 of 3)

		DNAN				Byproducts		
HPLC Type	Sample Time (min)	Concentration (%)	Concentration (ppm)	RT (min)	Area (meas. @ 253 nm)	RT (min)	Area (meas. @ 253 nm)	Mass Ratio (C_n / C_o)
C_o (starting Conc)	0		9.4945					1.0000
R1	5	87.1961	8.7289	1.135	643.8			0.9194
R2	10	81.1805	8.1267	1.134	599.6			0.8559
R3	15	78.2815	7.8365	1.137	578.3			0.8254
R4	20	76.2264	7.6307	1.136	563.2			0.8037
R5	25	74.1305	7.4209	1.137	547.8			0.7816
R6	35	72.5381	7.2615	1.136	536.1			0.7648
R7	45	71.9665	7.2043	1.135	531.9			0.7588
R8	60	69.1764	6.9250	1.137	511.4			0.7294

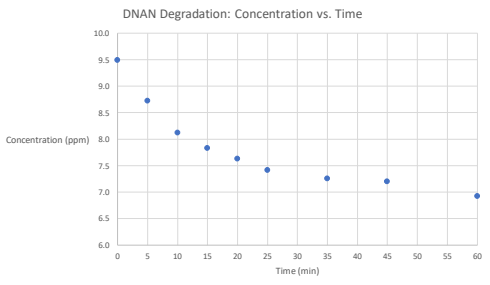

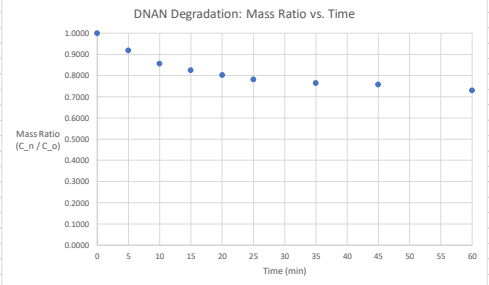

Quality Control Checks: QC 60%

Line	Area	Relative Error (< 10%)
9	441.8	0.7637
17	439.1	1.3702
27	442.4	0.6289

Data File Name	20200626A_DNAN_JH
DNAN Prepared	6/23/2020
DNAN Conc (mg/L or ppm)	10.0013
pH	7.094
H2O2 Vol (µl)	638
CAS weight (g)	0.2505
CAS Vol (µl)	100
Start Setup	6:19
Start Control	8:23
Stop Experiment	10:45
Ran in HPLC	11:00

Notes

DI water from tap not working. Used pre-made DI water.
New stir plate in use.

Calibration Curve

Concentration (%)	Concentration (ppm)	RT (min)	Area (meas. @ 253 nm)
0.0000	0.0000	0.000	0.0
10.0000	1.0001	1.129	76.1
20.0000	2.0003	1.128	151.0
40.0000	4.0005	1.128	295.8
60.0000	6.0008	1.131	440.7
80.0000	8.0010	1.129	587.8
100.0000	10.0013	1.134	735.6
Slope	0.1364		
y-intercept	-0.2887		

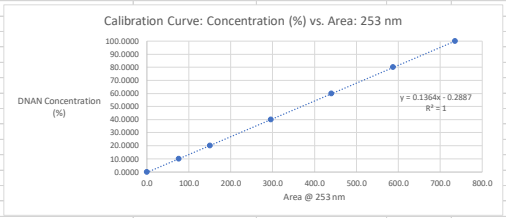

Control Experiment

HPLC Type	Sample Time (min)	Concentration (%)	Concentration (ppm)	RT (min)	Area (meas. @ 253 nm)	C_o = Avg Ctrl Conc. (ppm)
C1	0	91.7813	9.1793	1.131	675.0	9.6071
C2	10	96.0506	9.6063	1.131	706.3	
C3	20	96.6371	9.6650	1.131	710.6	
C4	30	96.7053	9.6718	1.132	711.1	
C5	40	96.8690	9.6882	1.132	712.3	
C6	50	96.8281	9.6841	1.132	712.0	
C7	60	97.5374	9.7550	1.132	717.2	

Experiment: 500:1 (1 of 3)

		DNAN				Byproducts		
HPLC Type	Sample Time (min)	Concentration (%)	Concentration (ppm)	RT (min)	Area (meas. @ 253 nm)	RT (min)	Area (meas. @ 253 nm)	Mass Ratio (C_n / C_o)
C_o (starting Conc)	0		9.6071					1.0000
R1	5	82.6698	8.2681	1.130	608.2			0.8606
R2	10	78.1413	7.8151	1.132	575.0			0.8135
R3	15	72.5898	7.2599	1.133	534.3			0.7557
R4	20	71.3895	7.1399	1.130	525.5			0.7432
R5	25	69.2753	6.9284	1.132	510.0			0.7212
R6	35	66.3563	6.6365	1.135	488.6			0.6908
R7	45	65.7835	6.5792	1.127	484.4			0.6848
R8	60	60.3820	6.0390	1.134	444.8			0.6286

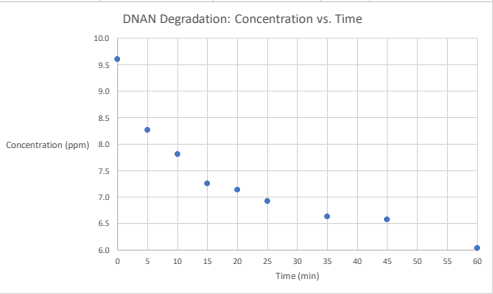

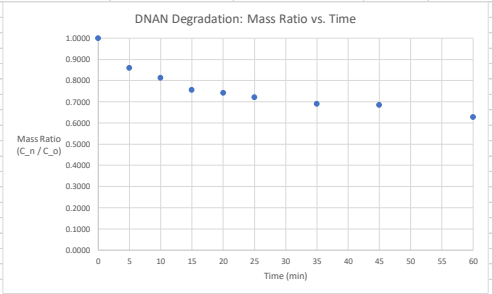

Quality Control Checks: QC 60%

Line	Area	Relative Error (< 10%)
9	437.1	0.8169
17	443.7	0.6807
27	438.6	0.4765

Data File Name	20200702_DNAN_A_JH
DNAN Prepared	6/29/2020
DNAN Conc (mg/L or ppm)	10.000
pH	7.079
H2O2 Vol (µl)	638
CAS weight (g)	0.2508
CAS Vol (µl)	100
Start Setup	4:30
Start Control	8:30
Stop Experiment	11:15
Ran in HPLC	14:00

Notes

Calibration Curve

Concentration (%)	Concentration (ppm)	RT (min)	Area (meas. @ 253 nm)
0.0000	0.0000	0.000	0.0
10.0000	1.0000	1.12	80.4
20.0000	2.0000	1.122	149.2
40.0000	4.0000	1.119	304.4
60.0000	6.0000	1.125	447.5
80.0000	8.0000	1.123	593.1
100.0000	10.0000	1.121	755.0
Slope	0.1337		
y-intercept	-0.2121		

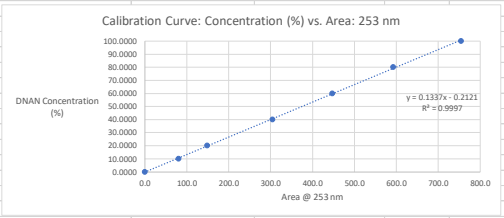

Control Experiment

HPLC Type	Sample Time (min)	Concentration (%)	Concentration (ppm)	RT (min)	Area (meas. @ 253 nm)	C_o = Avg Ctrl Conc. (ppm)
C1	0	87.9898	8.7990	1.124	659.7	9.1886
C2	10	91.6799	9.1680	1.122	687.3	
C3	20	96.7605	9.6761	1.125	725.3	
C4	30	91.7334	9.1733	1.125	687.7	
C5	40	90.1156	9.0116	1.123	675.6	
C6	50	92.7228	9.2723	1.123	695.1	
C7	60	92.2013	9.2201	1.124	691.2	

Experiment: 500:1 (2 of 3)

		DNAN				Byproducts		
HPLC Type	Sample Time (min)	Concentration (%)	Concentration (ppm)	RT (min)	Area (meas. @ 253 nm)	RT (min)	Area (meas. @ 253 nm)	Mass Ratio (C_n / C_o)
C_o (starting Conc)	0		9.1886					1.0000
R1	5	79.5801	7.9580	1.127	596.800			0.8661
R2	10	70.4885	7.0488	1.122	528.800			0.7671
R3	15	69.5272	6.9527	1.120	521.610			0.7567
R4	20	65.3673	6.5367	1.126	490.497			0.7114
R5	25	64.8886	6.4889	1.123	486.916			0.7062
R6	35	64.2179	6.4218	1.124	481.900			0.6989
R7	45	63.4024	6.3402	1.128	475.800			0.6900
R8	60	62.7740	6.2774	1.132	471.100			0.6832

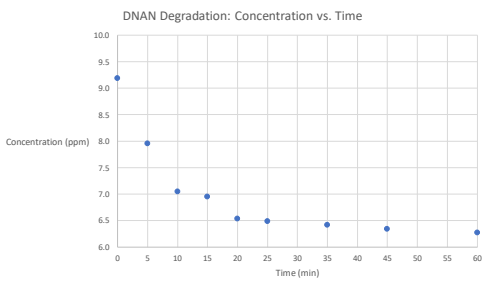

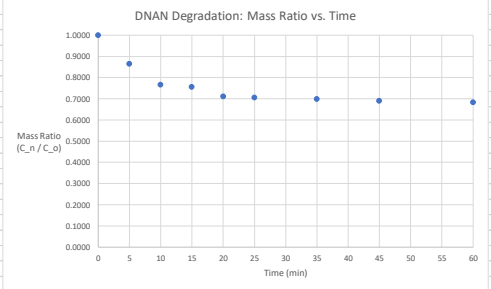

Quality Control Checks: QC 60%

Line	Area	Relative Error (< 10%)
9	447.4	0.0223
17	452.0	1.0056
27	444.7	0.6257

Data File Name	20200702_DNAN_B_JH
DNAN Prepared	6/29/2020
DNAN Conc (mg/L or ppm)	10.0107
pH	6.682
H2O2 Vol (µl)	638
CAS weight (g)	0.2508
CAS Vol (µl)	100
Start Setup	11:15
Start Control	11:30
Stop Experiment	13:40
Ran in HPLC	15:45

Notes

Conducted same day as 500:1 #2. Used separate batches of DNAN, same batch of CAS.

Calibration Curve

Concentration (%)	Concentration (ppm)	RT (min)	Area (meas. @ 253 nm)
0.0000	0.0000	0.000	0.0
10.0000	1.0011	1.126	78.9
20.0000	2.0021	1.128	145.6
40.0000	4.0043	1.126	295.6
60.0000	6.0064	1.127	438.7
80.0000	8.0085	1.128	591.4
100.0000	10.0107	1.128	745.7
Slope	0.1349		
y-intercept	0.0448		

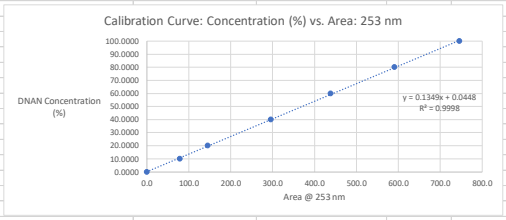

Control Experiment

HPLC Type	Sample Time (min)	Concentration (%)	Concentration (ppm)	RT (min)	Area (meas. @ 253 nm)	C_o = Avg Ctrl Conc. (ppm)
C1	0	90.0501	9.0146	1.125	667.2	9.3263
C2	10	92.1717	9.2270	1.127	682.9	
C3	20	93.6485	9.3748	1.128	693.9	
C4	30	94.7348	9.4836	1.129	701.9	
C5	40	93.2202	9.3320	1.127	690.7	
C6	50	94.6376	9.4739	1.129	701.2	
C7	60	93.6844	9.3784	1.128	694.1	

Experiment: 500:1 (3 of 3)

		DNAN				Byproducts		
HPLC Type	Sample Time (min)	Concentration (%)	Concentration (ppm)	RT (min)	Area (meas. @ 253 nm)	RT (min)	Area (meas. @ 253 nm)	Mass Ratio (C_n / C_o)
C_o (starting Conc)	0		9.3263					1.0000
R1	5	79.0324	7.9117	1.125	585.527			0.8483
R2	10	72.2197	7.2297	1.125	535.025			0.7752
R3	15	70.2465	7.0321	1.124	520.398			0.7540
R4	20	67.9667	6.8039	1.128	503.498			0.7295
R5	25	66.6001	6.6671	1.127	493.368			0.7149
R6	35	66.5370	6.6608	1.125	492.900			0.7142
R7	45	64.5810	6.4650	1.125	478.400			0.6932
R8	60	64.0914	6.4160	1.128	474.771			0.6879

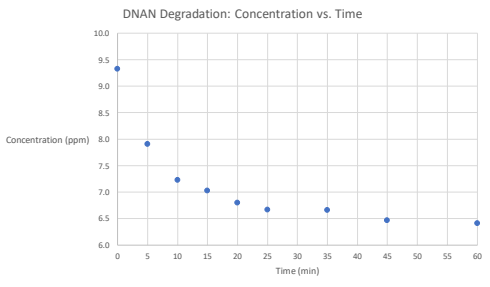

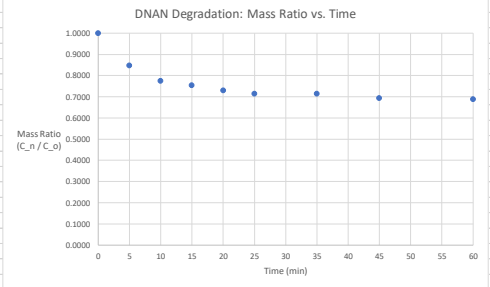

Quality Control Checks: QC 60%

Line	Area	Relative Error (< 10%)
9	441.4	0.6155
17	441.1	0.5471
27	437.3	0.3191

Data File Name	20200716_DNAN_JH
DNAN Prepared	7/13/2020
DNAN Conc (mg/L or ppm)	10.009300
pH	6.932
H2O2 Vol (µl)	1276
CAS weight (g)	0.2504
CAS Vol (µl)	100
Start Setup	6:45
Start Control	8:45
Stop Experiment	10:47
Ran in HPLC	11:00

Notes

DNAN pippetted @ 676 and 600 µl to get 1276 µl.

Calibration Curve

Concentration (%)	Concentration (ppm)	RT (min)	Area (meas. @ 253 nm)
0.0000	0.0000	0.000	0.0
10.0000	1.0009	1.104	81.7
20.0000	2.0019	1.108	139.8
40.0000	4.0037	1.11	284.2
60.0000	6.0056	1.114	427.1
80.0000	8.0074	1.113	569.2
100.0000	10.0093	1.114	722.4
Slope	0.1398		
y-intercept	-0.1256		

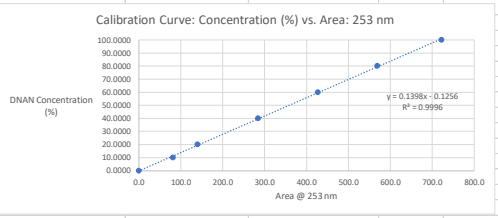

Control Experiment

HPLC Type	Sample Time (min)	Concentration (%)	Concentration (ppm)	RT (min)	Area (meas. @ 253 nm)	C_o = Avg Ctrl Conc. (ppm)
C1	0	91.4993	9.1584	1.113	655.4	9.3010
C2	10	94.7986	9.4887	1.116	679.0	
C3	20	93.8759	9.3963	1.114	672.4	
C4	30	93.1350	9.3222	1.113	667.1	
C5	40	92.1424	9.2228	1.112	660.0	
C6	50	91.7090	9.1794	1.114	656.9	
C7	60	93.3027	9.3390	1.114	668.3	

Experiment: 1000:1 (1 of 3)

		DNAN				Byproducts		
HPLC Type	Sample Time (min)	Concentration (%)	Concentration (ppm)	RT (min)	Area (meas. @ 253 nm)	RT (min)	Area (meas. @ 253 nm)	Mass Ratio (C_n / C_o)
C_o (starting Conc)	0		9.3010					1.0000
R1	5	78.1065	7.8179	1.112	559.600			0.8405
R2	10	73.9125	7.3981	1.115	529.600			0.7954
R3	15	69.8024	6.9867	1.113	500.200			0.7512
R4	20	68.2785	6.8342	1.114	489.300			0.7348
R5	25	67.6494	6.7712	1.114	484.800			0.7280
R6	35	66.2095	6.6271	1.113	474.500	0.832	0.760	0.7125
R7	45	67.0623	6.7125	1.113	480.600			0.7217
R8	60	66.3353	6.6397	1.114	475.400			0.7139

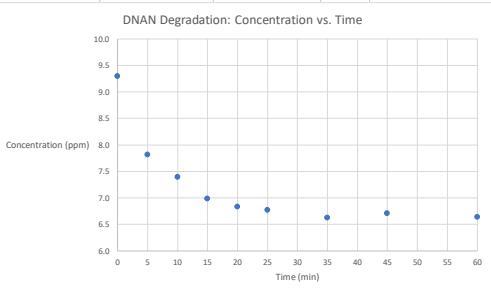

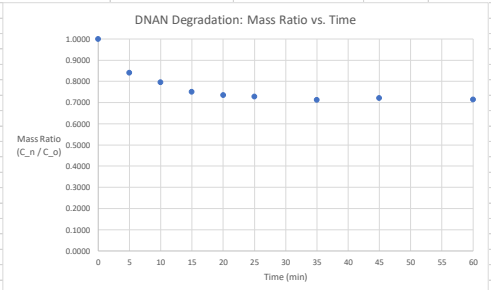

Quality Control Checks: QC 60%

Line	Area	Relative Error (< 10%)
9	428.1	0.2341
17	427.3	0.0468
27	423.5	0.8429

Data File Name	20200723_DNAN_A_JH
DNAN Prepared	7/20/2020
DNAN Conc (mg/L or ppm)	10.0053
pH	6.238
H2O2 Vol (µl)	1276
CAS weight (g)	0.2504
CAS Vol (µl)	100
Start Setup	5:15
Start Control	7:20
Stop Experiment	9:20
Ran in HPLC	9:28

Notes

Conducting this experiment, and 1000-1 # 3 on the same day. Used same CAS solution for both experiments. Total reset after completion of this experiment prior to starting 1000-1 # 3.

Calibration Curve

Concentration (%)	Concentration (ppm)	RT (min)	Area (meas. @ 253 nm)
0.0000	0.0000	0.000	0.0
10.0000	1.0005	1.088	69.4
20.0000	2.0011	1.09	143.6
40.0000	4.0021	1.09	289.8
60.0000	6.0032	1.093	431.6
80.0000	8.0042	1.093	573.1
100.0000	10.0053	1.094	722.6
Slope	0.1386		
y-intercept	0.1324		

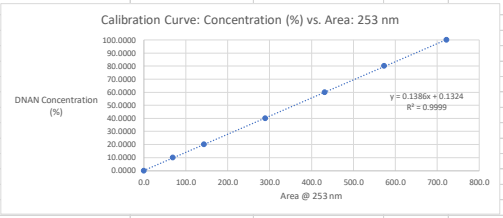

Control Experiment

HPLC Type	Sample Time (min)	Concentration (%)	Concentration (ppm)	RT (min)	Area (meas. @ 253 nm)	C_o = Avg Ctrl Conc. (ppm)
C1	0	91.2619	9.1310	1.094	657.5	9.5583
C2	10	96.5703	9.6621	1.094	695.8	
C3	20	96.9445	9.6996	1.093	698.5	
C4	30	95.6417	9.5692	1.094	689.1	
C5	40	96.4317	9.6483	1.095	694.8	
C6	50	95.7803	9.5831	1.094	690.1	
C7	60	96.0990	9.6150	1.093	692.4	

Experiment: 1000:1 (2 of 3)

		DNAN				Byproducts		
HPLC Type	Sample Time (min)	Concentration (%)	Concentration (ppm)	RT (min)	Area (meas. @ 253 nm)	RT (min)	Area (meas. @ 253 nm)	Mass Ratio (C_n / C_o)
C_o (starting Conc)	0		9.5583					1.0000
R1	5	79.3423	7.9384	1.095	571.500			0.8305
R2	10	75.8912	7.5931	1.095	546.600			0.7944
R3	15	73.4518	7.3491	1.095	529.000			0.7689
R4	20	72.2598	7.2298	1.094	520.400			0.7564
R5	25	71.4282	7.1466	1.095	514.400			0.7477
R6	35	68.8780	6.8915	1.094	496.000			0.7210
R7	45	67.7553	6.7791	1.094	487.900			0.7092
R8	60	67.4227	6.7458	1.096	485.500			0.7058

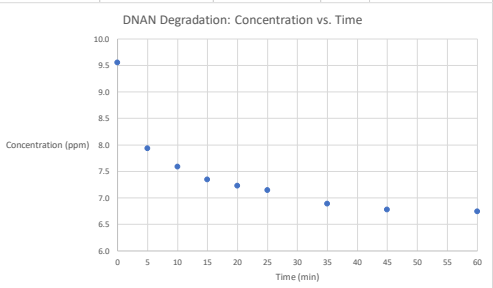

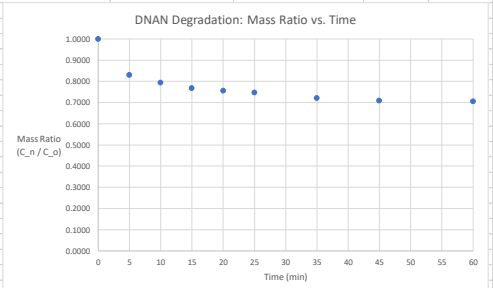

Quality Control Checks: QC 60%

Line	Area	Relative Error (< 10%)
9	428.4	0.7414
17	432.4	0.1854
27	430.9	0.1622

Data File Name	20200723_DNAN_B_JH
DNAN Prepared	7/20/2020
DNAN Conc (mg/L or ppm)	10.0067
pH	6.140
H2O2 Vol (µl)	1276
CAS weight (g)	0.2504
CAS Vol (µl)	100
Start Setup	9:30
Start Control	9:40
Stop Experiment	11:40
Ran in HPLC	11:50

Notes

Conducted back to back with 1000-1 #2. Full reset and clean of reactor before starting.

Calibration Curve

Concentration (%)	Concentration (ppm)	RT (min)	Area (meas. @ 253 nm)
0.0000	0.0000	0.000	0.0
10.0000	1.0007	1.096	70.5
20.0000	2.0013	1.094	145.8
40.0000	4.0027	1.095	292.3
60.0000	6.0040	1.094	434.9
80.0000	8.0054	1.095	579.6
100.0000	10.0067	1.094	725.6
Slope	0.1378		
y-intercept	0.0188		

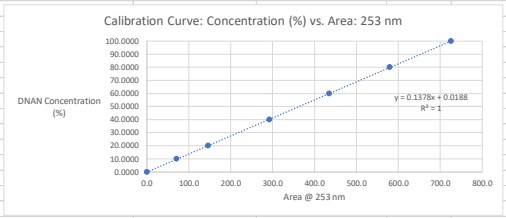

Control Experiment

HPLC Type	Sample Time (min)	Concentration (%)	Concentration (ppm)	RT (min)	Area (meas. @ 253 nm)	C_o = Avg Ctrl Conc. (ppm)
C1	0	93.9984	9.4061	1.095	682.0	9.6419
C2	10	96.3272	9.6392	1.094	698.9	
C3	20	96.5201	9.6585	1.095	700.3	
C4	30	96.1067	9.6171	1.096	697.3	
C5	40	96.9611	9.7026	1.094	703.5	
C6	50	97.0438	9.7109	1.095	704.1	
C7	60	97.5261	9.7591	1.095	707.6	

Experiment: 1000:1 (3 of 3)

		DNAN				Byproducts		
HPLC Type	Sample Time (min)	Concentration (%)	Concentration (ppm)	RT (min)	Area (meas. @ 253 nm)	RT (min)	Area (meas. @ 253 nm)	Mass Ratio (C_n / C_o)
C_o (starting Conc)	0		9.6419					1.0000
R1	5	73.5764	7.3626	1.096	533.800			0.7636
R2	10	67.9955	6.8041	1.095	493.300			0.7057
R3	15	65.5978	6.5642	1.095	475.900			0.6808
R4	20	64.3301	6.4373	1.094	466.700			0.6676
R5	25	62.9107	6.2953	1.097	456.400			0.6529
R6	35	62.1115	6.2153	1.095	450.600			0.6446
R7	45	61.5465	6.1588	1.095	446.500			0.6387
R8	60	60.3063	6.0347	1.096	437.500			0.6259

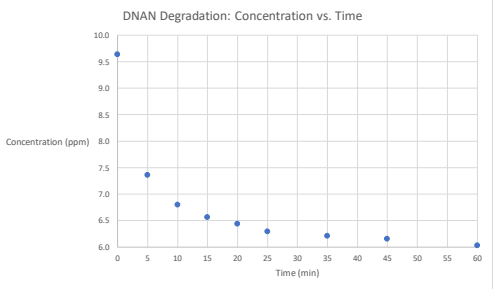

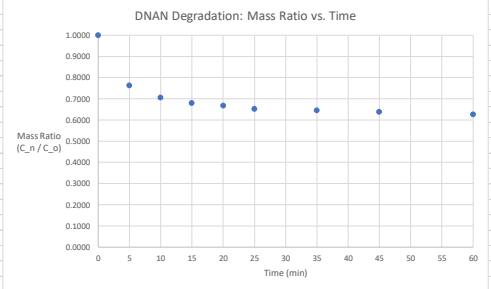

Quality Control Checks: QC 60%

Line	Area	Relative Error (< 10%)
9	434.7	0.0460
17	432.8	0.4829
27	430.9	0.9198

Data File Name	20200730_DNAN_JH
DNAN Prepared	7/27/2020
DNAN Conc (mg/L or ppm)	10.0040
pH	6.248
H2O2 Vol (µl)	0
CAS weight (g)	0.2503
CAS Vol (µl)	100
Start Setup	6:30
Start Control	8:15
Stop Experiment	10:15
Ran in HPLC	

Notes

This is a control with DNAN, CAS, and no H2O2. Initial control on 5/29 was DNAN and no CAS and no H2O2.

Calibration Curve

Concentration (%)	Concentration (ppm)	RT (min)	Area (meas. @ 253 nm)
0.0000	0.0000	0.000	0.0
10.0000	1.0004	1.081	74.2
20.0000	2.0008	1.082	154.0
40.0000	4.0016	1.081	299.4
60.0000	6.0024	1.083	447.7
80.0000	8.0032	1.085	600.9
100.0000	10.0040	1.088	748.1
Slope	0.1337		
y-intercept	-0.1097		

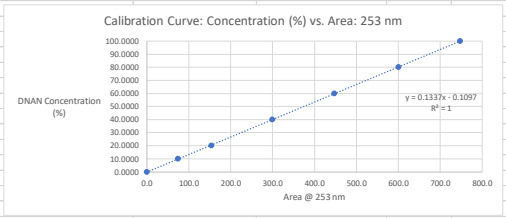

Control Experiment

HPLC Type	Sample Time (min)	Concentration (%)	Concentration (ppm)	RT (min)	Area (meas. @ 253 nm)	C_o = Avg Ctrl Conc. (ppm)
C1	0	91.2208	9.1257	1.095	683.1	9.5684
C2	10	96.7158	9.6755	1.086	724.2	
C3	20	95.8602	9.5899	1.081	717.8	
C4	30	97.7453	9.7784	1.076	731.9	
C5	40	96.3014	9.6340	1.075	721.1	
C6	50	95.7532	9.5792	1.076	717.0	
C7	60	95.9270	9.5965	1.080	718.3	

Experiment: 0:1

		DNAN				Byproducts		
HPLC Type	Sample Time (min)	Concentration (%)	Concentration (ppm)	RT (min)	Area (meas. @ 253 nm)	RT (min)	Area (meas. @ 253 nm)	Mass Ratio (C_n / C_o)
C_o (starting Conc)	0		9.5684					1.0000
R1	5	96.4217	9.6460	1.084	722.000			1.0081
R2	10	96.6624	9.6701	1.086	723.800			1.0106
R3	15	96.2345	9.6273	1.087	720.600			1.0062
R4	20	96.1409	9.6179	1.089	719.900			1.0052
R5	25	95.9671	9.6006	1.091	718.600			1.0034
R6	35	95.4190	9.5457	1.091	714.500			0.9976
R7	45	95.7398	9.5778	1.093	716.900			1.0010
R8	60	96.3014	9.6340	1.093	721.100			1.0068

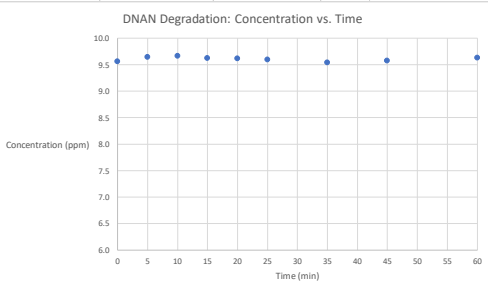

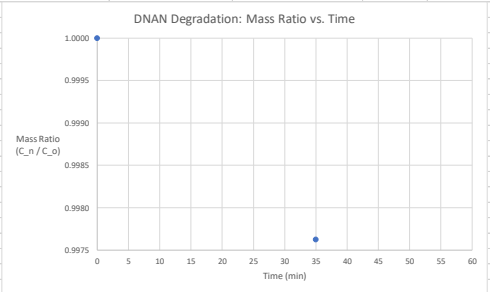

Quality Control Checks: QC 60%

Line	Area	Relative Error (< 10%)
9	447.8	0.0223
17	450.1	0.5361
27	445.6	0.4691

Data File Name	20200806_DNAN_1_JH
DNAN Prepared	8/3/2020
DNAN Conc (mg/L or ppm)	10.0013
pH	5.177
H2O2 Vol (µl)	319
CAS weight (g)	0.2501
CAS Vol (µl)	100
Start Setup	5:00
Start Control	6:45
Stop Experiment	8:45
Ran in HPLC	8:50

Notes

Conducted same day as 250:1 #1

Calibration Curve

Concentration (%)	Concentration (ppm)	RT (min)	Area (meas. @ 253 nm)
0.0000	0.0000	0.000	0.0
10.0000	1.0001	1.098	69.2
20.0000	2.0003	1.096	150.6
40.0000	4.0005	1.099	284.9
60.0000	6.0008	1.098	434.2
80.0000	8.0010	1.099	587.7
100.0000	10.0013	1.098	723.1
Slope	0.1375		
y-intercept	0.0828		

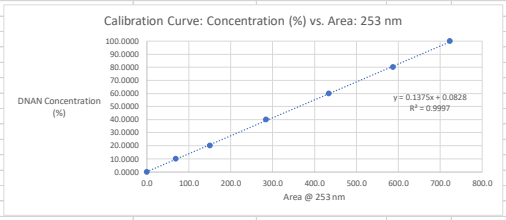

Control Experiment

HPLC Type	Sample Time (min)	Concentration (%)	Concentration (ppm)	RT (min)	Area (meas. @ 253 nm)	C_o = Avg Ctrl Conc. (ppm)
C1	0	92.0153	9.2027	1.099	668.6	9.5980
C2	10	95.3016	9.5314	1.098	692.5	
C3	20	95.5766	9.5589	1.098	694.5	
C4	30	95.8653	9.5878	1.098	696.6	
C5	40	97.1303	9.7143	1.099	705.8	
C6	50	98.8628	9.8876	1.098	718.4	
C7	60	97.0203	9.7033	1.098	705.0	

Experiment: 250:1 (1 of 3)

		DNAN				Byproducts		
HPLC Type	Sample Time (min)	Concentration (%)	Concentration (ppm)	RT (min)	Area (meas. @ 253 nm)	RT (min)	Area (meas. @ 253 nm)	Mass Ratio (C_n / C_o)
C_o (starting Conc)	0		9.5980					1.0000
R1	5	81.1391	8.1150	1.099	589.500			0.8455
R2	10	76.2853	7.6295	1.097	554.200			0.7949
R3	15	73.8653	7.3875	1.100	536.600			0.7697
R4	20	70.1116	7.0121	1.099	509.300			0.7306
R5	25	68.6403	6.8649	1.098	498.600			0.7152
R6	35	68.1178	6.8127	1.097	494.800			0.7098
R7	45	67.2516	6.7260	1.097	488.500			0.7008
R8	60	65.8216	6.5830	1.097	478.100			0.6859

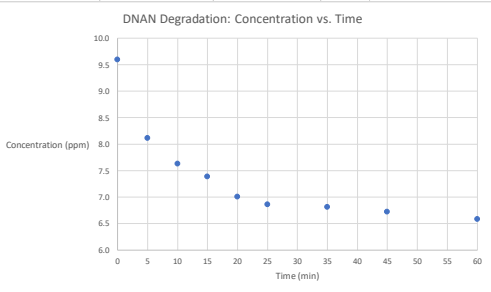

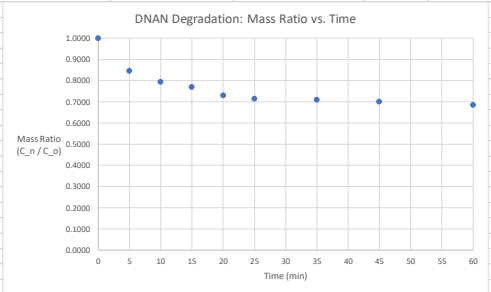

Quality Control Checks: QC 60%

Line	Area	Relative Error (< 10%)
9	428.0	1.4279
17	435.9	0.3915
27	429.4	1.1055

Data File Name	20200806_DNAN_2_JH
DNAN Prepared	8/3/2020
DNAN Conc (mg/L or ppm)	10.0040
pH	5.188
H2O2 Vol (µl)	319
CAS weight (g)	0.2501
CAS Vol (µl)	100
Start Setup	8:50
Start Control	9:00
Stop Experiment	11:00
Ran in HPLC	11:10

Notes

Conducted same day as 250:1 #1

Calibration Curve

Concentration (%)	Concentration (ppm)	RT (min)	Area (meas. @ 253 nm)
0.0000	0.0000	0.000	0.0
10.0000	1.0004	1.098	72.2
20.0000	2.0008	1.097	141.2
40.0000	4.0016	1.098	301.8
60.0000	6.0024	1.096	435.8
80.0000	8.0032	1.100	579.9
100.0000	10.0040	1.100	726.4
Slope	0.1376		
y-intercept	-0.0774		

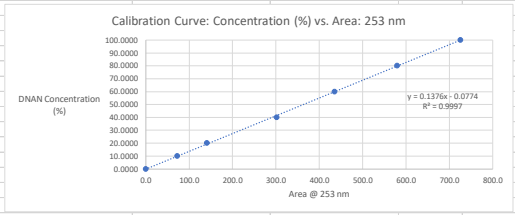

Control Experiment

HPLC Type	Sample Time (min)	Concentration (%)	Concentration (ppm)	RT (min)	Area (meas. @ 253 nm)	C_o = Avg Ctrl Conc. (ppm)
C1	0	96.8480	9.6887	1.099	704.4	9.7363
C2	10	96.8205	9.6859	1.098	704.2	
C3	20	97.4122	9.7451	1.100	708.5	
C4	30	96.3527	9.6391	1.099	700.8	
C5	40	98.7469	9.8786	1.098	718.2	
C6	50	98.0314	9.8071	1.100	713.0	
C7	60	97.0544	9.7093	1.099	705.9	

Experiment: 250:1 (2 of 3)

		DNAN				Byproducts		
HPLC Type	Sample Time (min)	Concentration (%)	Concentration (ppm)	RT (min)	Area (meas. @ 253 nm)	RT (min)	Area (meas. @ 253 nm)	Mass Ratio (C_n / C_o)
C_o (starting Conc)	0		9.7363					1.0000
R1	5	81.0103	8.1043	1.098	589.300			0.8324
R2	10	76.4832	7.6514	1.099	556.400			0.7859
R3	15	71.0618	7.1090	1.098	517.000			0.7302
R4	20	69.9748	7.0003	1.101	509.100			0.7190
R5	25	69.0391	6.9067	1.100	502.300			0.7094
R6	35	67.6218	6.7649	1.100	492.000			0.6948
R7	45	67.2916	6.7318	1.098	489.600			0.6914
R8	60	67.2640	6.7291	1.102	489.400			0.6911

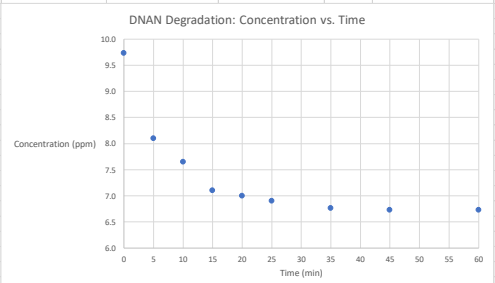

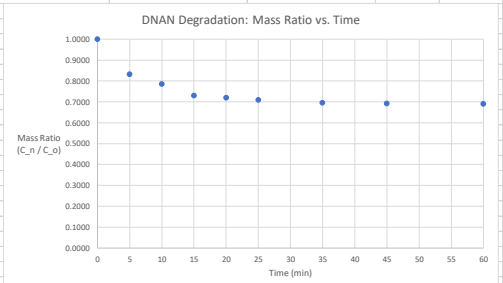

Quality Control Checks: QC 60%

Line	Area	Relative Error (< 10%)
9	438.2	0.5507
17	445.4	2.2028
27	433.5	0.5278

Data File Name	20200813_DNAN_1_JH
DNAN Prepared	8/10/2020
DNAN Conc (mg/L or ppm)	10.0013
pH	5.365
H2O2 Vol (µl)	319
CAS weight (g)	0.25
CAS Vol (µl)	100
Start Setup	5:15
Start Control	6:55
Stop Experiment	8:55
Ran in HPLC	9:05

Notes

Conducted same day as 50:1 #1

Calibration Curve

Concentration (%)	Concentration (ppm)	RT (min)	Area (meas. @ 253 nm)
0.0000	0.0000	0.000	0.0
10.0000	1.0001	1.091	64.2
20.0000	2.0003	1.093	137.7
40.0000	4.0005	1.094	290.2
60.0000	6.0008	1.093	429.6
80.0000	8.0010	1.093	568.2
100.0000	10.0013	1.094	721.6
Slope	0.1384		
y-intercept	0.5512		

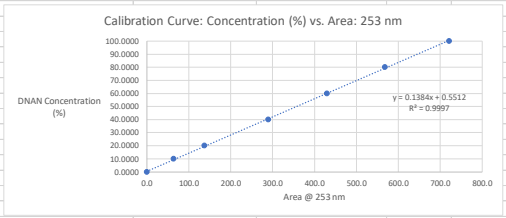

Control Experiment

HPLC Type	Sample Time (min)	Concentration (%)	Concentration (ppm)	RT (min)	Area (meas. @ 253 nm)	C_o = Avg Ctrl Conc. (ppm)
C1	0	91.4938	9.1506	1.095	657.1	9.5472
C2	10	94.8985	9.4911	1.095	681.7	
C3	20	96.9606	9.6973	1.094	696.6	
C4	30	96.7530	9.6766	1.093	695.1	
C5	40	96.1164	9.6129	1.094	690.5	
C6	50	95.6182	9.5631	1.093	686.9	
C7	60	96.3794	9.6392	1.093	692.4	

Experiment: 250:1 (3 of 3)

		DNAN				Byproducts		
HPLC Type	Sample Time (min)	Concentration (%)	Concentration (ppm)	RT (min)	Area (meas. @ 253 nm)	RT (min)	Area (meas. @ 253 nm)	Mass Ratio (C_n / C_o)
C_o (starting Conc)	0		9.5472					1.0000
R1	5	80.6986	8.0709	1.092	579.100			0.8454
R2	10	76.8926	7.6903	1.091	551.600			0.8055
R3	15	72.8237	7.2833	1.091	522.200			0.7629
R4	20	70.3048	7.0314	1.092	504.000			0.7365
R5	25	70.2910	7.0300	1.093	503.900			0.7363
R6	35	69.4744	6.9483	1.089	498.000			0.7278
R7	45	69.5851	6.9594	1.090	498.800			0.7289
R8	60	68.2426	6.8252	1.091	489.100			0.7149

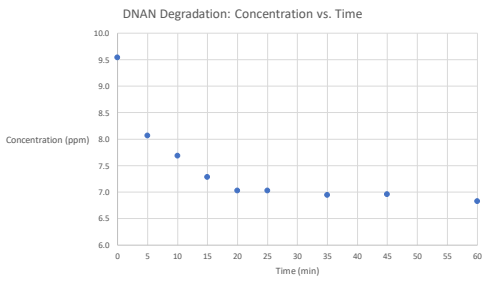

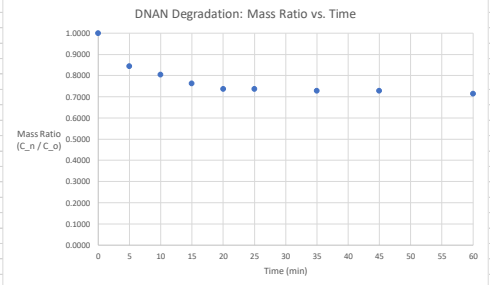

Quality Control Checks: QC 60%

Line	Area	Relative Error (< 10%)
9	427.0	0.6052
17	426.9	0.6285
27	437.3	1.7924

Data File Name	20200813_DNAN_2_JH
DNAN Prepared	8/10/2020
DNAN Conc (mg/L or ppm)	10.0147
pH	5.232
H2O2 Vol (µl)	64
CAS weight (g)	0.25
CAS Vol (µl)	100
Start Setup	9:00
Start Control	9:05
Stop Experiment	11:05
Ran in HPLC	12:00

Notes

Conducted same day as 250:1 #3.

Calibration Curve

Concentration (%)	Concentration (ppm)	RT (min)	Area (meas. @ 253 nm)
0.0000	0.0000	0.000	0.0
10.0000	1.0015	1.096	65.3
20.0000	2.0029	1.096	141.6
40.0000	4.0059	1.096	288.4
60.0000	6.0088	1.094	462.1
80.0000	8.0118	1.094	580.9
100.0000	10.0147	1.095	725.5
Slope	0.1359		
y-intercept	0.3414		

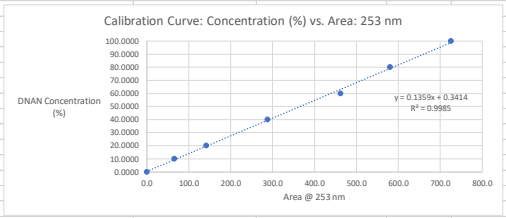

Control Experiment

HPLC Type	Sample Time (min)	Concentration (%)	Concentration (ppm)	RT (min)	Area (meas. @ 253 nm)	C_o = Avg Ctrl Conc. (ppm)
C1	0	93.0796	9.3216	1.092	682.4	9.5464
C2	10	95.0637	9.5203	1.093	697.0	
C3	20	95.6888	9.5830	1.093	701.6	
C4	30	95.6481	9.5789	1.093	701.3	
C5	40	96.2324	9.6374	1.093	705.6	
C6	50	95.8791	9.6020	1.092	703.0	
C7	60	95.6753	9.5816	1.094	701.5	

Experiment: 50:1 (1 of 3)

		DNAN				Byproducts		
HPLC Type	Sample Time (min)	Concentration (%)	Concentration (ppm)	RT (min)	Area (meas. @ 253 nm)	RT (min)	Area (meas. @ 253 nm)	Mass Ratio (C_n / C_o)
C_o (starting Conc)	0		9.5464					1.0000
R1	5	85.7817	8.5908	1.093	628.700			0.8999
R2	10	84.9256	8.5050	1.093	622.400			0.8909
R3	15	79.7478	7.9865	1.092	584.300			0.8366
R4	20	78.9324	7.9048	1.092	578.300			0.8280
R5	25	77.7365	7.7851	1.092	569.500			0.8155
R6	35	76.7036	7.6816	1.092	561.900			0.8047
R7	45	77.3559	7.7470	1.092	566.700			0.8115
R8	60	77.6277	7.7742	1.093	568.700			0.8144

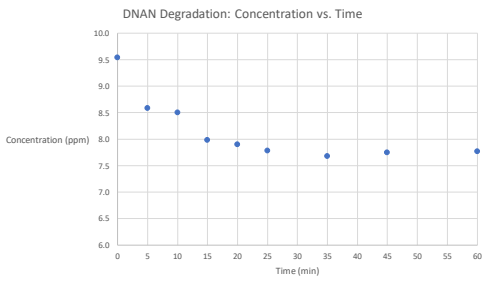

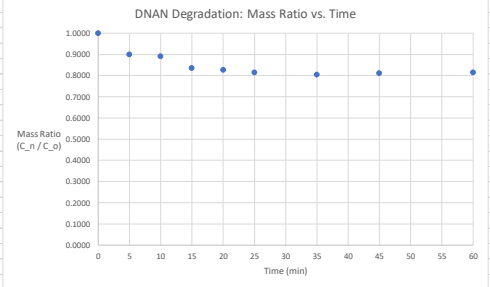

Quality Control Checks: QC 60%

Line	Area	Relative Error (< 10%)
9	457.2	1.0604
17	463.1	0.2164
27	465.8	0.8007

Data File Name	20200820_DNAN_1_JH
DNAN Prepared	8/17/2020
DNAN Conc (mg/L or ppm)	10.0027
pH	5.197
H2O2 Vol (µl)	64
CAS weight (g)	0.2502
CAS Vol (µl)	100
Start Setup	5:15
Start Control	7:05
Stop Experiment	9:05
Ran in HPLC	9:10

Notes

Conducted same day as 50:1 #3.

Calibration Curve

Concentration (%)	Concentration (ppm)	RT (min)	Area (meas. @ 253 nm)
0.0000	0.0000	0.000	0.0
10.0000	1.0003	1.099	72.8
20.0000	2.0005	1.099	139.2
40.0000	4.0011	1.097	288.3
60.0000	6.0016	1.101	437.9
80.0000	8.0022	1.099	588.0
100.0000	10.0027	1.100	723.9
Slope	0.1370		
y-intercept	0.2536		

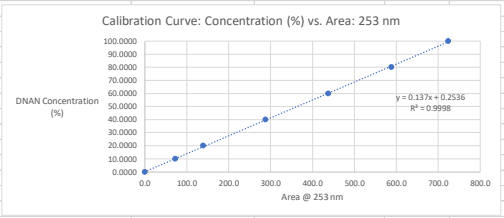

Control Experiment

HPLC Type	Sample Time (min)	Concentration (%)	Concentration (ppm)	RT (min)	Area (meas. @ 253 nm)	C_o = Avg Ctrl Conc. (ppm)
C1	0	92.5779	9.2603	1.101	673.9	9.5551
C2	10	95.5097	9.5535	1.099	695.3	
C3	20	96.4002	9.6426	1.100	701.8	
C4	30	96.7701	9.6796	1.100	704.5	
C5	40	96.2221	9.6248	1.099	700.5	
C6	50	95.2905	9.5316	1.098	693.7	
C7	60	95.9070	9.5933	1.101	698.2	

Experiment: 50:1 (2 of 3)

		DNAN				Byproducts		
HPLC Type	Sample Time (min)	Concentration (%)	Concentration (ppm)	RT (min)	Area (meas. @ 253 nm)	RT (min)	Area (meas. @ 253 nm)	Mass Ratio (C_n / C_o)
C_o (starting Conc)	0		9.5551					1.0000
R1	5	86.7965	8.6820	1.098	631.700			0.9086
R2	10	83.1112	8.3134	1.099	604.800			0.8700
R3	15	81.1247	8.1147	1.099	590.300			0.8492
R4	20	79.6862	7.9708	1.100	579.800			0.8342
R5	25	78.8642	7.8885	1.098	573.800			0.8256
R6	35	78.4258	7.8447	1.098	570.600			0.8210
R7	45	78.4121	7.8433	1.099	570.500			0.8209
R8	60	77.4805	7.7501	1.102	563.700			0.8111

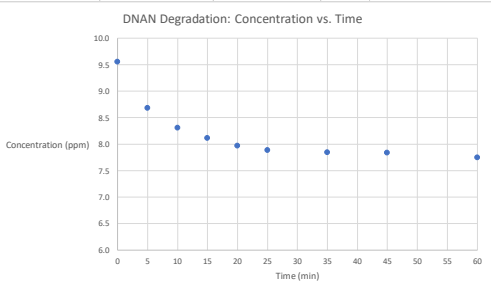

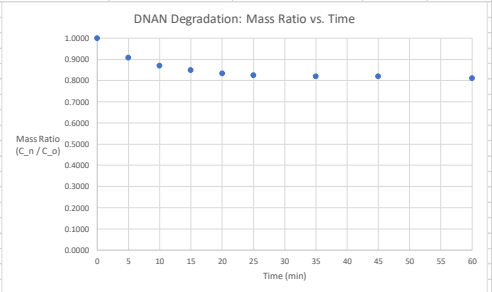

Quality Control Checks: QC 60%

Line	Area	Relative Error (< 10%)
9	429.9	1.8269
17	425.0	2.9459
27	439.3	0.3197

Data File Name	20200820_DNAN_2_JH
DNAN Prepared	8/17/2020
DNAN Conc (mg/L or ppm)	10.0013
pH	5.232
H2O2 Vol (µl)	64
CAS weight (g)	0.2502
CAS Vol (µl)	100
Start Setup	9:10
Start Control	9:15
Stop Experiment	11:15
Ran in HPLC	11:20

Notes

Conducted same day as 50:1 #2. B

Calibration Curve

Concentration (%)	Concentration (ppm)	RT (min)	Area (meas. @ 253 nm)
0.0000	0.0000	0.000	0.0
10.0000	1.0001	1.1	72.1
20.0000	2.0003	1.099	142.9
40.0000	4.0005	1.101	283.8
60.0000	6.0008	1.1	431.5
80.0000	8.0010	1.099	587.0
100.0000	10.0013	1.098	722.9
Slope	0.1375		
y-intercept	0.2763		

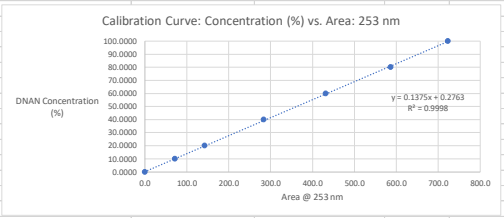

Control Experiment

HPLC Type	Sample Time (min)	Concentration (%)	Concentration (ppm)	RT (min)	Area (meas. @ 253 nm)	C_o = Avg Ctrl Conc. (ppm)
C1	0	94.7663	9.4779	1.098	687.2	9.6456
C2	10	96.3751	9.6388	1.098	698.9	
C3	20	96.6638	9.6676	1.098	701.0	
C4	30	97.0488	9.7061	1.097	703.8	
C5	40	96.5263	9.6539	1.097	700.0	
C6	50	96.8701	9.6883	1.097	702.5	
C7	60	96.8563	9.6869	1.098	702.4	

Experiment: 50:1 (3 of 3)

		DNAN				Byproducts		
HPLC Type	Sample Time (min)	Concentration (%)	Concentration (ppm)	RT (min)	Area (meas. @ 253 nm)	RT (min)	Area (meas. @ 253 nm)	Mass Ratio (C_n / C_o)
C_o (starting Conc)	0		9.6456					1.0000
R1	5	86.9426	8.6954	1.100	630.300			0.9015
R2	10	83.4776	8.3488	1.101	605.100			0.8656
R3	15	81.8138	8.1824	1.100	593.000			0.8483
R4	20	78.6651	7.8675	1.098	570.100			0.8157
R5	25	78.8301	7.8840	1.103	571.300			0.8174
R6	35	77.8263	7.7836	1.100	564.000			0.8070
R7	45	77.9088	7.7919	1.098	564.600			0.8078
R8	60	77.4413	7.7451	1.099	561.200			0.8030

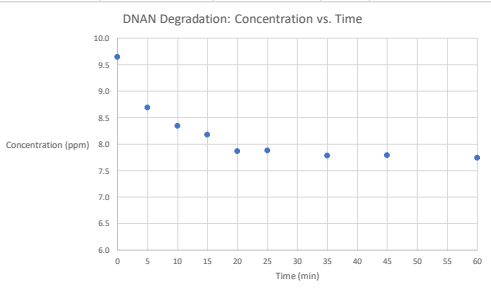

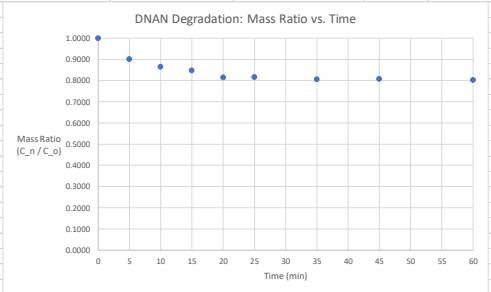

Quality Control Checks: QC 60%

Line	Area	Relative Error (< 10%)
9	431.6	0.0232
17	421.2	2.3870
27	430.7	0.1854

Appendix C: AOP ANOVA, t-Test, and Regression Analysis

Oneway Analysis of k_s By Treatment

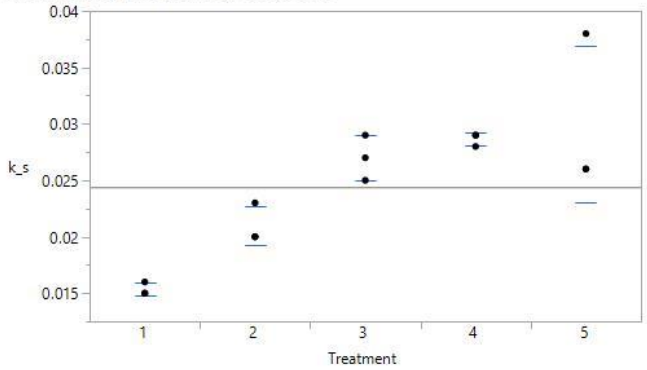

Wilcoxon / Kruskal-Wallis Tests (Rank Sums)

Level	Count	Score Sum	Expected Score	Score Mean	(Mean-Mean0)/Std0
1	3	6.000	24.000	2.0000	-2.542
2	3	15.000	24.000	5.0000	-1.235
3	3	30.000	24.000	10.0000	0.799
4	3	37.000	24.000	12.3333	1.816
5	3	32.000	24.000	10.6667	1.089

1-way Test, ChiSquare Approximation

ChiSquare	DF	Prob>ChiSq
11.3755	4	0.0227*

Small sample sizes. Refer to statistical tables for tests, rather than large-sample approximations.

Tests that the Variances are Equal

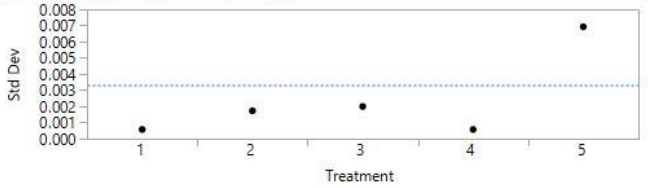

Level	Count	Std Dev	MeanAbsDif to Mean	MeanAbsDif to Median
1	3	0.0005774	0.0004444	0.0003333
2	3	0.0017321	0.0013333	0.0010000
3	3	0.0020000	0.0013333	0.0013333
4	3	0.0005774	0.0004444	0.0003333
5	3	0.0069282	0.0053333	0.0040000

Test	F Ratio	DFNum	DFDen	Prob > F
O'Brien[.5]	1.6309	4	10	0.2414
Brown-Forsythe	0.6509	4	10	0.6392
Levene	8.7958	4	10	0.0026*
Bartlett	3.2878	4	.	0.0106*

Warning: Small sample sizes. Use Caution.

Welch's Test

Welch Anova testing Means Equal, allowing Std Devs Not Equal

F Ratio	DFNum	DFDen	Prob > F
144.2129	4	4.6829	<.0001*

This treatment was for five levels, 1-5. Non-linear scaling.

1: 50
2: 100
3: 250
4: 500
5: 1000

Bivariate Fit of k_s By Log(ratio)

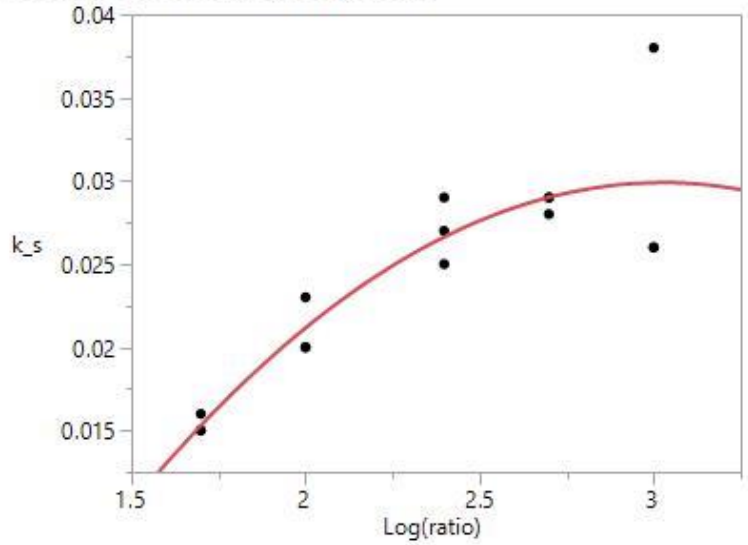

Polynomial Fit Degree=2

Polynomial Fit Degree=2

k_s = 0.0001202 + 0.0110604*Log(ratio) - 0.008301*(Log(ratio)-2.35918)^2

Summary of Fit

RSquare	0.800158
RSquare Adj	0.766851
Root Mean Square Error	0.003058
Mean of Response	0.0244
Observations (or Sum Wgts)	15

Analysis of Variance

Source	DF	Sum of Squares	Mean Square	F Ratio
Model	2	0.00044937	0.000225	24.0237
Error	12	0.00011223	9.353e-6	Prob > F
C. Total	14	0.00056160		<.0001*

Parameter Estimates

Term	Estimate	Std Error	t Ratio	Prob>|t|
Intercept	0.0001202	0.004269	0.03	0.9780
Log(ratio)	0.0110604	0.001694	6.53	<.0001*
(Log(ratio)-2.35918)^2	-0.008301	0.004575	-1.81	0.0946

Trial	Ratio	k_s (Y)	Treatment			
1	100	0.023	2			
2	100	0.02	2			
3	100	0.02	2			
4	500	0.029	4			
5	500	0.029	4			
6	500	0.028	4			
7	1000	0.026	5			
8	1000	0.026	5			
9	1000	0.038	5			
10	250	0.027	3			
11	250	0.029	3			
12	250	0.025	3			
13	50	0.015	1			
14	50	0.015	1			
15	50	0.016	1			
Ratio	Treatment	Mean	Stdev	tvalue	family alpha	0.05
100	1	0.0210	0.0017	5.597568367	comparison alpha	0.005
500	2	0.0287	0.0006			
1000	3	0.0300	0.0069			
250	4	0.0270	0.0020			
50	5	0.0153	0.0006			
Comparison	Margin of error	LB	UB	Significant		
50 - 100	0.0051	-0.0108	-0.0006	Y		
50 - 250	0.0058	-0.0175	-0.0058	Y		
50 - 500	0.0023	-0.0156	-0.0110	Y		
50 - 1000	0.0195	-0.0341	0.0048	N		
100 - 250	0.0074	-0.0134	0.0014	N		
100 - 500	0.0051	-0.0128	-0.0026	Y		
100 - 1000	0.0200	-0.0290	0.0110	N		
250 - 500	0.0058	-0.0075	0.0042	N		
250 - 1000	0.0202	-0.0232	0.0172	N		
500 - 1000	0.0195	-0.0208	0.0181	N		

H2O2:DNAN	$(H2O2:DNAN)^2$	k_s (min^{-1})
0	0	0
50	2500	0.015
50	2500	0.015
50	2500	0.016
100	10000	0.023
100	10000	0.02
100	10000	0.02
250	62500	0.027
250	62500	0.029
250	62500	0.025
500	250000	0.029
500	250000	0.029
500	250000	0.028
1000	1000000	0.026
1000	1000000	0.026
1000	1000000	0.038

SUMMARY OUTPUT: LINEAR

Regression Statistics	
Multiple R	0.833230718
R Square	0.69427343
Adjusted R Sq	0.627606763
Standard Erro	0.013909126
Observations	16

ANOVA

	df	*SS*	*MS*	*F*	*Significance F*
Regression	1	0.006590043	0.006590043	34.06344906	4.32009E-05
Residual	15	0.002901957	0.000193464		
Total	16	0.009492			

	Coefficients	*Standard Error*	*t Stat*	*P-value*	*Lower 95%*	*Upper 95%*	*Lower 95.0%*	*Upper 95.0%*
Intercept	0	#N/A	#N/A	#N/A	#N/A	#N/A	#N/A	#N/A
H2O2:DNAN	4.0717E-05	6.9764E-06	5.836390071	3.2751E-05	2.58471E-05	5.55868E-05	2.58471E-05	5.55868E-05

RESIDUAL OUTPUT

Observation	*Predicted ks (min-1)*	*Residuals*
1	0	0
2	0.002035849	0.012964151
3	0.002035849	0.012964151
4	0.002035849	0.013964151
5	0.004071698	0.018928302
6	0.004071698	0.015928302
7	0.004071698	0.015928302
8	0.010179245	0.016820755
9	0.010179245	0.018820755
10	0.010179245	0.014820755
11	0.020358491	0.008641509
12	0.020358491	0.008641509
13	0.020358491	0.007641509
14	0.040716981	-0.014716981
15	0.040716981	-0.014716981
16	0.040716981	-0.002716981

SUMMARY OUTPUT: QUADRATIC FORCED THROUGH INTERCEPT

Regression Statistics	
Multiple R	0.950181394
R Square	0.902844681
Adjusted R Sq	0.824476444
Standard Erro	0.008116114
Observations	16

ANOVA

	df	*SS*	*MS*	*F*	*Significance F*
Regression	2	0.008569802	0.004284901	65.0495805	1.6943E-07
Residual	14	0.000922198	6.58713E-05		
Total	16	0.009492			

	Coefficients	*Standard Error*	*t Stat*	*P-value*	*Lower 95%*	*Upper 95%*	*Lower 95.0%*	*Upper 95.0%*
Intercept	0	#N/A	#N/A	#N/A	#N/A	#N/A	#N/A	#N/A
H2O2:DNAN	0.000117706	1.46215E-05	8.050213817	1.27316E-06	8.63462E-05	0.000149066	8.63462E-05	0.000149066
(H2O2:DNAN)	-8.9346E-08	1.62974E-08	-5.482238799	8.07563E-05	-1.243E-07	-5.43916E-08	-1.243E-07	-5.43916E-08

RESIDUAL OUTPUT

Observation	*Predicted ks (min-1)*	*Residuals*
1	0	0
2	0.005661947	0.009338053
3	0.005661947	0.009338053
4	0.005661947	0.010338053
5	0.010877164	0.012122836
6	0.010877164	0.009122836
7	0.010877164	0.009122836
8	0.023842435	0.003157565
9	0.023842435	0.005157565
10	0.023842435	0.001157565
11	0.036516625	-0.007516625
12	0.036516625	-0.007516625
13	0.036516625	-0.008516625
14	0.028360265	-0.002360265
15	0.028360265	-0.002360265
16	0.028360265	0.009639735

SUMMARY OUTPUT QUADRATIC

Regression Statistics	
Multiple R	0.837674088
R Square	0.701697878
Adjusted R Sq	0.655805244
Standard Erro	0.005068939
Observations	16

ANOVA

	df	*SS*	*MS*	*F*	*Significance F*
Regression	2	0.000785726	0.000392863	15.28998915	0.000384828
Residual	13	0.000334024	2.56941E-05		
Total	15	0.00111975			

	Coefficients	*Standard Error*	*t Stat*	*P-value*	*Lower 95%*	*Upper 95%*	*Lower 95.0%*	*Upper 95.0%*
Intercept	0.011710863	0.00244767	4.784494521	0.000356625	0.006422994	0.016998732	0.006422994	0.016998732
H2O2:DNAN	6.28003E-05	1.46658E-05	4.282096484	0.000892405	3.11168E-05	9.44839E-05	3.11168E-05	9.44839E-05
(H2O2:DNAN)	-4.51159E-08	1.375E-08	-3.281153575	0.005959972	-7.4821E-08	-1.54108E-08	-7.4821E-08	-1.54108E-08

RESIDUAL OUTPUT

Observation	*Predicted ks (min-1)*	*Residuals*
1	0.011710863	-0.011710863
2	0.01473809	0.00026191
3	0.01473809	0.00026191
4	0.01473809	0.00126191
5	0.017539738	0.005460262
6	0.017539738	0.002460262
7	0.017539738	0.002460262
8	0.024591203	0.002408797
9	0.024591203	0.004408797
10	0.024591203	0.000408797
11	0.031832055	-0.002832055
12	0.031832055	-0.002832055
13	0.031832055	-0.003832055
14	0.029395293	-0.003395293
15	0.029395293	-0.003395293
16	0.029395293	0.008604707

Appendix D: MATLAB Code

```
%DNAN Code
%June, 2020
%Author: W. Harper & J. Hart
%Project: UV LED Project (sponsored by AFCEC/DERA)
%This program is used to model DNAN removal in a UV LED reactor

%the clock is here to help determine the runtime. It does not affect the process simulation
tstart = clock;

%global declarations - the purpose of these declarations is to make these parameter values
%available to light3.

%global declarations
global rateconstant reactorvolume flow xo Cinit
global realdata11 realdata12 realdata13 realdata14 realdata15 realdata16 realdata17 realdata18
realdata19 realdata110 realdata111 realdata112 realdata113 realdata114 realdata115 realdata21
realdata22 realdata23 realdata24 realdata25 realdata26 realdata27 realdata28 realdata29 realdata210
realdata211 realdata212 realdata213 realdata214 realdata215

%The parameters in the matrix are respectively:
%effluent concentration of DNAN (1)

%the units of the rateconstant are inverse time (1/min)

%the units of volume are ml
reactorvolume = 35;

%the units of flow are ml/minutes
flow = 2.0;

tau = reactorvolume./flow;

%parameters needed for simulation
alpha = 0.001;
beta = 0.001;
gamma = 0.05;

%additional matrices needed for data processing
nnn = 100000;
ZZZ1 = zeros(7,nnn);
BEST = zeros(6,1);
BEST1 = zeros(1,1);
ZZZ2 = zeros(7,nnn);
BEST2 = zeros(1,1);
ZZZ3 = zeros(7,nnn);
BEST3 = zeros(1,1);
ZZZ4 = zeros(7,nnn);
BEST4 = zeros(1,1);
ZZZ5 = zeros(7,nnn);
```

```
BEST5 = zeros(1,1);
ZZZ6 = zeros(7,nnn);
BEST6 = zeros(1,1);
ZZZ7 = zeros(7,nnn);
BEST7 = zeros(1,1);
ZZZ8 = zeros(7,nnn);
BEST8 = zeros(1,1);
ZZZ9 = zeros(7,nnn);
BEST9 = zeros(1,1);
ZZZ10 = zeros(7,nnn);
BEST10 = zeros(1,1);
ZZZ11 = zeros(7,nnn);
BEST11 = zeros(1,1);
ZZZ12 = zeros(7,nnn);
BEST12 = zeros(1,1);
ZZZ13 = zeros(7,nnn);
BEST13 = zeros(1,1);
ZZZ14 = zeros(7,nnn);
BEST14 = zeros(1,1);
ZZZ15 = zeros(7,nnn);
BEST15 = zeros(1,1);


%the following are process parameters
to = 0;
%the units are minutes
tf = 60;

HartDNANdata2020

%aaa is needed to determine the best parameter combination
aaa1 = 10000000000;
aaa2 = aaa1;
aaa3 = aaa1;
aaa4 = aaa1;
aaa5 = aaa1;
aaa6 = aaa1;
aaa7 = aaa1;
aaa8 = aaa1;
aaa9 = aaa1;
aaa10 = aaa1;
aaa11 = aaa1;
aaa12 = aaa1;
aaa13 = aaa1;
aaa14 = aaa1;
aaa15 = aaa1;

%this is a counter
counttt = 1;

%the simulation logic begins here
```

```
%This is for the first experimental data set: 100:1 #1
for rateconstant = alpha:beta:gamma
%_____________________________________________________
%Initial Conditions Matrix
xo = Cinit(1,1);
%Solve the differential equations
[t,x] = ode45('light3',realdata11,xo,[],tau);

MMM1 = abs((realdata21 - x(:,1)./Cinit(1,1))).^2;
ttt1 = cumsum(MMM1);
bbb1 = ttt1(end)./size(realdata21,1);
rrr1 = ((bbb1)^(0.5))./max(realdata21);

ZZZ1(1,counttt) = rrr1;
ZZZ1(2,counttt) = rateconstant;

if ZZZ1(1,counttt) < aaa1
   aaa1 = ZZZ1(1,counttt);
   BEST(1,1) = rateconstant;
   zipa = x(:,1)./Cinit(1,1);
   zipat = t;
end
counttt = counttt + 1;
end

%_____________________________________________________________________________

counttt = 1;


%This is for the second experimental data set: 100:1 #2
for rateconstant = alpha:beta:gamma
%_____________________________________________________
%Initial Conditions Matrix
xo = Cinit(2,1);
%Solve the differential equations
[t,x] = ode45('light3',realdata12,xo,[],tau);

MMM2 = abs((realdata22 - x(:,1)./Cinit(2,1))).^2;
ttt2 = cumsum(MMM2);
bbb2 = ttt2(end)./size(realdata22,1);
rrr2 = ((bbb2)^(0.5))./max(realdata22);

ZZZ2(1,counttt) = rrr2;
ZZZ2(2,counttt) = rateconstant;

if ZZZ2(1,counttt) < aaa2
   aaa2 = ZZZ2(1,counttt);
   BEST(2,1) = rateconstant;
   zipb = x(:,1)./Cinit(2,1);
   zipbt = t;
```

```
end
counttt = counttt + 1;
end

counttt = 1;

%This is for the third experimental data set: 100:1 #3
for rateconstant = alpha:beta:gamma
%_____________________________________________________
%Initial Conditions Matrix
xo = Cinit(3,1);
%Solve the differential equations
[t,x] = ode45('light3',realdata13,xo,[],tau);

MMM3 = abs((realdata23 - x(:,1)./Cinit(3,1))).^2;
ttt3 = cumsum(MMM3);
bbb3 = ttt3(end)./size(realdata23,1);
rrr3 = ((bbb3)^(0.5))./max(realdata23);

ZZZ3(1,counttt) = rrr3;
ZZZ3(2,counttt) = rateconstant;

if ZZZ3(1,counttt) < aaa3
   aaa3 = ZZZ3(1,counttt);
   BEST(3,1) = rateconstant;
   zipc = x(:,1)./Cinit(3,1);
   zipct = t;
end
counttt = counttt + 1;
end

counttt = 1;

%This is for the fourth experimental data set: 500:1 #1
for rateconstant = alpha:beta:gamma
%_____________________________________________________
%Initial Conditions Matrix
xo = Cinit(4,1);
%Solve the differential equations
[t,x] = ode45('light3',realdata14,xo,[],tau);

MMM4 = abs((realdata24 - x(:,1)./Cinit(4,1))).^2;
ttt4 = cumsum(MMM4);
bbb4 = ttt4(end)./size(realdata24,1);
rrr4 = ((bbb4)^(0.5))./max(realdata24);

ZZZ4(1,counttt) = rrr4;
ZZZ4(2,counttt) = rateconstant;

if ZZZ4(1,counttt) < aaa4
   aaa4 = ZZZ4(1,counttt);
```

```
   BEST(4,1) = rateconstant;
   zipd = x(:,1)./Cinit(4,1);
   zipdt = t;
end
counttt = counttt + 1;
end

counttt = 1;

%This is for the fifth experimental data set: 500:1 #2
for rateconstant = alpha:beta:gamma
%_____________________________________________________
%Initial Conditions Matrix
xo = Cinit(5,1);
%Solve the differential equations
[t,x] = ode45('light3',realdata15,xo,[],tau);

MMM5 = abs((realdata25 - x(:,1)./Cinit(5,1))).^2;
ttt5 = cumsum(MMM5);
bbb5 = ttt5(end)./size(realdata25,1);
rrr5 = ((bbb5)^(0.5))./max(realdata25);

ZZZ5(1,counttt) = rrr5;
ZZZ5(2,counttt) = rateconstant;

if ZZZ5(1,counttt) < aaa5
   aaa5 = ZZZ5(1,counttt);
   BEST(5,1) = rateconstant;
   zipe = x(:,1)./Cinit(5,1);
   zipet = t;
end
counttt = counttt + 1;
end


counttt = 1;

%This is for the sixth experimental data set: 500:1 #3
for rateconstant = alpha:beta:gamma
%_____________________________________________________
%Initial Conditions Matrix
xo = Cinit(6,1);
%Solve the differential equations
[t,x] = ode45('light3',realdata16,xo,[],tau);

MMM6 = abs((realdata26 - x(:,1)./Cinit(6,1))).^2;
ttt6 = cumsum(MMM6);
bbb6 = ttt6(end)./size(realdata26,1);
rrr6 = ((bbb6)^(0.5))./max(realdata26);

ZZZ6(1,counttt) = rrr6;
```

```
ZZZ6(2,counttt) = rateconstant;

if ZZZ6(1,counttt) < aaa6
   aaa6 = ZZZ6(1,counttt);
   BEST(6,1) = rateconstant;
   zipf = x(:,1)./Cinit(6,1);
   zipft = t;
end
counttt = counttt + 1;
end

%This is for the seventh experimental data set: 1000:1 #1
for rateconstant = alpha:beta:gamma
%_____________________________________________________
%Initial Conditions Matrix
xo = Cinit(7,1);
%Solve the differential equations
[t,x] = ode45('light3',realdata17,xo,[],tau);

MMM7 = abs((realdata27 - x(:,1)./Cinit(7,1))).^2;
ttt7 = cumsum(MMM7);
bbb7 = ttt7(end)./size(realdata27,1);
rrr7 = ((bbb7)^(0.5))./max(realdata27);

ZZZ7(1,counttt) = rrr7;
ZZZ7(2,counttt) = rateconstant;

if ZZZ7(1,counttt) < aaa7
   aaa7 = ZZZ7(1,counttt);
   BEST(7,1) = rateconstant;
   zipg = x(:,1)./Cinit(7,1);
   zipgt = t;
end
counttt = counttt + 1;
end

%This is for the eigth experimental data set: 1000:1 #2
for rateconstant = alpha:beta:gamma
%_____________________________________________________
%Initial Conditions Matrix
xo = Cinit(8,1);
%Solve the differential equations
[t,x] = ode45('light3',realdata18,xo,[],tau);

MMM8 = abs((realdata28 - x(:,1)./Cinit(8,1))).^2;
ttt8 = cumsum(MMM8);
bbb8 = ttt8(end)./size(realdata28,1);
rrr8 = ((bbb8)^(0.5))./max(realdata28);

ZZZ8(1,counttt) = rrr8;
ZZZ8(2,counttt) = rateconstant;
```

```
if ZZZ8(1,counttt) < aaa8
   aaa8 = ZZZ8(1,counttt);
   BEST(8,1) = rateconstant;
   ziph = x(:,1)./Cinit(8,1);
   zipht = t;
end
counttt = counttt + 1;
end

%This is for the ninth experimental data set: 1000:1 #3
for rateconstant = alpha:beta:gamma
%_____________________________________________________
%Initial Conditions Matrix
xo = Cinit(9,1);
%Solve the differential equations
[t,x] = ode45('light3',realdata19,xo,[],tau);

MMM9 = abs((realdata29 - x(:,1)./Cinit(9,1))).^2;
ttt9 = cumsum(MMM9);
bbb9 = ttt9(end)./size(realdata29,1);
rrr9 = ((bbb9)^(0.5))./max(realdata29);

ZZZ9(1,counttt) = rrr9;
ZZZ9(2,counttt) = rateconstant;

if ZZZ9(1,counttt) < aaa9
   aaa9 = ZZZ9(1,counttt);
   BEST(9,1) = rateconstant;
   zipi = x(:,1)./Cinit(9,1);
   zipit = t;
end
counttt = counttt + 1;
end

%This is for the tenth experimental data set: 250:1 #1
for rateconstant = alpha:beta:gamma
%_____________________________________________________
%Initial Conditions Matrix
xo = Cinit(10,1);
%Solve the differential equations
[t,x] = ode45('light3',realdata110,xo,[],tau);

MMM10 = abs((realdata210 - x(:,1)./Cinit(10,1))).^2;
ttt10 = cumsum(MMM10);
bbb10 = ttt10(end)./size(realdata210,1);
rrr10 = ((bbb10)^(0.5))./max(realdata210);

ZZZ10(1,counttt) = rrr10;
ZZZ10(2,counttt) = rateconstant;
```

```
if ZZZ10(1,counttt) < aaa10
   aaa10 = ZZZ10(1,counttt);
   BEST(10,1) = rateconstant;
   zipj = x(:,1)./Cinit(10,1);
   zipjt = t;
end
counttt = counttt + 1;
end

%This is for the eleventh experimental data set: 250:1 #2
for rateconstant = alpha:beta:gamma
%_____________________________________________________
%Initial Conditions Matrix
xo = Cinit(11,1);
%Solve the differential equations
[t,x] = ode45('light3',realdata111,xo,[],tau);

MMM11 = abs((realdata211 - x(:,1)./Cinit(11,1))).^2;
ttt11 = cumsum(MMM11);
bbb11 = ttt11(end)./size(realdata211,1);
rrr11 = ((bbb11)^(0.5))./max(realdata211);

ZZZ11(1,counttt) = rrr11;
ZZZ11(2,counttt) = rateconstant;

if ZZZ11(1,counttt) < aaa11
   aaa11 = ZZZ11(1,counttt);
   BEST(11,1) = rateconstant;
   zipk = x(:,1)./Cinit(11,1);
   zipkt = t;
end
counttt = counttt + 1;
end

%This is for the twelfth experimental data set: 250:1 #3
for rateconstant = alpha:beta:gamma
%_____________________________________________________
%Initial Conditions Matrix
xo = Cinit(12,1);
%Solve the differential equations
[t,x] = ode45('light3',realdata112,xo,[],tau);

MMM12 = abs((realdata212 - x(:,1)./Cinit(12,1))).^2;
ttt12 = cumsum(MMM12);
bbb12 = ttt12(end)./size(realdata212,1);
rrr12 = ((bbb12)^(0.5))./max(realdata212);

ZZZ12(1,counttt) = rrr12;
ZZZ12(2,counttt) = rateconstant;

if ZZZ12(1,counttt) < aaa12
```

```
   aaa12 = ZZZ12(1,counttt);
   BEST(12,1) = rateconstant;
   zipl = x(:,1)./Cinit(12,1);
   ziplt = t;
end
counttt = counttt + 1;
end

%This is for the thirteenth experimental data set: 50:1 #1
for rateconstant = alpha:beta:gamma
%_____________________________________________________
%Initial Conditions Matrix
xo = Cinit(13,1);
%Solve the differential equations
[t,x] = ode45('light3',realdata113,xo,[],tau);

MMM13 = abs((realdata213 - x(:,1)./Cinit(13,1))).^2;
ttt13 = cumsum(MMM13);
bbb13 = ttt13(end)./size(realdata213,1);
rrr13 = ((bbb13)^(0.5))./max(realdata213);

ZZZ13(1,counttt) = rrr13;
ZZZ13(2,counttt) = rateconstant;

if ZZZ13(1,counttt) < aaa13
   aaa13 = ZZZ13(1,counttt);
   BEST(13,1) = rateconstant;
   zipm = x(:,1)./Cinit(13,1);
   zipmt = t;
end
counttt = counttt + 1;
end

%This is for the fourteenth experimental data set: 50:1 #2
for rateconstant = alpha:beta:gamma
%_____________________________________________________
%Initial Conditions Matrix
xo = Cinit(14,1);
%Solve the differential equations
[t,x] = ode45('light3',realdata114,xo,[],tau);

MMM14 = abs((realdata214 - x(:,1)./Cinit(14,1))).^2;
ttt14 = cumsum(MMM14);
bbb14 = ttt14(end)./size(realdata214,1);
rrr14 = ((bbb14)^(0.5))./max(realdata214);

ZZZ14(1,counttt) = rrr14;
ZZZ14(2,counttt) = rateconstant;

if ZZZ14(1,counttt) < aaa14
   aaa14 = ZZZ14(1,counttt);
```

```
   BEST(14,1) = rateconstant;
   zipn = x(:,1)./Cinit(14,1);
   zipnt = t;
end
counttt = counttt + 1;
end

%This is for the fifteenth experimental data set: 50:1 #3
for rateconstant = alpha:beta:gamma
%_____________________________________________________
%Initial Conditions Matrix
xo = Cinit(15,1);
%Solve the differential equations
[t,x] = ode45('light3',realdata115,xo,[],tau);

MMM15 = abs((realdata215 - x(:,1)./Cinit(15,1))).^2;
ttt15 = cumsum(MMM15);
bbb15 = ttt15(end)./size(realdata215,1);
rrr15 = ((bbb15)^(0.5))./max(realdata215);

ZZZ15(1,counttt) = rrr15;
ZZZ15(2,counttt) = rateconstant;

if ZZZ15(1,counttt) < aaa15
   aaa15 = ZZZ15(1,counttt);
   BEST(15,1) = rateconstant;
   zipo = x(:,1)./Cinit(15,1);
   zipot = t;
end
counttt = counttt + 1;
end

%End of calculations and use of ODE function
%_____________________________________________________________________________________
_____________________________________________________________

%These are individual (each trial for each experiment) plots:

figure(1)
plot(realdata11,realdata21,'bd',zipat,zipa(:,1),'k-.')
title('DNAN Removal, Molar Ratio 100:1, 1 of 3')
xlabel('Time (minutes)')
ylabel('Relative concentration C/Co')
legend('data','model')
axis([0 60 0.50 1])

figure(2)
plot(realdata12,realdata22,'bd',zipbt,zipb(:,1),'k-.')
title('DNAN Removal, Molar Ratio 100:1, 2 of 3')
xlabel('Time (minutes)')
ylabel('Relative concentration C/Co')
```

```
legend('data','model')
axis([0 60 0.50 1])

figure(3)
plot(realdata13,realdata23,'bd',zipct,zipc(:,1),'k-.')
title('DNAN Removal, Molar Ratio 100:1, 3 of 3')
xlabel('Time (minutes)')
ylabel('Relative concentration C/Co')
legend('data','model')
axis([0 60 0.50 1])

figure(4)
plot(realdata14,realdata24,'bd',zipdt,zipd(:,1),'k-.')
title('DNAN Removal, Molar Ratio 500:1, 1 of 3')
xlabel('Time (minutes)')
ylabel('Relative concentration C/Co')
legend('data','model')
axis([0 60 0.50 1])

figure(5)
plot(realdata15,realdata25,'bd',zipet,zipe(:,1),'k-.')
title('DNAN Removal, Molar Ratio 500:1, 2 of 3')
xlabel('Time (minutes)')
ylabel('Relative concentration C/Co')
legend('data','model')
axis([0 60 0.50 1])

figure(6)
plot(realdata16,realdata26,'bd',zipft,zipf(:,1),'k-.')
title('DNAN Removal, Molar Ratio 500:1, 3 of 3')
xlabel('Time (minutes)')
ylabel('Relative concentration C/Co')
legend('data','model')
axis([0 60 0.50 1])

figure(7)
plot(realdata17,realdata27,'bd',zipgt,zipg(:,1),'k-.')
title('DNAN Removal, Molar Ratio 1000:1, 1 of 3')
xlabel('Time (minutes)')
ylabel('Relative concentration C/Co')
legend('data','model')
axis([0 60 0.50 1])

figure(8)
plot(realdata18,realdata28,'bd',zipht,ziph(:,1),'k-.')
title('DNAN Removal, Molar Ratio 1000:1, 2 of 3')
xlabel('Time (minutes)')
ylabel('Relative concentration C/Co')
legend('data','model')
axis([0 60 0.50 1])
```

```
figure(9)
plot(realdata19,realdata29,'bd',zipit,zipi(:,1),'k-.')
title('DNAN Removal, Molar Ratio 1000:1, 3 of 3')
xlabel('Time (minutes)')
ylabel('Relative concentration C/Co')
legend('data','model')
axis([0 60 0.50 1])

figure(10)
plot(realdata110,realdata210,'bd',zipjt,zipj(:,1),'k-.')
title('DNAN Removal, Molar Ratio 250:1, 1 of 3')
xlabel('Time (minutes)')
ylabel('Relative concentration C/Co')
legend('data','model')
axis([0 60 0.50 1])

figure(11)
plot(realdata111,realdata211,'bd',zipkt,zipk(:,1),'k-.')
title('DNAN Removal, Molar Ratio 250:1, 2 of 3')
xlabel('Time (minutes)')
ylabel('Relative concentration C/Co')
legend('data','model')
axis([0 60 0.50 1])

figure(12)
plot(realdata112,realdata212,'bd',ziplt,zipl(:,1),'k-.')
title('DNAN Removal, Molar Ratio 250:1, 3 of 3')
xlabel('Time (minutes)')
ylabel('Relative concentration C/Co')
legend('data','model')
axis([0 60 0.50 1])

figure(13)
plot(realdata113,realdata213,'bd',zipmt,zipm(:,1),'k-.')
title('DNAN Removal, Molar Ratio 50:1, 1 of 3')
xlabel('Time (minutes)')
ylabel('Relative concentration C/Co')
legend('data','model')
axis([0 60 0.50 1])

figure(14)
plot(realdata114,realdata214,'bd',zipnt,zipn(:,1),'k-.')
title('DNAN Removal, Molar Ratio 50:1, 2 of 3')
xlabel('Time (minutes)')
ylabel('Relative concentration C/Co')
legend('data','model')
axis([0 60 0.50 1])

figure(15)
plot(realdata115,realdata215,'bd',zipot,zipo(:,1),'k-.')
title('DNAN Removal, Molar Ratio 50:1, 3 of 3')
```

```
xlabel('Time (minutes)')
ylabel('Relative concentration C/Co')
legend('data','model')
axis([0 60 0.50 1])

%_____
_____

%These are plots categorized by molar ratio with x3 trials plotted:

figure(100)
plot(realdata11,realdata21,'bd',zipat,zipa(:,1),'b-.')
title('DNAN Removal, Molar Ratio 100:1, 3 Trials')
xlabel('Time (minutes)')
ylabel('Relative concentration C/Co')
axis([0 60 0.50 1])
hold on
plot(realdata12,realdata22,'rd',zipbt,zipb(:,1),'r-.')
plot(realdata13,realdata23,'gd',zipct,zipc(:,1),'g-.')
legend ('Trial 1','Model 1','Trial 2','Model 2','Trial 3','Model 3')
hold off

figure(500)
plot(realdata14,realdata24,'bd',zipdt,zipd(:,1),'b-.')
title('DNAN Removal, Molar Ratio 500:1, 3 Trials')
xlabel('Time (minutes)')
ylabel('Relative concentration C/Co')
axis([0 60 0.50 1])
hold on
plot(realdata15,realdata25,'rd',zipet,zipe(:,1),'r-.')
plot(realdata16,realdata26,'gd',zipft,zipf(:,1),'g-.')
legend ('Trial 1','Model 1','Trial 2','Model 2','Trial 3','Model 3')
hold off

figure(1000)
plot(realdata17,realdata27,'bd',zipgt,zipg(:,1),'b-.')
title('DNAN Removal, Molar Ratio 1000:1,  Trials')
xlabel('Time (minutes)')
ylabel('Relative concentration C/Co')
axis([0 60 0.50 1])
hold on
plot(realdata18,realdata28,'rd',zipht,ziph(:,1),'r-.')
plot(realdata19,realdata29,'gd',zipit,zipi(:,1),'g-.')
legend ('Trial 1','Model 1','Trial 2','Model 2','Trial 3','Model 3')
hold off

figure(250)
plot(realdata110,realdata210,'bd',zipjt,zipj(:,1),'b-.')
title('DNAN Removal, Molar Ratio 250:1, 3 Trials')
xlabel('Time (minutes)')
ylabel('Relative concentration C/Co')
```

```
axis([0 60 0.50 1])
hold on
plot(realdata111,realdata211,'rd',zipkt,zipk(:,1),'r-.')
plot(realdata112,realdata212,'gd',ziplt,zipl(:,1),'g-.')
legend ('Trial 1','Model 1','Trial 2','Model 2','Trial 3','Model 3')
hold off

figure(50)
plot(realdata113,realdata213,'bd',zipmt,zipm(:,1),'b-.')
title('DNAN Removal, Molar Ratio 50:1, 3 Trials')
xlabel('Time (minutes)')
ylabel('Relative concentration C/Co')
axis([0 60 0.50 1])
hold on
plot(realdata114,realdata214,'rd',zipnt,zipn(:,1),'r-.')
plot(realdata115,realdata215,'gd',zipot,zipo(:,1),'g-.')
legend ('Trial 1','Model 1','Trial 2','Model 2','Trial 3','Model 3')
hold off

xlswrite('DNANregressions.xls',zipa,'100-1#1','B6');
xlswrite('DNANregressions.xls',zipat,'100-1#1','C6');
xlswrite('DNANregressions.xls',zipb,'100-1#2','B6');
xlswrite('DNANregressions.xls',zipbt,'100-1#2','C6');
xlswrite('DNANregressions.xls',zipc,'100-1#3','B6');
xlswrite('DNANregressions.xls',zipct,'100-1#3','C6');
xlswrite('DNANregressions.xls',zipd,'500-1#1','B6');
xlswrite('DNANregressions.xls',zipdt,'500-1#1','C6');
xlswrite('DNANregressions.xls',zipe,'500-1#2','B6');
xlswrite('DNANregressions.xls',zipet,'500-1#2','C6');
xlswrite('DNANregressions.xls',zipf,'500-1#3','B6');
xlswrite('DNANregressions.xls',zipft,'500-1#3','C6');
xlswrite('DNANregressions.xls',zipg,'1000-1#1','B6');
xlswrite('DNANregressions.xls',zipgt,'1000-1#1','C6');
xlswrite('DNANregressions.xls',ziph,'1000-1#2','B6');
xlswrite('DNANregressions.xls',zipht,'1000-1#2','C6');
xlswrite('DNANregressions.xls',zipi,'1000-1#3','B6');
xlswrite('DNANregressions.xls',zipit,'1000-1#3','C6');
xlswrite('DNANregressions.xls',zipj,'250-1#1','B6');
xlswrite('DNANregressions.xls',zipjt,'250-1#1','C6');
xlswrite('DNANregressions.xls',zipk,'250-1#2','B6');
xlswrite('DNANregressions.xls',zipkt,'250-1#2','C6');
xlswrite('DNANregressions.xls',zipl,'250-1#3','B6');
xlswrite('DNANregressions.xls',ziplt,'250-1#3','C6');
xlswrite('DNANregressions.xls',zipm,'50-1#1','B6');
xlswrite('DNANregressions.xls',zipmt,'50-1#1','C6');
xlswrite('DNANregressions.xls',zipn,'50-1#2','B6');
xlswrite('DNANregressions.xls',zipnt,'50-1#2','C6');
xlswrite('DNANregressions.xls',zipo,'50-1#3','B6');
xlswrite('DNANregressions.xls',zipot,'50-1#3','C6');

xlswrite('DNANregressions.xls',BEST(:,1),'BEST','C6');
```

```
%the following block is needed to calculate and display the runtime.
tstop = clock;
runtime = etime(tstop,tstart)./60;
disp('length of run in minutes:')
disp(runtime)
```

Matlab DNAN Data File

```
%June 2020 - AFIT
%Authors: W. Harper and J. Hart
%Project: 2019-20 UV LED project

global Cinit realdata11 realdata12 realdata13 realdata14 realdata15 realdata16 realdata17 realdata18
realdata19 realdata110 realdata111 realdata112 realdata113 realdata114 realdata115 realdata21
realdata22 realdata23 realdata24 realdata25 realdata26 realdata27 realdata28 realdata29 realdata210
realdata211 realdata212 realdata213 realdata214 realdata215

%this is a data file
%realdata1* entries are time in minutes
%realdata2* entries are relative concentration
%Cinit is the matrix of initial concentrations
%
%_____________________________________________________________
Cinit = [9.5831
9.3578
9.4945
9.6071
9.1886
9.3263
9.3010
9.5583
9.6419
9.5980
9.7363
9.4572
9.5464
9.5551
9.6456];
%_____________________________________________________

%_____________________________________________________________________________________________
_____________________________________________________________
%molar ratio = 100:1
%Experiment #1 of 3
%time data:
realdata11 = [0
5
```

```
10
15
20
25
35
45
60];

%relative concentration C/Co
%NOTE: These relative concentrations use the concentration (C_t) calculated
%by the calibration curve slope and measured concentration for that
%particular experiment (which changes for each day). The initial
%concentration which each C_t is divided by to normalize the data is an
%average of the control experiment concentrations measured over 1 hour
%prior to the actual experiment with the UV LED powered. Therefore, the
%starting concentration for the DNAN solution entering the reactor changes
%for each day and this is normalized so that the relative concentration is
%1.0 for each experiment.
realdata21 = [1.0000
0.8936
0.8271
0.7860
0.7753
0.7525
0.7324
0.7320
0.7187];
%_____
_____
%_____
_____
%molar ratio = 100:1
%Experiment #2 of 3
%time data:
realdata12 = [0
5
10
15
20
25
35
45
60];

%relative concentration C/Co
%Note: None
realdata22 = [1.0000
0.9199
0.8536
0.8224
0.7913
```

```
0.7654
0.7548
0.7500
0.7444];
%Note: Check this graph and rate constant to ensure it isn't messing up due to the lack of a value for
60min.
%_____
_____
%_____
_____
%molar ratio = 100:1
%Experiment #3 of 3
%time data:
realdata13 = [0
5
10
15
20
25
35
45
60];

%relative concentration C/Co
realdata23 = [1.0000
0.9194
0.8559
0.8254
0.8037
0.7816
0.7648
0.7588
0.7294];
%_____
_____
%_____
_____
%molar ratio = 500:1
%Experiment #1 of 3
%time data:
realdata14 = [0
5
10
15
20
25
35
45
60];

%relative concentration C/Co
```

```
realdata24 = [1.0000
0.8606
0.8135
0.7557
0.7432
0.7212
0.6908
0.6848
0.6286];
%_____
_____
%_____
_____
%molar ratio = 500:1
%Experiment #2 of 3
%time data:
realdata15 = [0
5
10
15
20
25
35
45
60];

%relative concentration C/Co
realdata25 = [1.0000
0.8661
0.7671
0.7567
0.7114
0.7062
0.6989
0.6900
0.6832];
%_____
_____
%_____
_____
%molar ratio = 500:1
%Experiment #3 of 3
%time data:
realdata16 = [0
5
10
15
20
25
35
45
```

```
60];

%relative concentration C/Co
realdata26 = [1.0000
0.8483
0.7752
0.7540
0.7295
0.7149
0.7142
0.6932
0.6879];
%_____
_____
%_____
_____
%molar ratio = 1000:1
%Experiment #1 of 3
%time data:
realdata17 = [0
5
10
15
20
25
35
45
60];

%relative concentration C/Co
realdata27 = [1.0000
0.8405
0.7954
0.7512
0.7348
0.7280
0.7125
0.7217
0.7139];
%_____
_____
%_____
_____
%molar ratio = 1000:1
%Experiment #2 of 3
%time data:
realdata18 = [0
5
10
15
20
```

```
25
35
45
60];

%relative concentration C/Co
realdata28 = [1.0000
0.8305
0.7944
0.7689
0.7564
0.7477
0.7210
0.7092
0.7058];
%_____
_____
%_____
_____
%molar ratio = 1000:1
%Experiment #3 of 3
%time data:
realdata19 = [0
5
10
15
20
25
35
45
60];

%relative concentration C/Co
realdata29 = [1.0000
0.7636
0.7057
0.6808
0.6676
0.6529
0.6446
0.6387
0.6259];

%_____
_____
%_____
_____
%molar ratio = 250:1
%Experiment #1 of 3
%time data:
realdata110 = [0
```

```
5
10
15
20
25
35
45
60];

%relative concentration C/Co
realdata210 = [1.0000
0.8455
0.7949
0.7697
0.7306
0.7152
0.7098
0.7008
0.6859];

%_____
_____
%_____
_____
%molar ratio = 250:1
%Experiment #2 of 3
%time data:
realdata111 = [0
5
10
15
20
25
35
45
60];

%relative concentration C/Co
realdata211= [1.0000
0.8324
0.7859
0.7302
0.7190
0.7094
0.6948
0.6914
0.6911];

%_____
_____
```

```
%_____
_____
%molar ratio = 250:1
%Experiment #3 of 3
%time data:
realdata112 = [0
5
10
15
20
25
35
45
60];

%relative concentration C/Co
realdata212 = [1.0000
0.8454
0.8055
0.7629
0.7365
0.7363
0.7278
0.7289
0.7149];

%_____
_____
%_____
_____
%molar ratio = 50:1
%Experiment #1 of 3
%time data:
realdata113 = [0
5
10
15
20
25
35
45
60];

%relative concentration C/Co
realdata213 = [1.0000
0.8999
0.8909
0.8366
0.8280
0.8155
0.8047
```

```
0.8115
0.8144];

%_____
_____
%_____
_____
%molar ratio = 50:1
%Experiment #2 of 3
%time data:
realdata114 = [0
5
10
15
20
25
35
45
60];

%relative concentration C/Co
realdata214 = [1.0000
0.9086
0.8700
0.8492
0.8342
0.8256
0.8210
0.8209
0.8111];

%_____
_____
%_____
_____
%molar ratio = 50:1
%Experiment #3 of 3
%time data:
realdata115 = [0
5
10
15
20
25
35
45
60];

%relative concentration C/Co
realdata215 = [1.0000
0.9015
```

```
0.8656
0.8483
0.8157
0.8174
0.8070
0.8078
0.8030];

%_____
_____
%_____
_____
```

Appendix E: HPLC Method File Data

Data File : D:\data\20200529_DNAN_A 2020-05-29 10-57-18\1ED-1301.D
Acq. Method: 20200220_BBP_D_DAD_MS_DLF.M

The Acq. Method's Instrument Parameters for the Run were :

==========
FLD
==========

FLD (G1321B)
============

Detection Mode: Fluorescence Mode
Peakwidth: > 0.2 min (4 s resp. time) (2.31 Hz)
PMT gain: 10
Baseline Behaviour Mode: Append
Fit spectra range on: Yes
Analog Output Source Channel 1: 1
Analog Output Source Channel 2: 2
Signal polarity: Positive (+)

Posttime
Posttime Mode: Off

Multiple Wavelengths
Multi Wavelength Mode: Off

Analog Output 1
Analog 1 Attenuation: 100 LU
Analog 1 Zero Offset: 5 %

Analog Output 2
Analog 2 Attenuation: 100 LU
Analog 2 Zero Offset: 5 %

Lamp Settings
Lamp on only during run: Yes
Lamp on required for analysis: No
Lamp economy mode on: No
Lamp energy reference mode on: No

Fluorescence Scan Range

Excitation Scan
Scan Excitation WL From: 220 nm
Scan Excitation WL To: 380 nm
Scan Excitation WL Step: 5 nm

Emission Scan
Scan Emission WL From: 300 nm
Scan Emission WL To: 500 nm
Scan Emission WL Step: 5 nm

Signal A

Excitation
Use Signal: Yes
Signal: Signal A
Wavelength Mode: Zero order

Emission
Use Signal: Yes
Signal: Signal A
Wavelength Mode: Zero order

Stoptime
Stoptime Mode: As pump/injector

Timetable

==========
DAD
==========

DAD (G1315C)
============

Peakwidth: >0.10 min (2.0 s response time) (2.5 Hz)
Slit: 4 nm
UV Lamp Required: Yes
Vis Lamp Required: Yes

Analog Output 1
Analog 1 Attenuation: 1000 mAU
Analog 1 Zero Offset: 5 %

Analog Output 2
Analog 2 Attenuation: 1000 mAU
Analog 2 Zero Offset: 5 %

Signals
Signal table

Use Sig.	Signal	Wavelength nm	Bandwidth nm	Use Ref.
Yes	Signal A	253	10	No

Yes Signal B 300 200 No
Yes Signal C 300 20 No
Yes Signal D 270 10 No
No Signal E
No Signal F
No Signal G
No Signal H

Prepare Mode
Margin for negative Absorbance: 100 mAU

Autobalance
Autobalance Prerun: Yes
Autobalance Postrun: No

Spectrum
Spectrum Store: None

Stoptime
Stoptime Mode: As pump/injector

Posttime
Posttime Mode: Off

Timetable

Instrument Curves
Store Board Temperature: No
Store Optical Unit Temperature: No
Store UV Lamp Anode Voltage: No

==========
Column Comp.
==========

Column Comp. (G1316A)
==========

Valve Position: Port 1 -> 2

Left Temperature Control
Temperature Control Mode: Temperature Set
Temperature: 30.00 °C

Enable Analysis Left Temperature
Enable Analysis Left Temperature On: Yes
Enable Analysis Left Temperature Value: 0.80 °C

Right Temperature Control
Right temperature Control Mode: Temperature Set
Right temperature: 30.00 °C

Enable Analysis Right Temperature
Enable Analysis Right Temperature On: Yes
Enable Analysis Right Temperature Value: 0.80 °C

Stop Time
Stoptime Mode: As pump/injector

Post Time
Posttime Mode: Off

Timetable

Instrument Curves
Store Left Temperature: Yes
Store Right Temperature: No

==========

HiP Sampler

==========

HiP Sampler (G1367E)
==========

Auxiliary
Draw Speed: 100.0 µl/min
Eject Speed: 100.0 µl/min
Draw Position Offset: 0.0 mm
Wait Time After Drawing: 2.0 s
Sample Flush Out Factor: 5.0
Vial/Well bottom sensing: No

Injection
Injection Mode: Standard injection
Injection Volume: 20.00 µL

High throughput
Automaitc Delay Volume Reduction: No
Overlapped Injection
Enable Overlapped Injection: No

Valve Switching
Valve Movements: 0

Valve Switch Time 1
Switch Time 1 Enabled: No

Valve Switch Time 2
Switch Time 2 Enabled: No

Valve Switch Time 3
Switch Time 3 Enabled: No

Valve Switch Time 4
Switch Time 4 Enabled: No

Stop Time
Stoptime Mode: As pump/No limit

Post Time
Posttime Mode: Off

Timetable

Instrument Curves
Store Temperature: No

==========
Valve
==========

Valve (G1170A)
==========

Position Switching Mode: Use valve position
Valve position: 1
After Run Position Switching Mode: Do not switch

Stop Time
Stoptime Mode: As pump/injector

Post Time
Posttime Mode: Off

Timetable

Position Description
Position Position Description

---
1 dad
2

3	flo
4	Channel 4
5	Channel 5
6	Channel 6
7	Channel 7
8	Channel 8
9	by pass
10	MS
11	Channel 11
12	Channel 12

==========

Quat. Pump

==========

Quat. Pump (G1311B)

==========

Flow:	0.600 ml/min
Low Pressure Limit:	0.00 bar
High Pressure Limit:	550.00 bar
Maximum Flow Gradient:	100.000 ml/min²
Primary Channel:	Automatic

Stroke

Automatic Stroke Calculation:	Yes

Compress

Compressibility Mode:	Compressibility Value Set
Compressibility:	100 10e-6/bar

Stop Time

Stoptime Mode:	Time set
Stoptime:	2.50 min

Post Time

Posttime Mode:	Off

Timetable

Solvent Composition

Channel	Name 1	Used	Percent %
A	Yes	50.0	
B	No		
C	Yes	10.0	
D	Yes	40.0	

Instrument Curves
Store Pressure: Yes
Store Flow: Yes
Store Solvent Ratio A: Yes
Store Solvent Ratio B: Yes
Store Solvent Ratio C: Yes
Store Solvent Ratio D: Yes
Store Direction of Piston A: No

==========

Mass Spectrometer Detector

==========

General Information

Use MSD : Enabled
Tune File : tunes20200218.tun
StopTime : No Limit
Time Filter : Enabled
Data Storage : Condensed
Peakwidth : 0.05 min
Fast Scan : Disabled
Fast Scan Data Reconstruction: Disabled
Polarity Switch Delay : 50 ms
Ionization Switch Delay : 50 ms

Signals

[Signal 1]

Ionization Mode : API-ES
Polarity : Positive
Fragmentor Ramp : Disabled
Percent Cycle Time : 100.00 %

Scan Parameters

Time (min)	Mass Range Low	High	Frag-mentor	Gain EMV	Thres-hold	Step-size
0.00	175.00	250.00	35	1.0	150	0.20

[Signal 2]
Not Active

[Signal 3]
Not Active

[Signal 4]
Not Active

Spray Chamber
----- -------
[MSZones]

Gas Temp : 300 C maximum 350 C
DryingGas : 10.0 l/min maximum 13.0 l/min
Neb Pres : 45 psig maximum 60 psig
Quad Temp : 0 C maximum 0 C

VCap (Positive) : 4000 V
VCap (Negative) : 3500 V

[Time Table]
Time Table is empty.

END OF MS ACQUISITION PARAMETERS

==========

FIA Series

==========

FIA Series in this Method : Disabled

Time Setting
Time between Injections : 0.15 min
Injection Loop Flush Time : 0.17 min

==========

Column(s)

==========

Column Description : Eclipse XDB-C18
Serial# : autoID-11
Product# : 993967-902 Batch# :
Diameter : 4.6 mm Length : 150.0 mm
Particle size : 5.0 µm Void volume : 60.0 %
Maximum Pressure : 400.0 bar Maximum pH : 9.0
Minimum pH : 2.0
Maximum Temperature: 60.0 °C
Comment :

Appendix F: HPLC Chromatograms

Calibration Curve 250:1 Blank

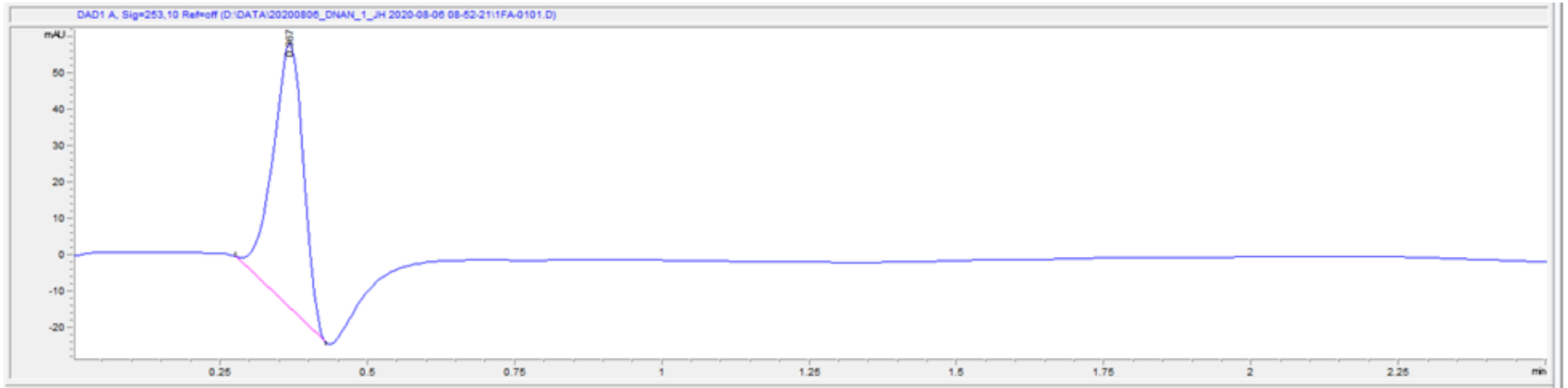

File Information	
LC-File	1FA-0101.D
File Path	D:\DATA\20200806_DNAN_1_JH 2020-08-06 08-52-21\
Date	06-Aug-20, 08:53:36
Sample	Blank
Sample Info	
Barcode	
Operator	user
Method	20200220_BBP_D_DAD_MS_DLF.M
Analysis Time	2.5 min
Sampling Rate	0.0067 min (0.402 sec), 376 datapoints

#	Time	Area	Height	Width	Area%	Symmetry
1	0.367	262.2	72.6	0.0562	100.000	1.168

Calibration Curve 250:1 10%

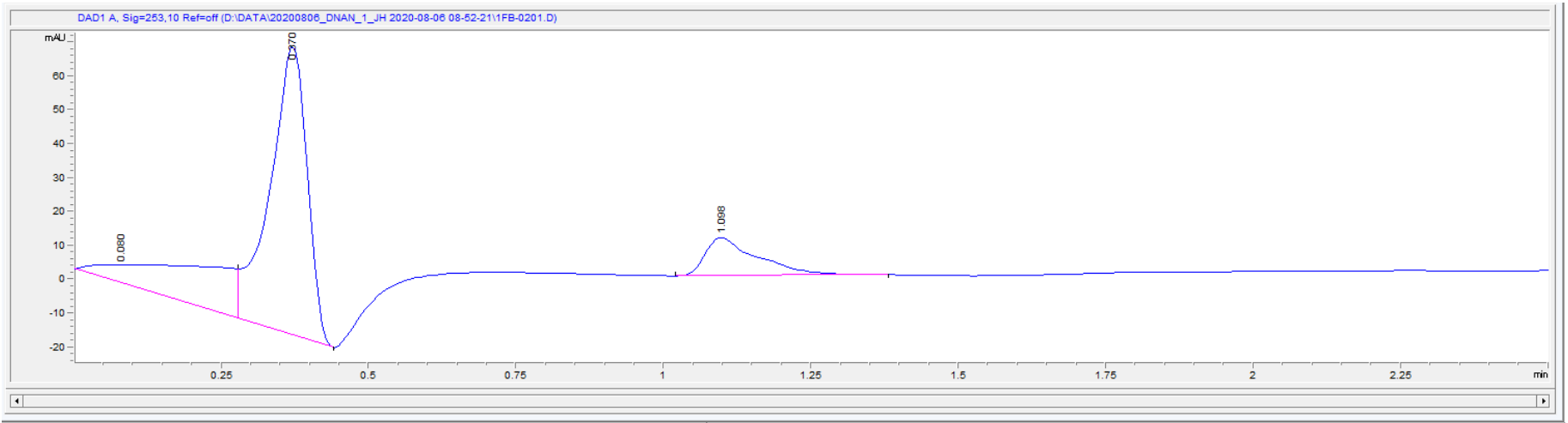

File Information

LC-File	1FB-0201.D
File Path	D:\DATA\20200806_DNAN_1_JH 2020-08-06 08-52-21\
Date	06-Aug-20, 08:57:15
Sample	10%
Sample Info	
Barcode	
Operator	user
Method	20200220_BBP_D_DAD_MS_DLF.M
Analysis Time	2.5 min
Sampling Rate	0.0067 min (0.402 sec), 376 datapoints

#	Time	Area	Height	Width	Area%	Symmetry
1	8.004E-2	135	5.3	0.3178	23.471	0.123
2	0.37	371.1	85.1	0.0649	64.504	1.5
3	1.098	69.2	11.3	0.0851	12.025	0.402

Calibration Curve 250:1 20%

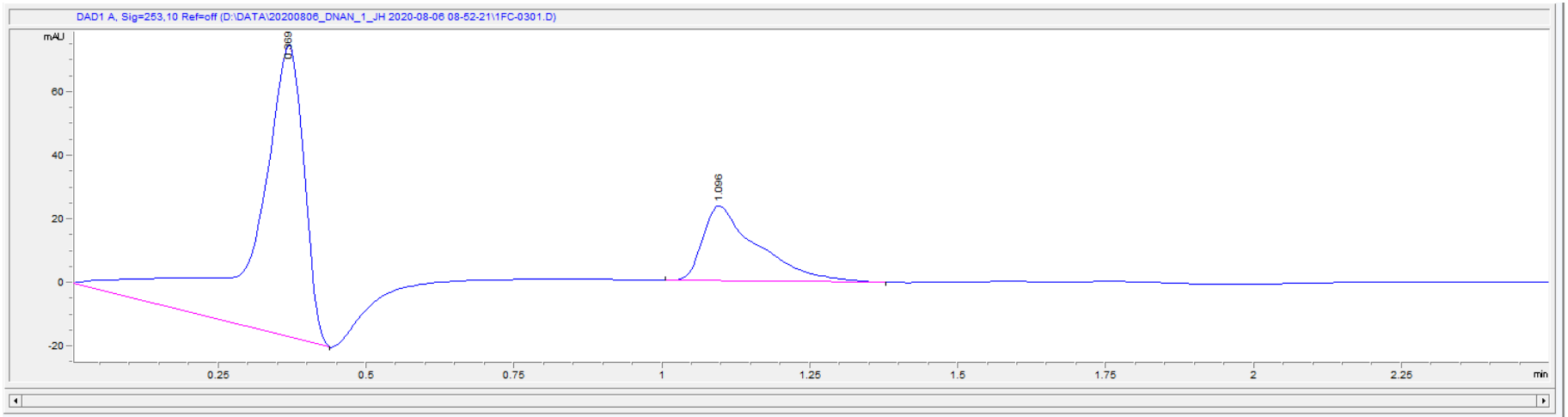

File Information

LC-File	1FC-0301.D
File Path	D:\DATA\20200806_DNAN_1_JH 2020-08-06 08-52-21\
Date	06-Aug-20, 09:00:52
Sample	20%
Sample Info	
Barcode	
Operator	user
Method	20200220_BBP_D_DAD_MS_DLF.M
Analysis Time	2.493 min
Sampling Rate	0.0067 min (0.402 sec), 375 datapoints

#	Time	Area	Height	Width	Area%	Symmetry
1	0.369	538.2	92.1	0.0822	78.137	2.362
2	1.096	150.6	23.6	0.0884	21.863	0.388

Calibration Curve 250:1 40%

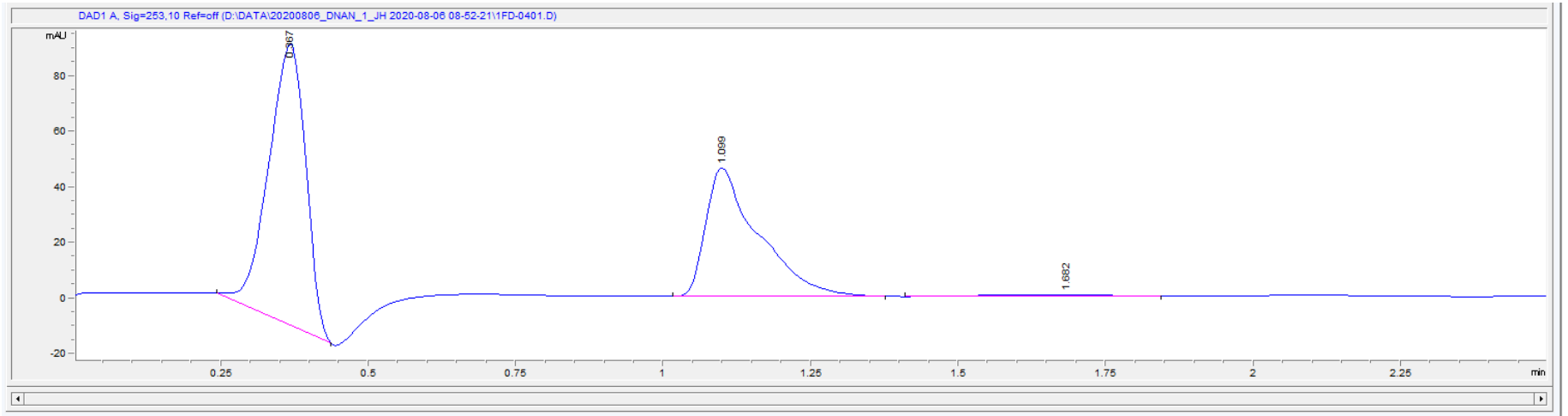

File Information

LC-File	1FD-0401.D
File Path	D:\DATA\20200806_DNAN_1_JH 2020-08-06 08-52-21\
Date	06-Aug-20, 09:04:32
Sample	40%
Sample Info	
Barcode	
Operator	user
Method	20200220_BBP_D_DAD_MS_DLF.M
Analysis Time	2.493 min
Sampling Rate	0.0067 min (0.402 sec), 375 datapoints

#	Time	Area	Height	Width	Area%	Symmetry
1	0.367	443	101.3	0.069	60.092	1.341
2	1.099	284.9	46.4	0.0856	38.637	0.4
3	1.682	9.4	6.7E-1	0.1921	1.271	1.799

Calibration Curve 250:1 60%

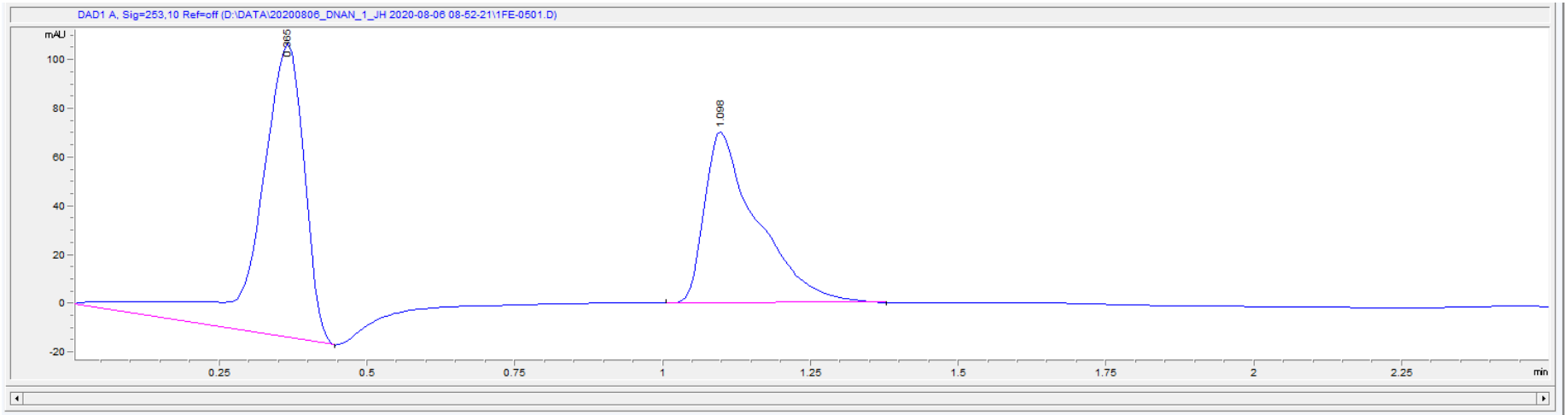

File Information

LC-File	1FE-0501.D
File Path	D:\DATA\20200806_DNAN_1_JH 2020-08-06 08-52-21\
Date	06-Aug-20, 09:08:11
Sample	60%
Sample Info	
Barcode	
Operator	user
Method	20200220_BBP_D_DAD_MS_DLF.M
Analysis Time	2.493 min
Sampling Rate	0.0067 min (0.402 sec), 375 datapoints

#	Time	Area	Height	Width	Area%	Symmetry
1	0.365	663.2	120.4	0.0843	60.434	1.843
2	1.098	434.2	70.3	0.0881	39.566	0.399

Calibration Curve 250:1 80%

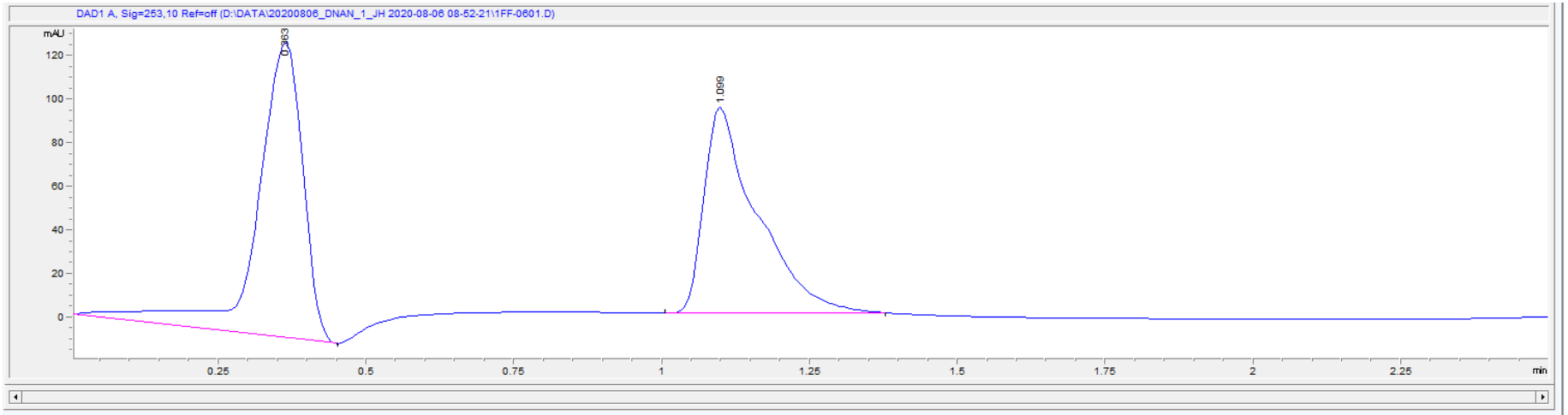

File Information

LC-File	1FF-0601.D
File Path	D:\DATA\20200806_DNAN_1_JH 2020-08-06 08-52-21\
Date	06-Aug-20, 09:11:50
Sample	80%
Sample Info	
Barcode	
Operator	user
Method	20200220_BBP_D_DAD_MS_DLF.M
Analysis Time	2.493 min
Sampling Rate	0.0067 min (0.402 sec), 375 datapoints

#	Time	Area	Height	Width	Area%	Symmetry
1	0.363	730.3	135.7	0.0848	55.409	1.667
2	1.099	587.7	94.5	0.0886	44.591	0.397

Calibration Curve 250:1 100%

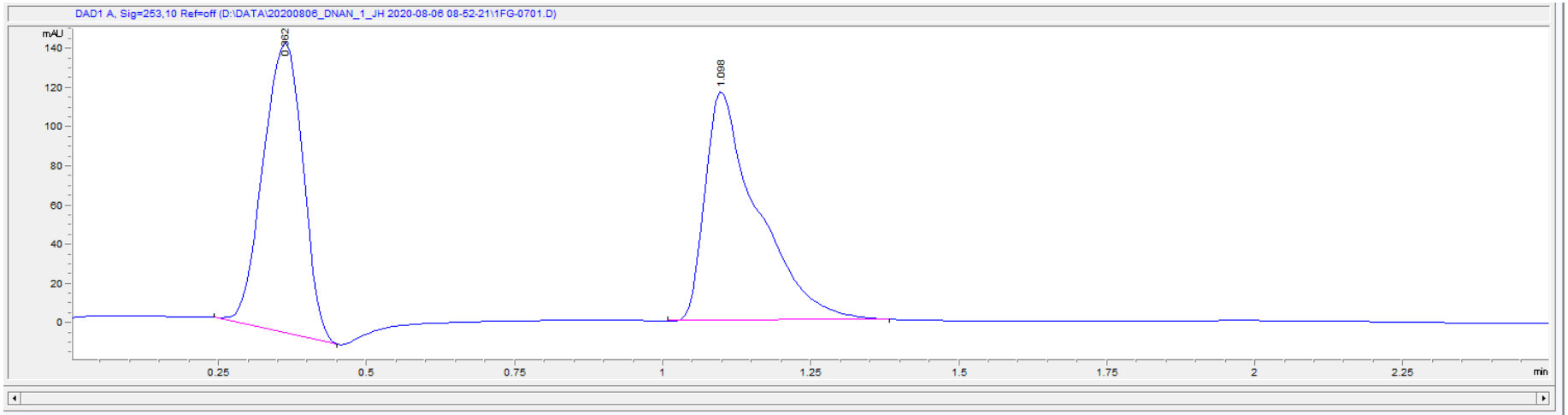

File Information	
LC-File	1FG-0701.D
File Path	D:\DATA\20200806_DNAN_1_JH 2020-08-06 08-52-21\
Date	06-Aug-20, 09:15:29
Sample	100%
Sample Info	
Barcode	
Operator	user
Method	20200220_BBP_D_DAD_MS_DLF.M
Analysis Time	2.493 min
Sampling Rate	0.0067 min (0.402 sec), 375 datapoints

#	Time	Area	Height	Width	Area%	Symmetry
1	0.362	692.7	147.9	0.0766	48.927	1.177
2	1.098	723.1	117.2	0.086	51.073	0.398

Control 250:1 0 min

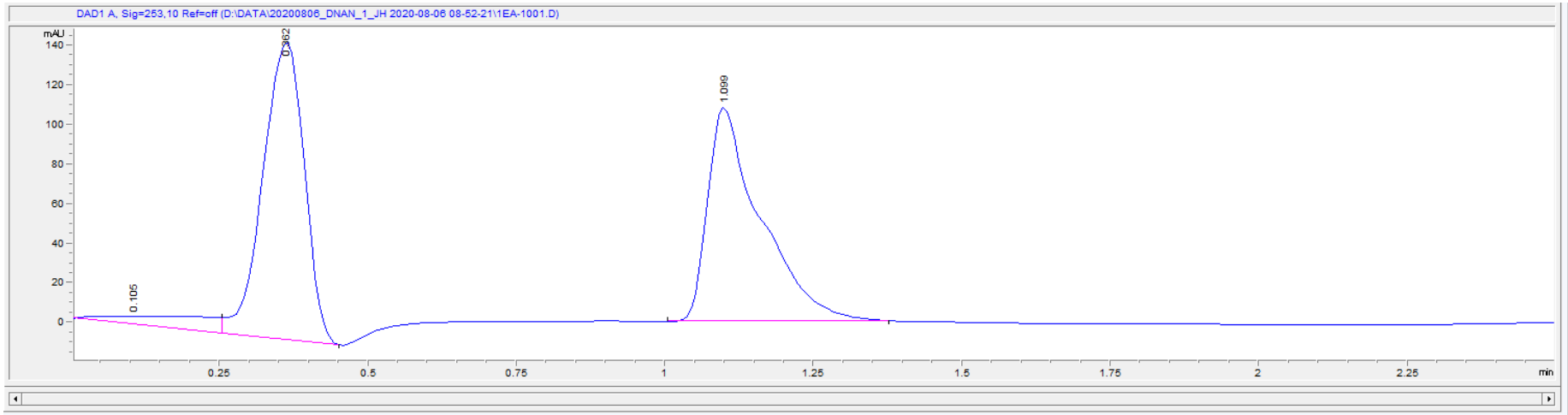

File Information	
LC-File	1EA-1001.D
File Path	D:\DATA\20200806_DNAN_1_JH 2020-08-06 08-52-21\
Date	06-Aug-20, 09:26:23
Sample	C1 0min
Sample Info	
Barcode	
Operator	user
Method	20200220_BBP_D_DAD_MS_DLF.M
Analysis Time	2.493 min
Sampling Rate	0.0067 min (0.402 sec), 375 datapoints

#	Time	Area	Height	Width	Area%	Symmetry
1	0.105	70.2	4.2	0.2193	4.787	0.278
2	0.362	728.5	150.1	0.0786	49.649	1.259
3	1.099	668.6	108.1	0.0882	45.564	0.403

Control 250:1 10 min

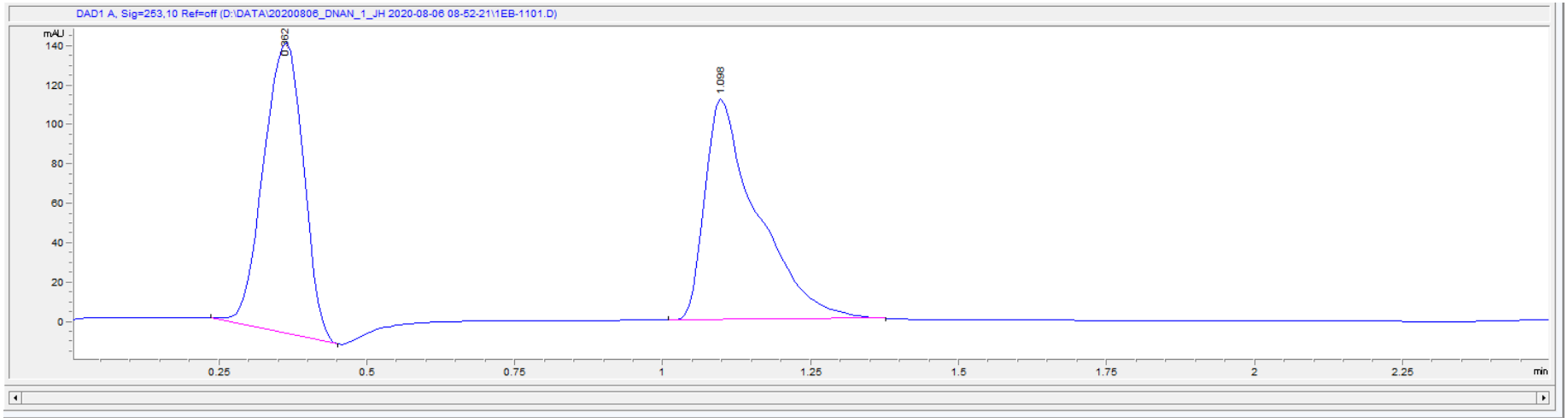

File Information	
LC-File	1EB-1101.D
File Path	D:\DATA\20200806_DNAN_1_JH 2020-08-06 08-52-21\
Date	06-Aug-20, 09:30:03
Sample	C2 10min
Sample Info	
Barcode	
Operator	user
Method	20200220_BBP_D_DAD_MS_DLF.M
Analysis Time	2.493 min
Sampling Rate	0.0067 min (0.402 sec), 375 datapoints

#	Time	Area	Height	Width	Area%	Symmetry
1	0.362	691.1	147.4	0.0767	49.947	1.182
2	1.098	692.5	112.3	0.088	50.053	0.402

Control 250:1 20 min

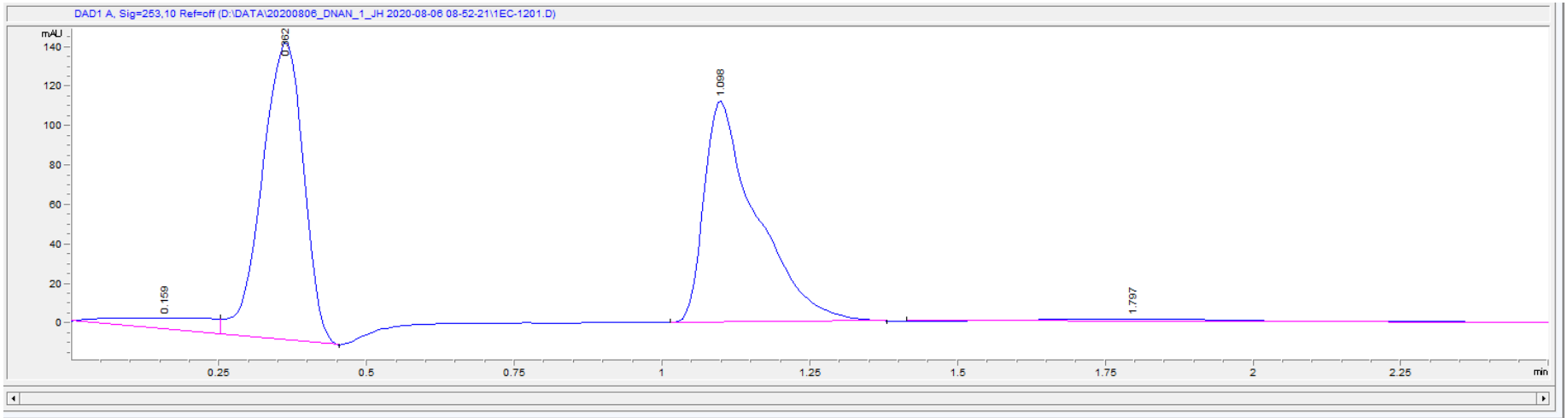

File Information	
LC-File	1EC-1201.D
File Path	D:\DATA\20200806_DNAN_1_JH 2020-08-06 08-52-21\
Date	06-Aug-20, 09:33:41
Sample	C3 20min
Sample Info	
Barcode	
Operator	user
Method	20200220_BBP_D_DAD_MS_DLF.M
Analysis Time	2.5 min
Sampling Rate	0.0067 min (0.402 sec), 376 datapoints

#	Time	Area	Height	Width	Area%	Symmetry
1	0.159	70.4	5.8	0.1814	4.570	0.982
2	0.362	734.9	150.7	0.0789	47.713	1.248
3	1.098	694.5	112.5	0.0861	45.088	0.405
4	1.797	40.5	1.5	0.3473	2.629	0.721

Control 250:1 30 min

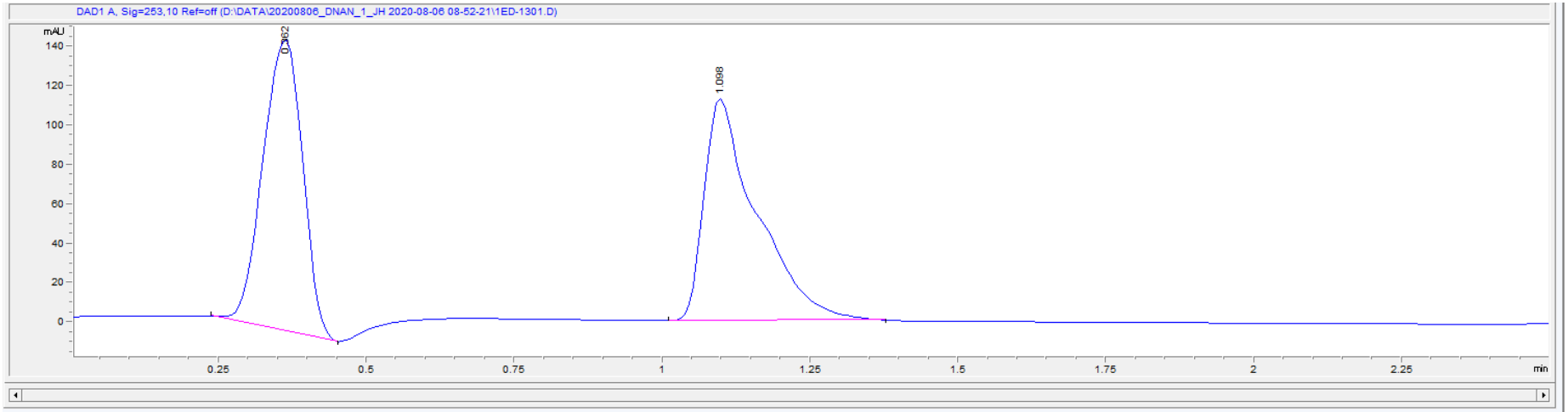

File Information

LC-File	1ED-1301.D
File Path	D:\DATA\20200806_DNAN_1_JH 2020-08-06 08-52-21\
Date	06-Aug-20, 09:37:20
Sample	C4 30min
Sample Info	
Barcode	
Operator	user
Method	20200220_BBP_D_DAD_MS_DLF.M
Analysis Time	2.493 min
Sampling Rate	0.0067 min (0.402 sec), 375 datapoints

#	Time	Area	Height	Width	Area%	Symmetry
1	0.362	691.9	147.8	0.0766	49.829	1.185
2	1.098	696.6	112.6	0.0882	50.171	0.399

Control 250:1 40 min

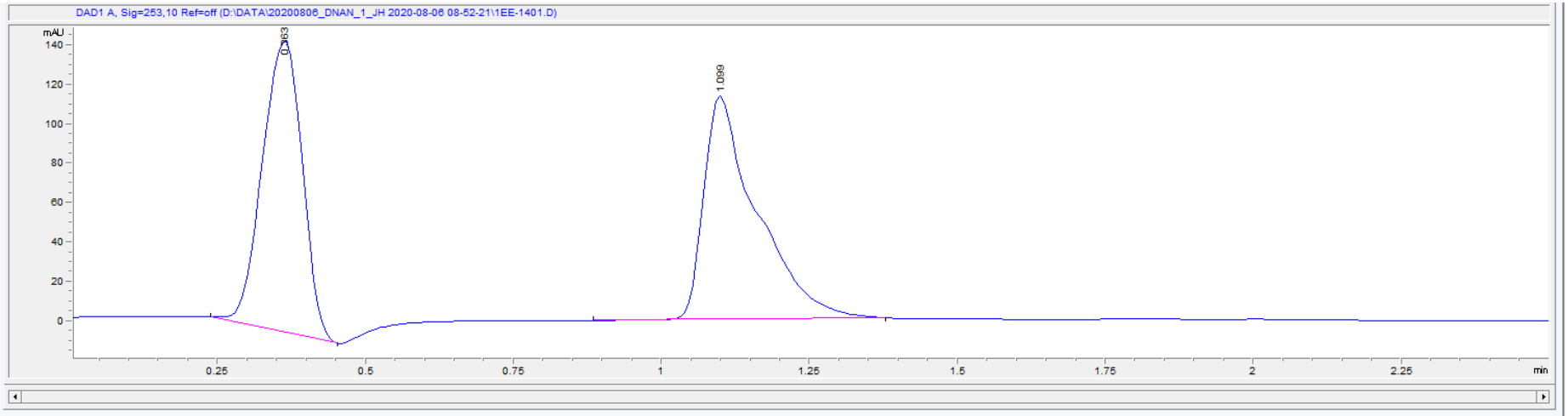

File Information

LC-File	1EE-1401.D
File Path	D:\DATA\20200806_DNAN_1_JH 2020-08-06 08-52-21\
Date	06-Aug-20, 09:40:58
Sample	C5 40min
Sample Info	
Barcode	
Operator	user
Method	20200220_BBP_D_DAD_MS_DLF.M
Analysis Time	2.493 min
Sampling Rate	0.0067 min (0.402 sec), 375 datapoints

#	Time	Area	Height	Width	Area%	Symmetry
1	0.363	693.2	147.9	0.0767	49.548	1.179
2	1.099	705.8	113.4	0.0886	50.452	0.403

Control 250:1 50 min

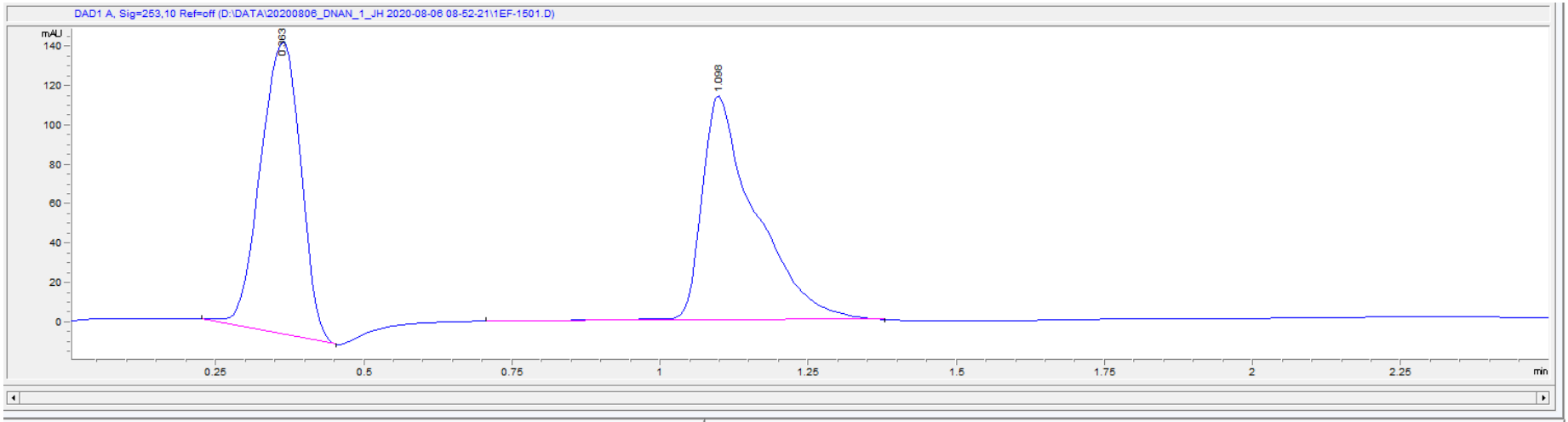

File Information	
LC-File	1EF-1501.D
File Path	D:\DATA\20200806_DNAN_1_JH 2020-08-06 08-52-21\
Date	06-Aug-20, 09:44:37
Sample	C6 50min
Sample Info	
Barcode	
Operator	user
Method	20200220_BBP_D_DAD_MS_DLF.M
Analysis Time	2.493 min
Sampling Rate	0.0067 min (0.402 sec), 375 datapoints

#	Time	Area	Height	Width	Area%	Symmetry
1	0.363	701.7	148.3	0.0772	49.415	1.188
2	1.098	718.4	113.9	0.0896	50.585	0.416

Control 250:1 60 min

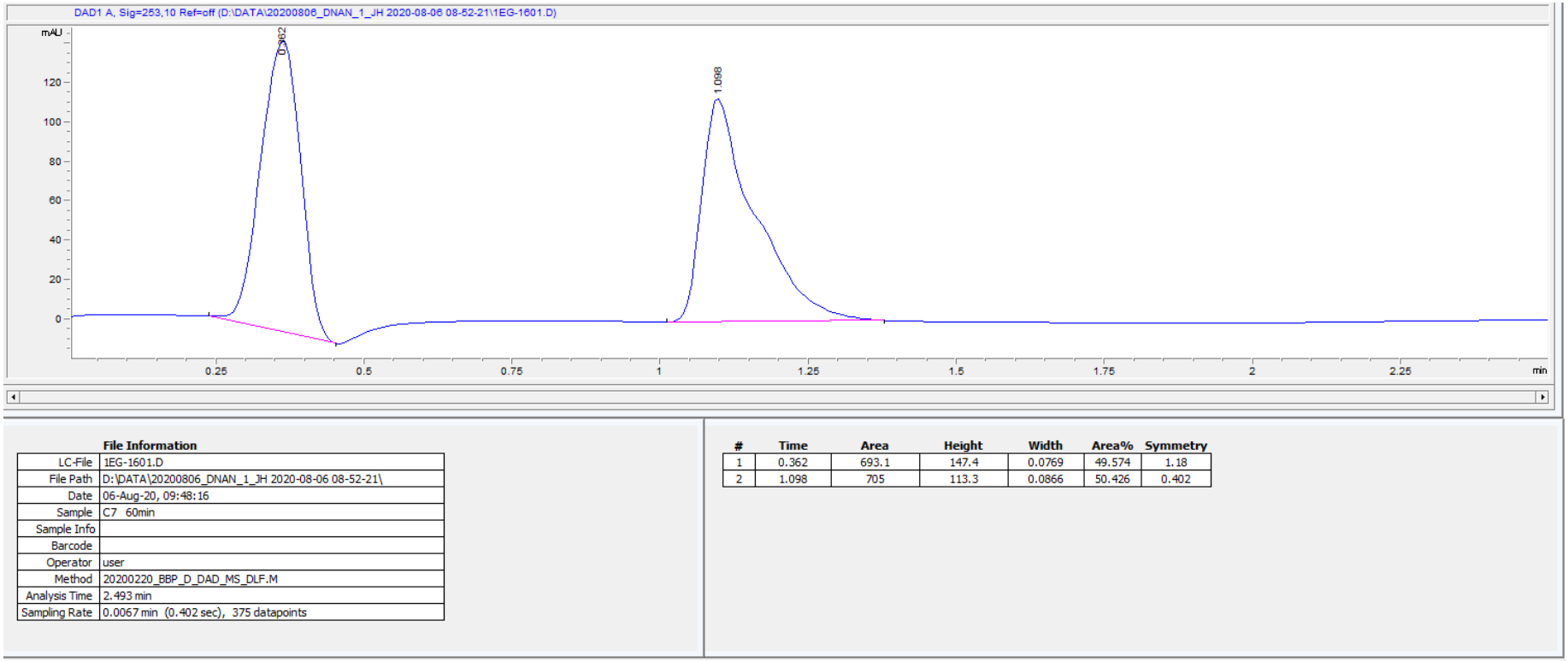

File Information	
LC-File	1EG-1601.D
File Path	D:\DATA\20200806_DNAN_1_JH 2020-08-06 08-52-21\
Date	06-Aug-20, 09:48:16
Sample	C7 60min
Sample Info	
Barcode	
Operator	user
Method	20200220_BBP_D_DAD_MS_DLF.M
Analysis Time	2.493 min
Sampling Rate	0.0067 min (0.402 sec), 375 datapoints

#	Time	Area	Height	Width	Area%	Symmetry
1	0.362	693.1	147.4	0.0769	49.574	1.18
2	1.098	705	113.3	0.0866	50.426	0.402

Experiment 250:1 5 min

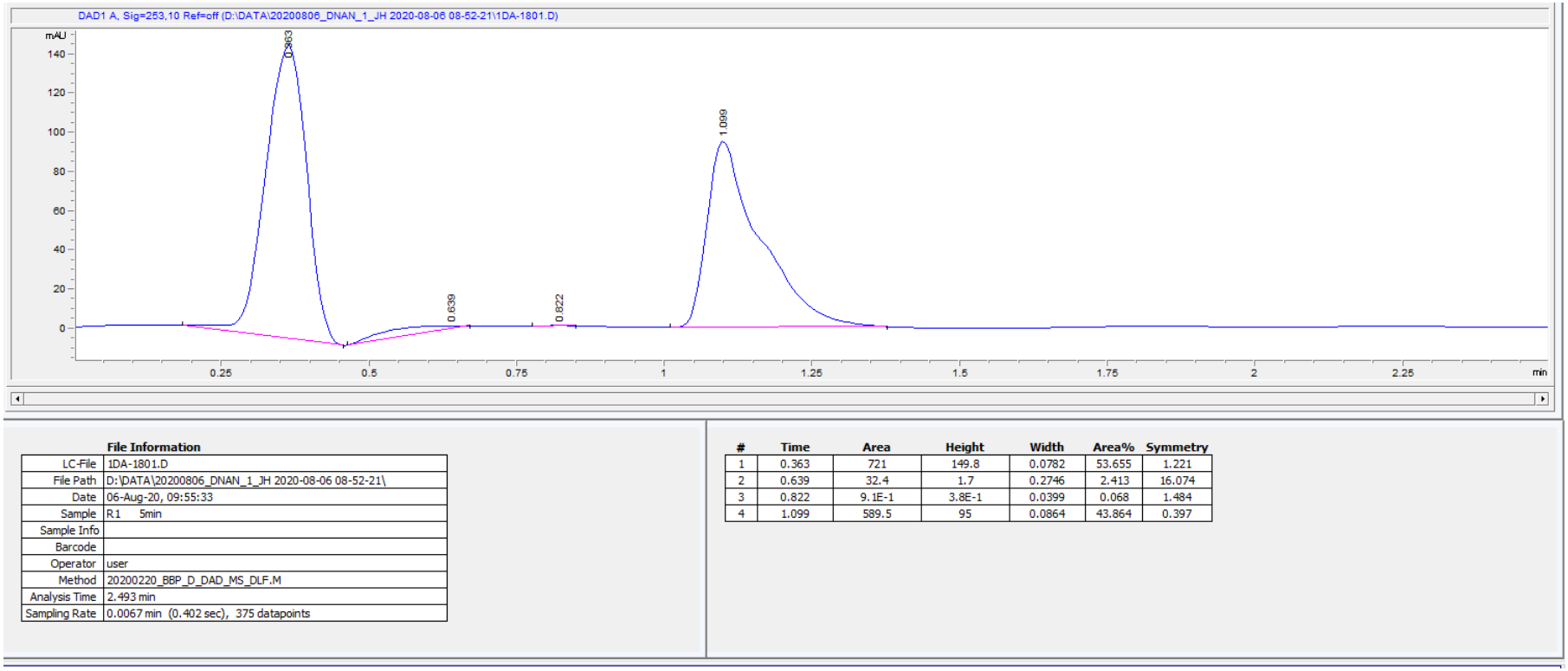

File Information	
LC-File	1DA-1801.D
File Path	D:\DATA\20200806_DNAN_1_JH 2020-08-06 08-52-21\
Date	06-Aug-20, 09:55:33
Sample	R1 5min
Sample Info	
Barcode	
Operator	user
Method	20200220_BBP_D_DAD_MS_DLF.M
Analysis Time	2.493 min
Sampling Rate	0.0067 min (0.402 sec), 375 datapoints

#	Time	Area	Height	Width	Area%	Symmetry
1	0.363	721	149.8	0.0782	53.655	1.221
2	0.639	32.4	1.7	0.2746	2.413	16.074
3	0.822	9.1E-1	3.8E-1	0.0399	0.068	1.484
4	1.099	589.5	95	0.0864	43.864	0.397

Experiment 250:1 10 min

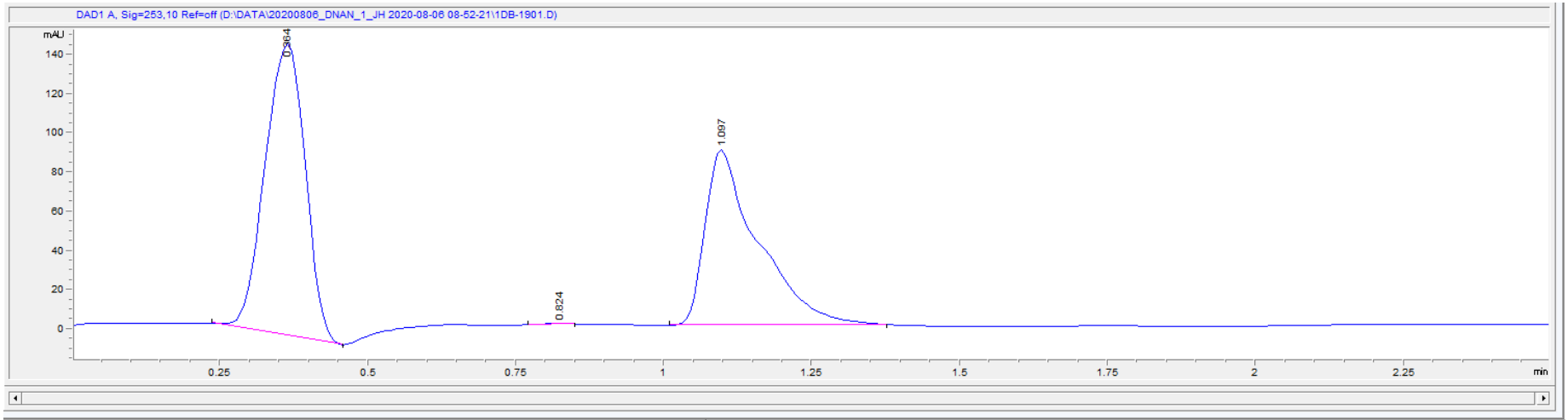

File Information	
LC-File	1DB-1901.D
File Path	D:\DATA\20200806_DNAN_1_JH 2020-08-06 08-52-21\
Date	06-Aug-20, 09:59:10
Sample	R2 10min
Sample Info	
Barcode	
Operator	user
Method	20200220_BBP_D_DAD_MS_DLF.M
Analysis Time	2.493 min
Sampling Rate	0.0067 min (0.402 sec), 375 datapoints

#	Time	Area	Height	Width	Area%	Symmetry
1	0.364	704.9	148.8	0.0773	55.930	1.179
2	0.824	1.2	4.7E-1	0.0419	0.094	1.694
3	1.097	554.2	89.2	0.0885	43.977	0.397

Experiment 250:1 15 min

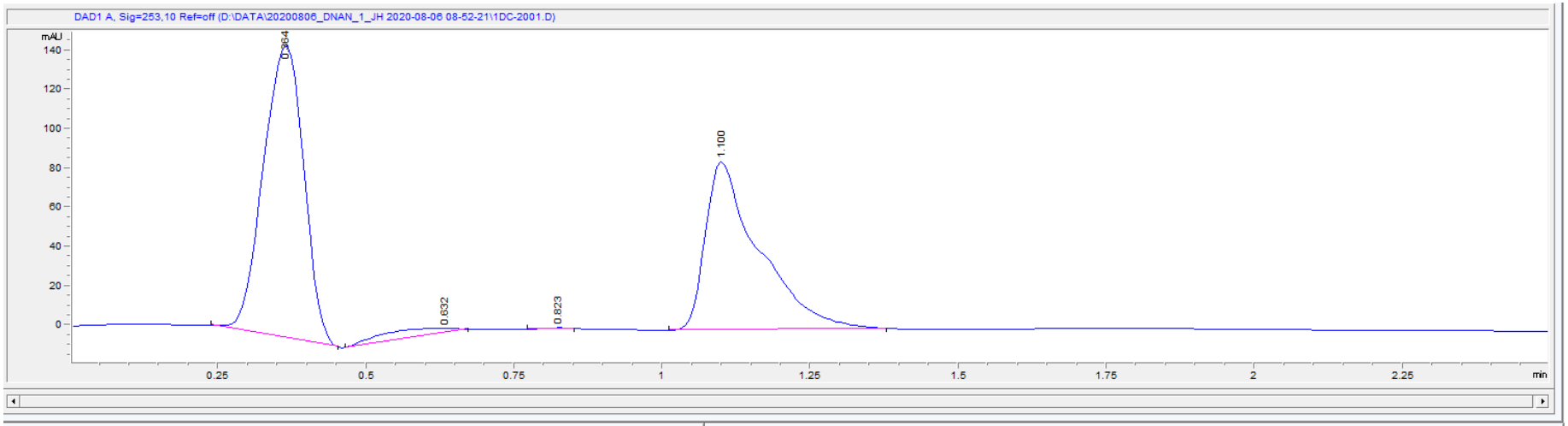

File Information	
LC-File	1DC-2001.D
File Path	D:\DATA\20200806_DNAN_1_JH 2020-08-06 08-52-21\
Date	06-Aug-20, 10:02:50
Sample	R3 15min
Sample Info	
Barcode	
Operator	user
Method	20200220_BBP_D_DAD_MS_DLF.M
Analysis Time	2.493 min
Sampling Rate	0.0067 min (0.402 sec), 375 datapoints

#	Time	Area	Height	Width	Area%	Symmetry
1	0.364	706.5	148.9	0.0774	55.297	1.178
2	0.632	33.2	2.1	0.232	2.595	10.03
3	0.823	1.3	5.2E-1	0.0439	0.104	1.522
4	1.1	536.6	85.7	0.0891	42.003	0.395

Experiment 250:1 20 min

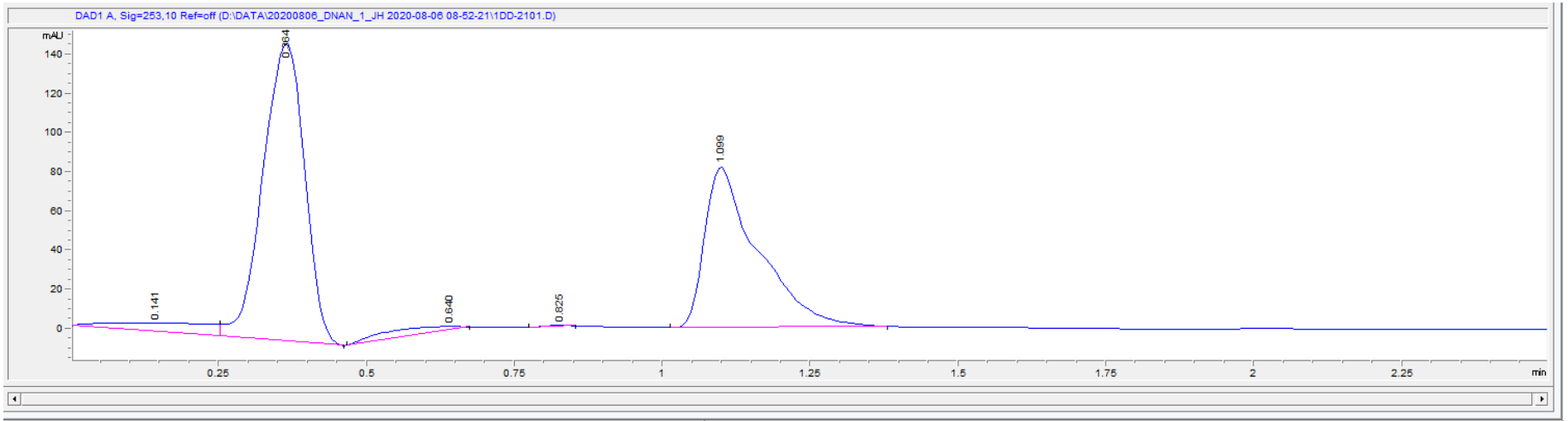

File Information	
LC-File	1DD-2101.D
File Path	D:\DATA\20200806_DNAN_1_JH 2020-08-06 08-52-21\
Date	06-Aug-20, 10:06:29
Sample	R4 20min
Sample Info	
Barcode	
Operator	user
Method	20200220_BBP_D_DAD_MS_DLF.M
Analysis Time	2.5 min
Sampling Rate	0.0067 min (0.402 sec), 376 datapoints

#	Time	Area	Height	Width	Area%	Symmetry
1	0.141	57.4	4.3	0.1818	4.279	0.74
2	0.364	743.7	151.5	0.0793	55.392	1.227
3	0.64	30.6	1.8	0.2459	2.281	12.481
4	0.825	1.6	5.7E-1	0.0458	0.116	1.831
5	1.099	509.3	81.8	0.0866	37.933	0.399

Experiment 250:1 25 min

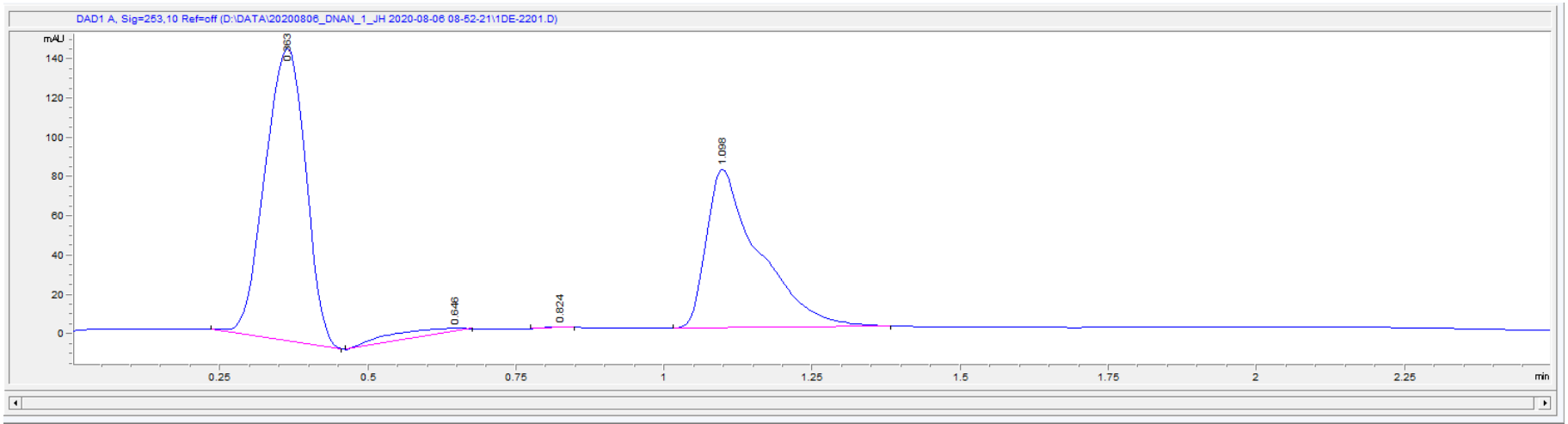

File Information	
LC-File	1DE-2201.D
File Path	D:\DATA\20200806_DNAN_1_JH 2020-08-06 08-52-21\
Date	06-Aug-20, 10:10:08
Sample	R5 25min
Sample Info	
Barcode	
Operator	user
Method	20200220_BBP_D_DAD_MS_DLF.M
Analysis Time	2.5 min
Sampling Rate	0.0067 min (0.402 sec), 376 datapoints

#	Time	Area	Height	Width	Area%	Symmetry
1	0.363	710.4	149.2	0.0796	57.213	1.169
2	0.646	31.5	1.6	0.2763	2.537	17.692
3	0.824	1.2	4.9E-1	0.0417	0.098	2.119
4	1.098	498.6	81	0.0858	40.152	0.401

Experiment 250:1 35 min

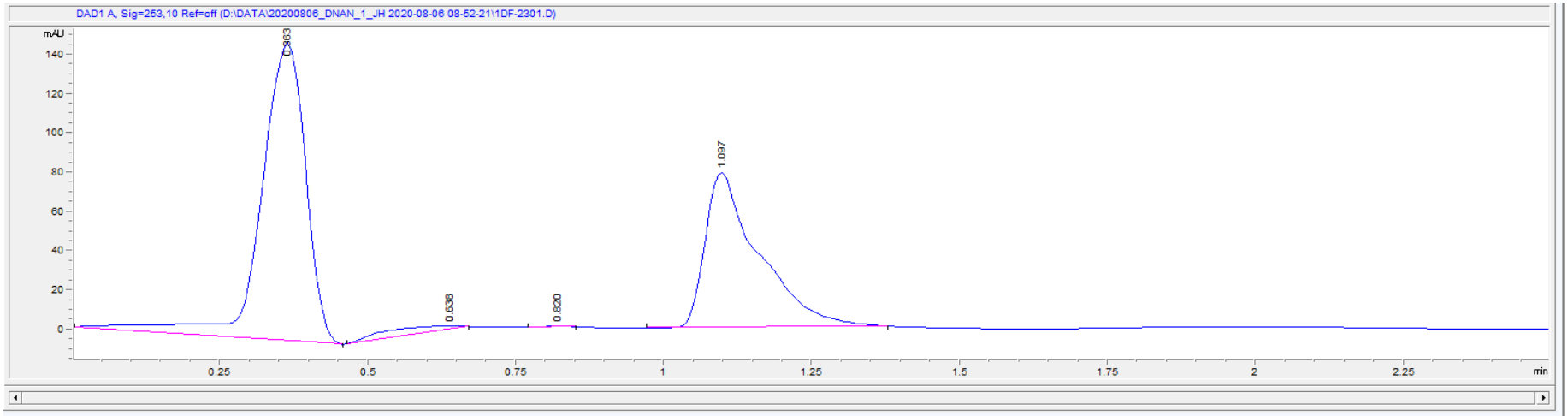

File Information	
LC-File	1DF-2301.D
File Path	D:\DATA\20200806_DNAN_1_JH 2020-08-06 08-52-21\
Date	06-Aug-20, 10:13:48
Sample	R6 35min
Sample Info	
Barcode	
Operator	user
Method	20200220_BBP_D_DAD_MS_DLF.M
Analysis Time	2.493 min
Sampling Rate	0.0067 min (0.402 sec), 375 datapoints

#	Time	Area	Height	Width	Area%	Symmetry
1	0.363	796	151.8	0.0832	60.198	1.44
2	0.638	30.1	1.7	0.2543	2.278	13.394
3	0.82	1.4	5.4E-1	0.0434	0.103	1.31
4	1.097	494.8	78.9	0.0892	37.421	0.393

Experiment 250:1 45 min

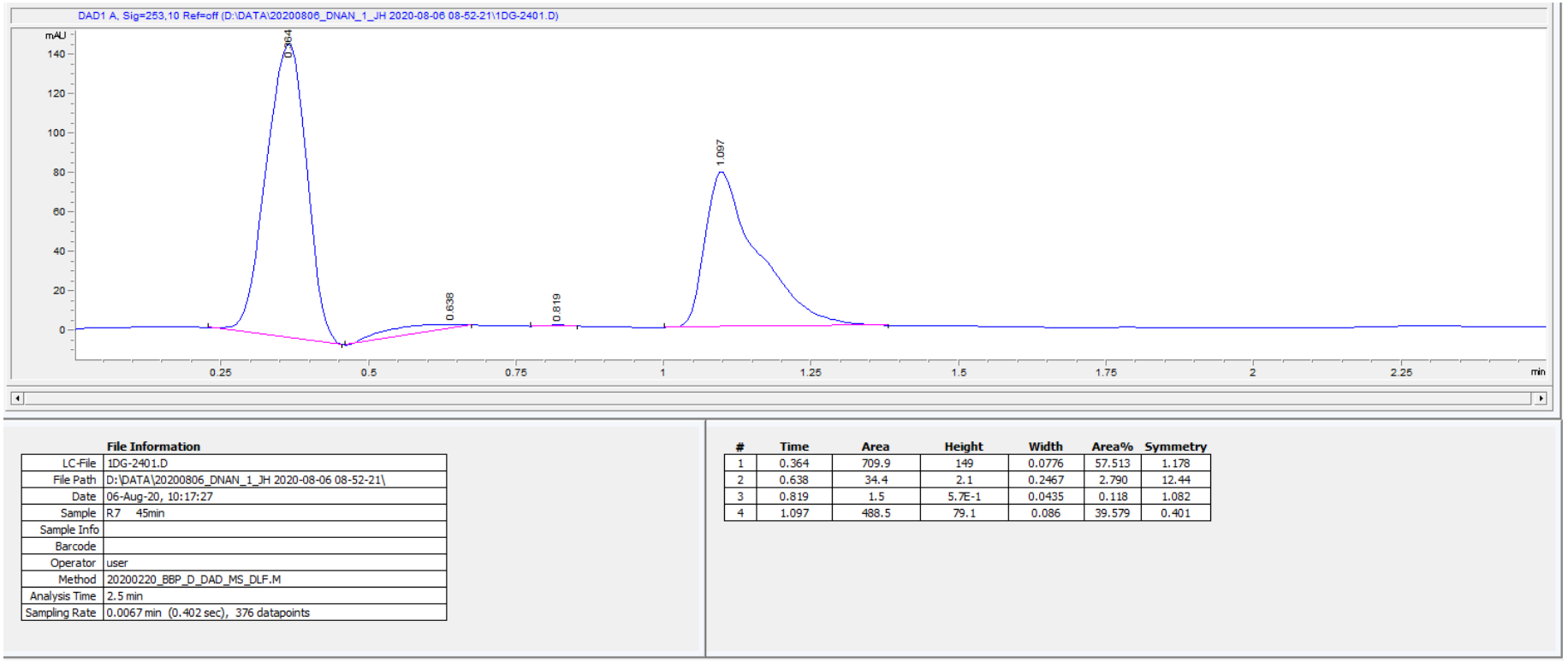

File Information	
LC-File	1DG-2401.D
File Path	D:\DATA\20200806_DNAN_1_JH 2020-08-06 08-52-21\
Date	06-Aug-20, 10:17:27
Sample	R7 45min
Sample Info	
Barcode	
Operator	user
Method	20200220_BBP_D_DAD_MS_DLF.M
Analysis Time	2.5 min
Sampling Rate	0.0067 min (0.402 sec), 376 datapoints

#	Time	Area	Height	Width	Area%	Symmetry
1	0.364	709.9	149	0.0776	57.513	1.178
2	0.638	34.4	2.1	0.2467	2.790	12.44
3	0.819	1.5	5.7E-1	0.0435	0.118	1.082
4	1.097	488.5	79.1	0.086	39.579	0.401

Experiment 250:1 60 min

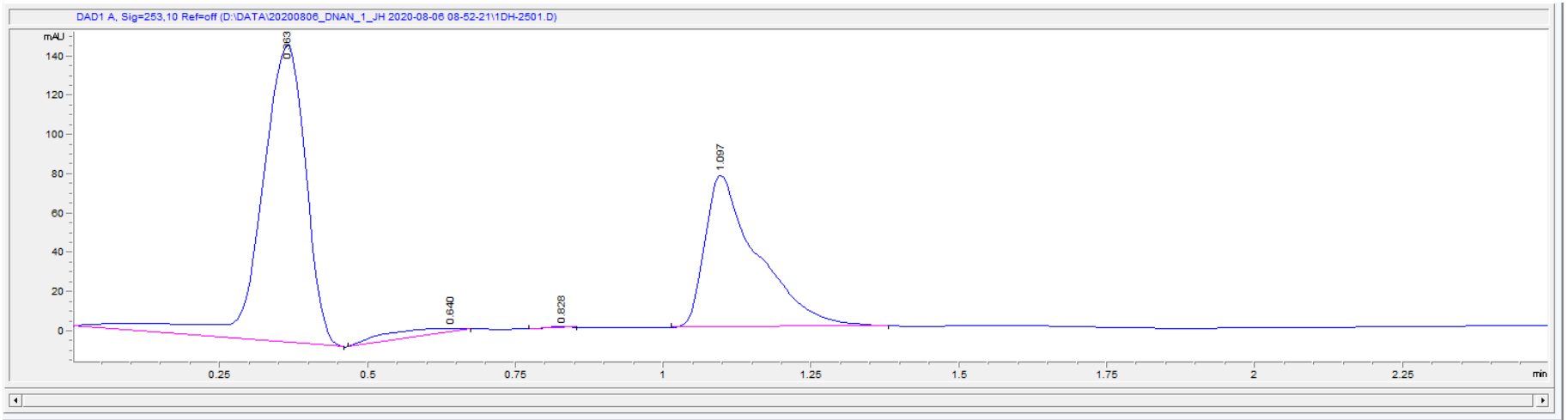

File Information	
LC-File	1DH-2501.D
File Path	D:\DATA\20200806_DNAN_1_JH 2020-08-06 08-52-21\
Date	06-Aug-20, 10:21:05
Sample	R8 60min
Sample Info	
Barcode	
Operator	user
Method	20200220_BBP_D_DAD_MS_DLF.M
Analysis Time	2.5 min
Sampling Rate	0.0067 min (0.402 sec), 376 datapoints

#	Time	Area	Height	Width	Area%	Symmetry
1	0.363	801.8	151.3	0.0838	61.156	1.449
2	0.64	29.8	1.7	0.2544	2.274	13.561
3	0.828	1.4	5.1E-1	0.0454	0.106	2.32
4	1.097	478.1	77.3	0.0861	36.464	0.399

Appendix G: Potential Byproduct Mass Spectroscopy

100:1 Trial

Sequence Name	Line	Vial	Sample Name	Region	RT	AMU
20200622_DNAN_JH_MS	2	P1-D-04	R4-H	H	1.175	240

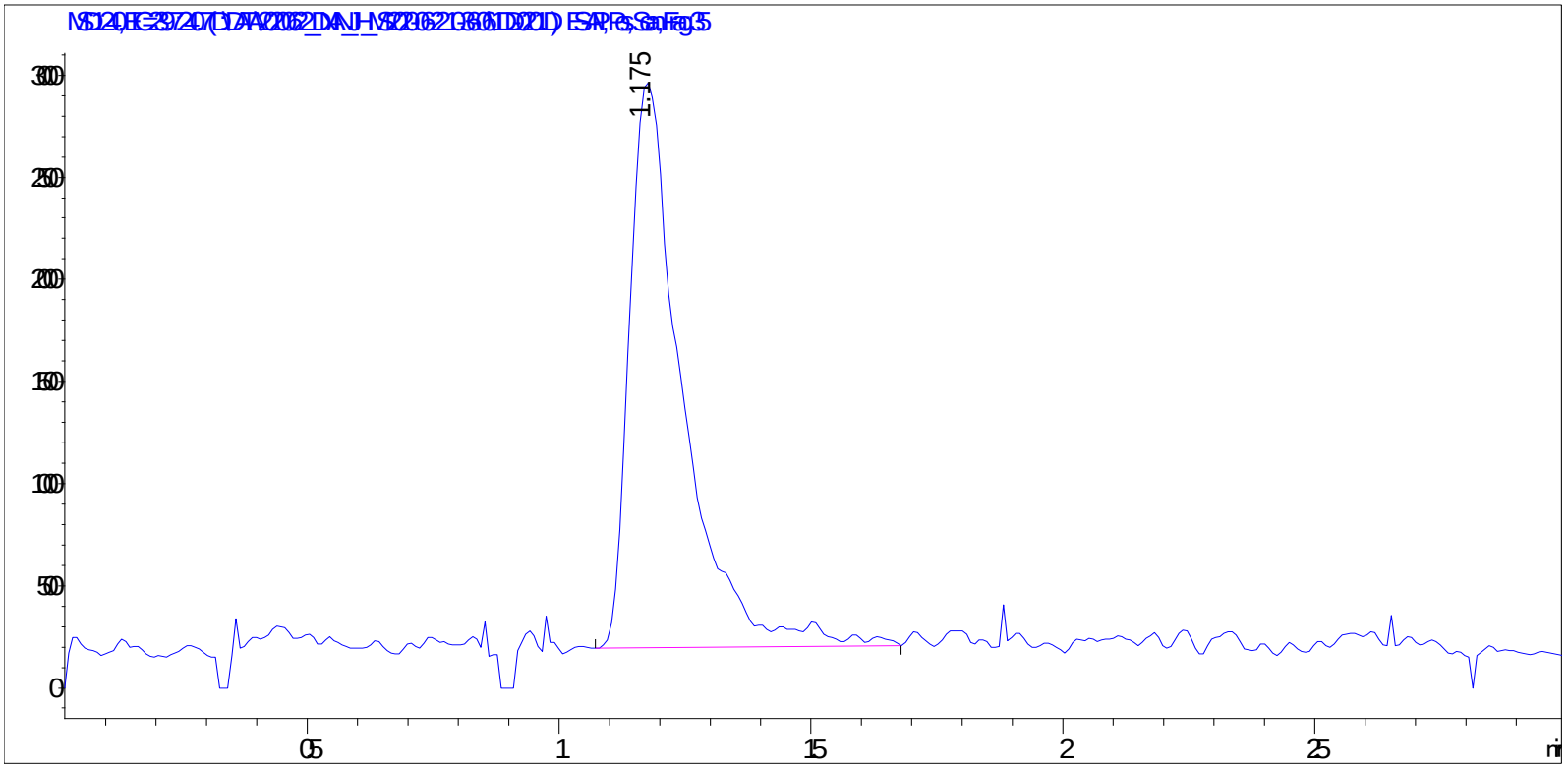

100:1 Trial

Sequence Name	Line	Vial	Sample Name	Region	RT	AMU
20200622_DNAN_JH_MS	2	P1-D-04	R4-H	H	1.175	240

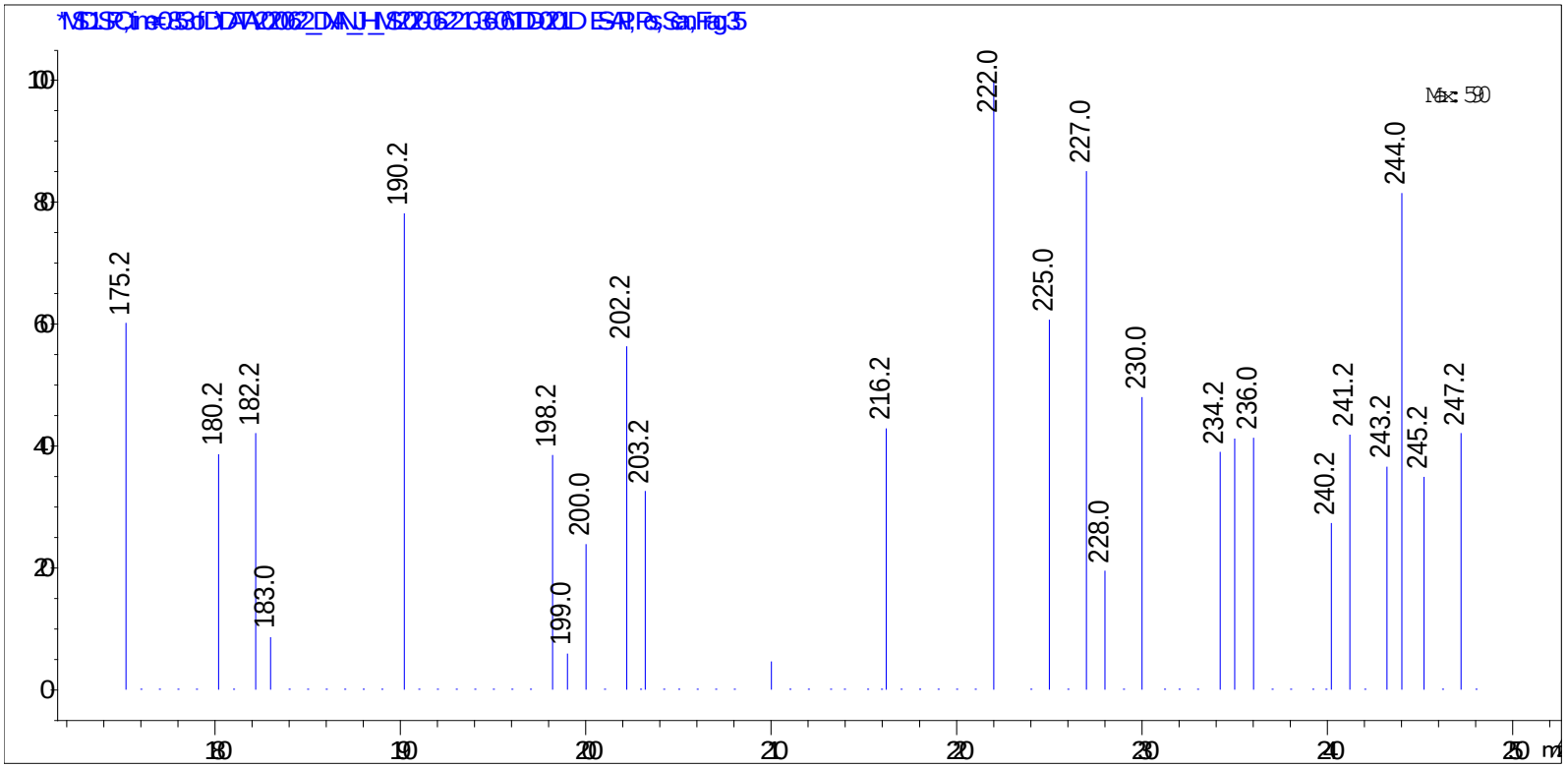

100:1 Trial

Sequence Name	Line	Vial	Sample Name	Region	RT	AMU
20200622_DNAN_JH_MS	3	P1-D-04	R4-M	M	0.371	146

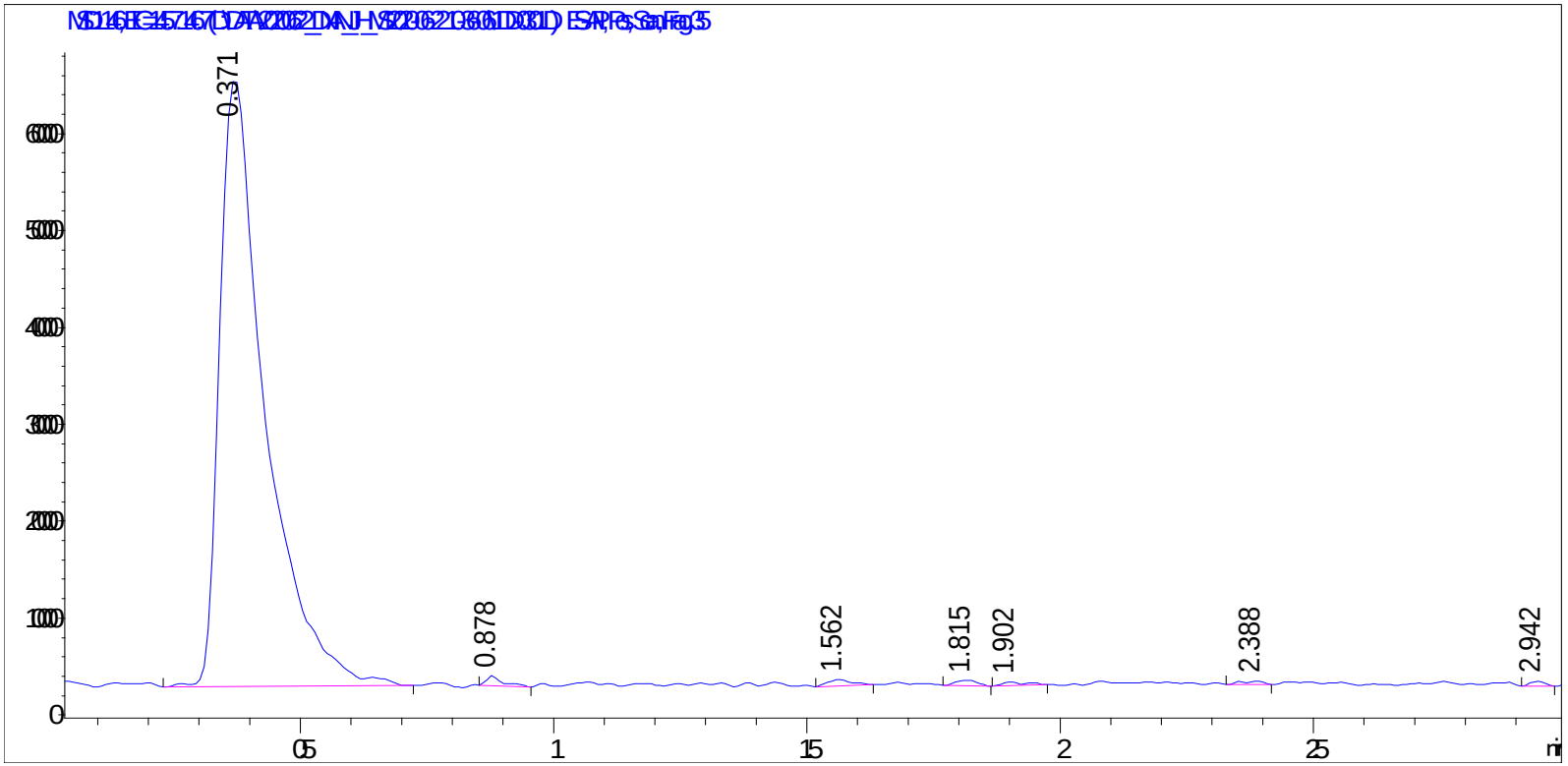

100:1 Trial

Sequence Name	Line	Vial	Sample Name	Region	RT	AMU
20200622_DNAN_JH_MS	3	P1-D-04	R4-M	M	0.371	146

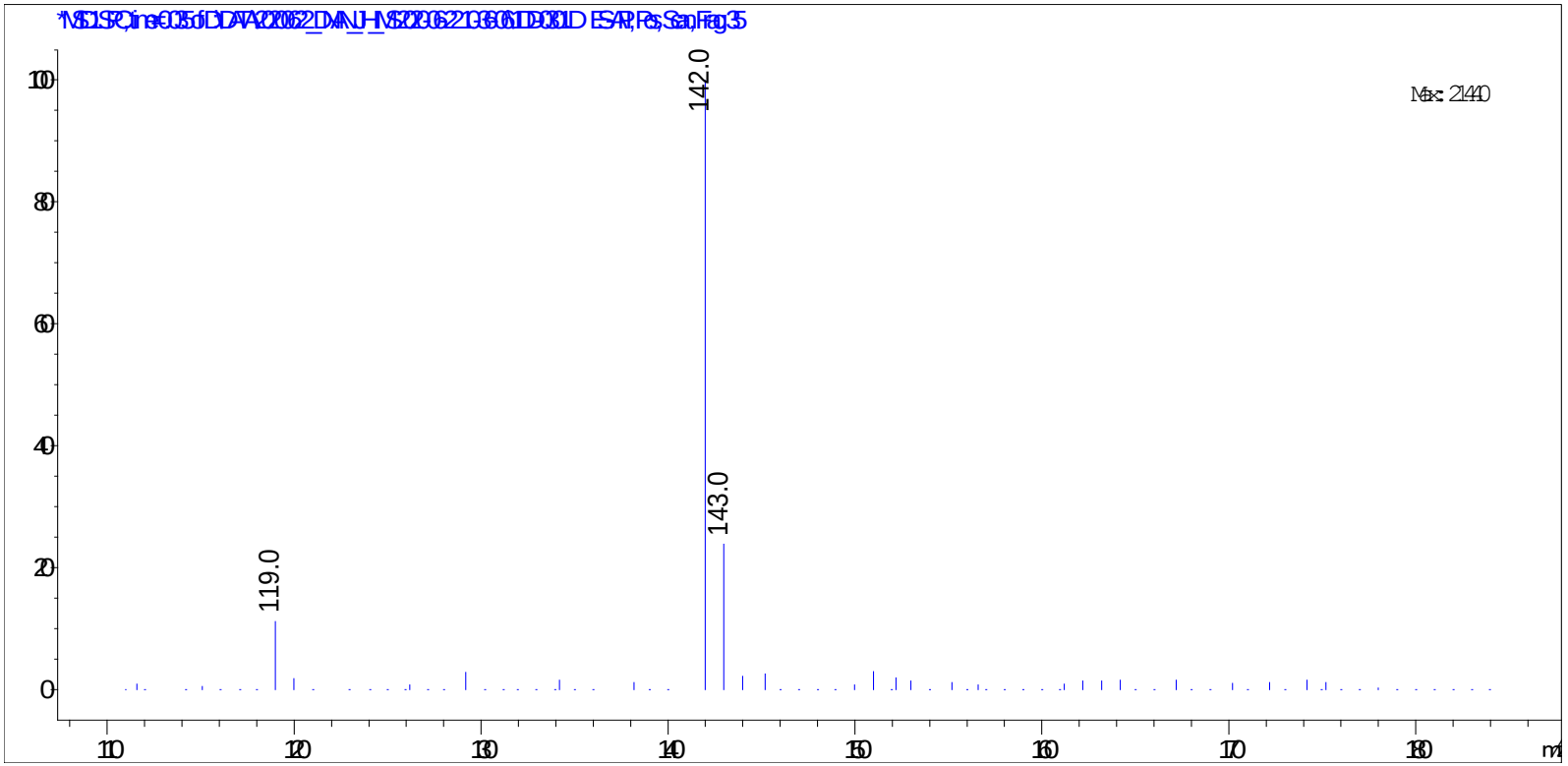

100:1 Trial

Sequence Name	Line	Vial	Sample Name	Region	RT	AMU
20200622_DNAN_JH_MS	9	P1-D-08	R8-H	H	1.164	240

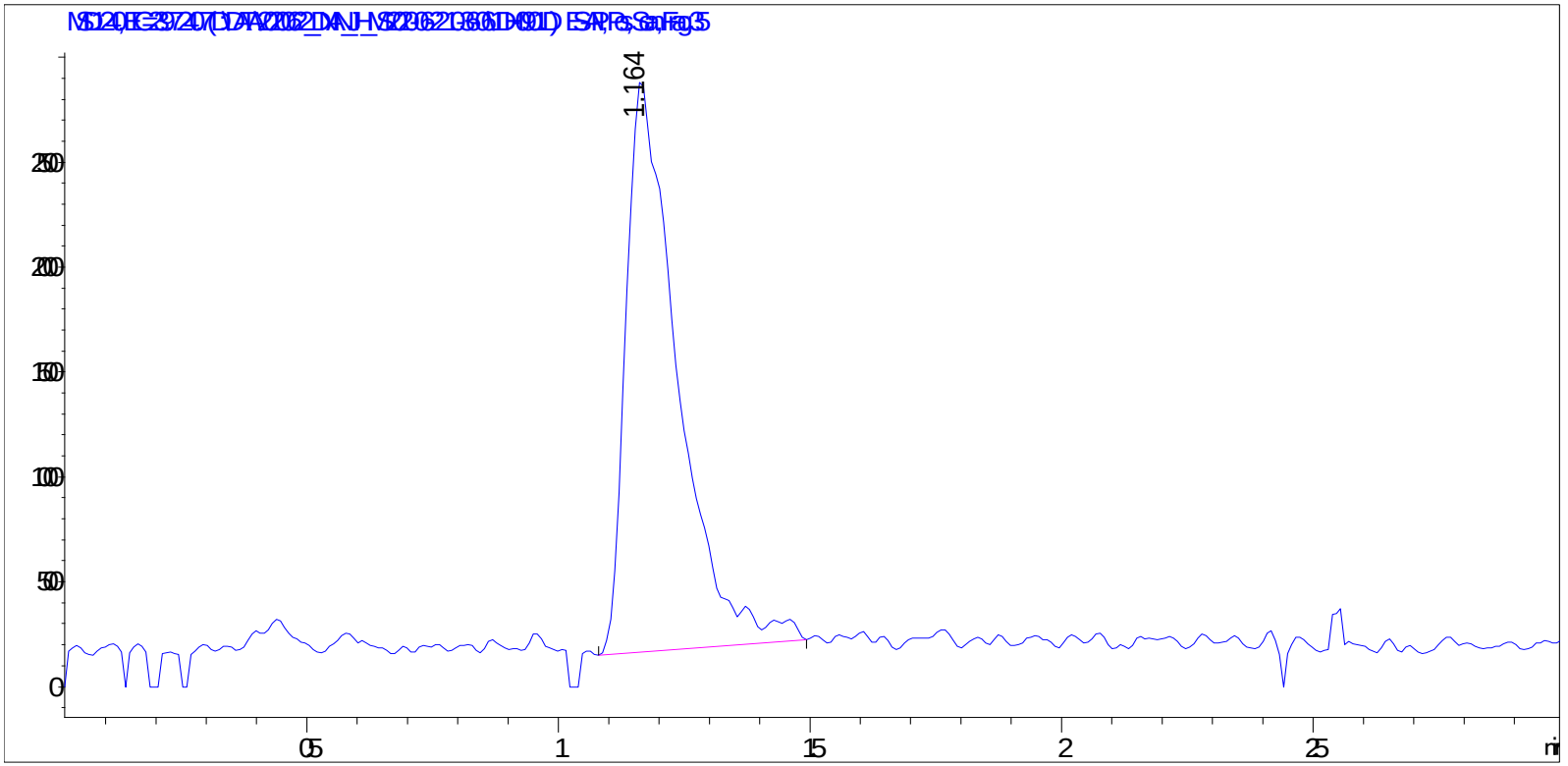

100:1 Trial

Sequence Name	Line	Vial	Sample Name	Region	RT	AMU
20200622_DNAN_JH_MS	9	P1-D-08	R8-H	H	1.164	240

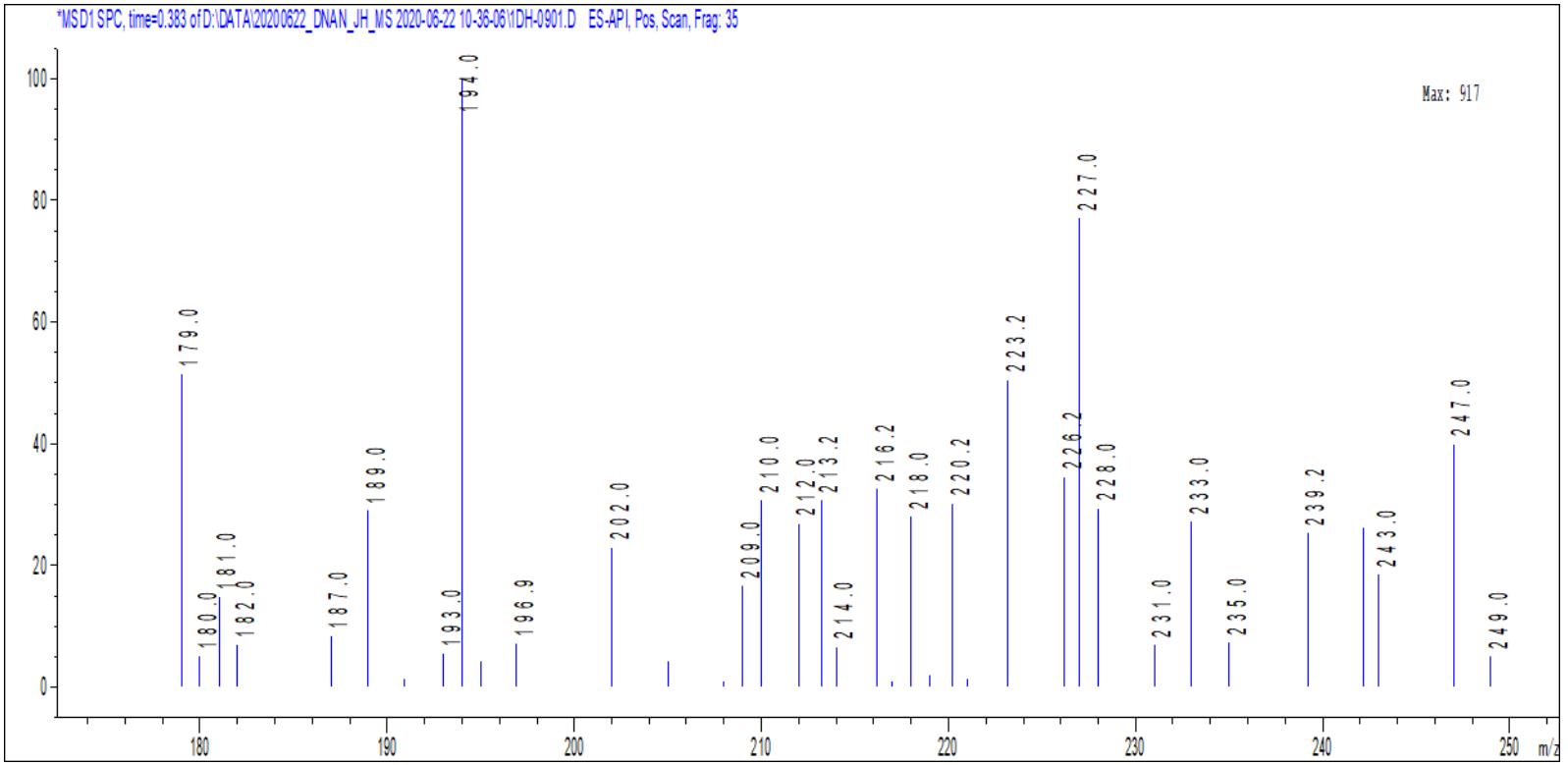

100:1 Trial

Sequence Name	Line	Vial	Sample Name	Region	RT	AMU
20200622_DNAN_JH_MS	10	P1-D-08	R8-M	M	0.372	146

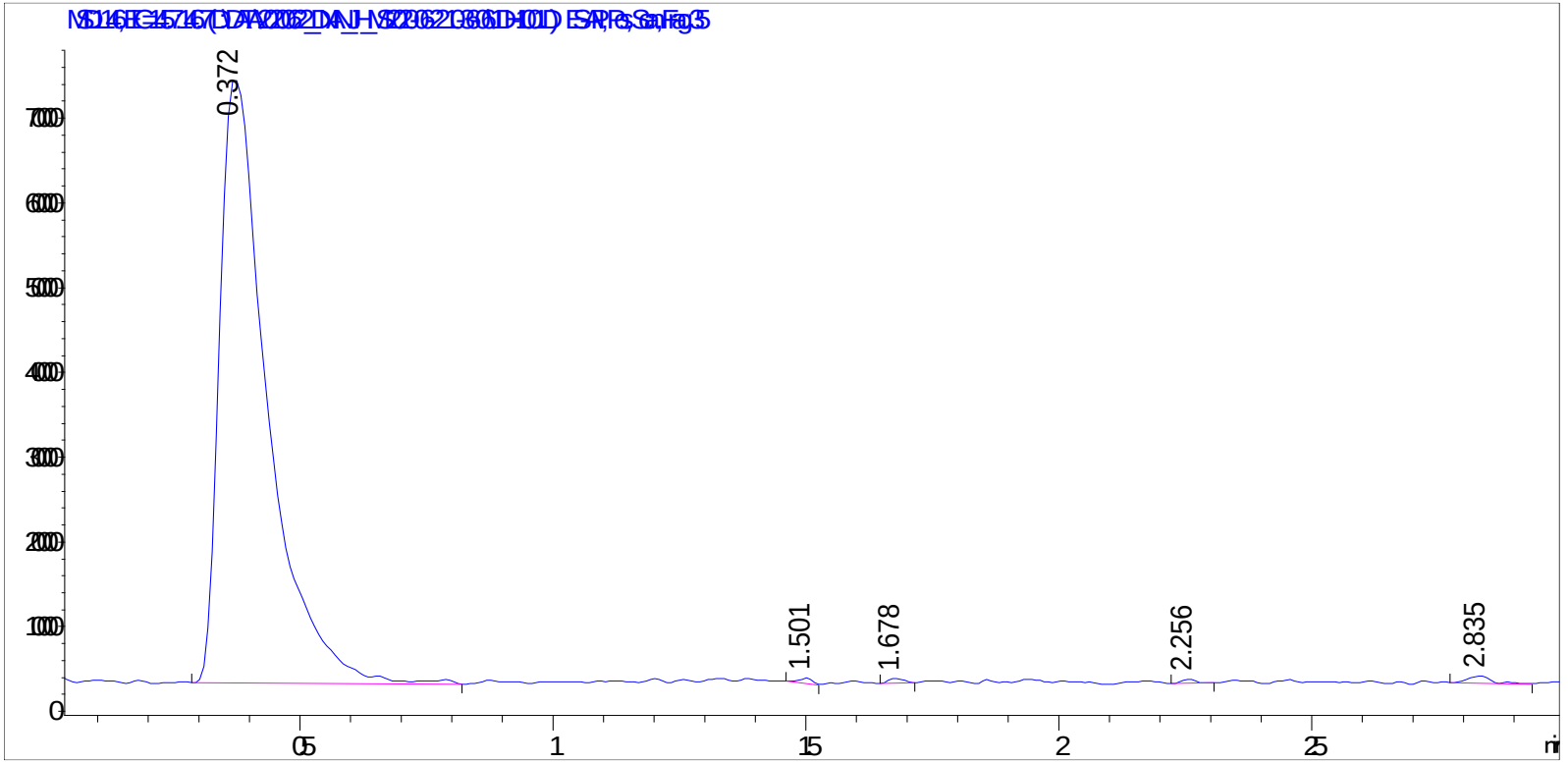

100:1 Trial

Sequence Name	Line	Vial	Sample Name	Region	RT	AMU
20200622_DNAN_JH_MS	10	P1-D-08	R8-M	M	0.372	146

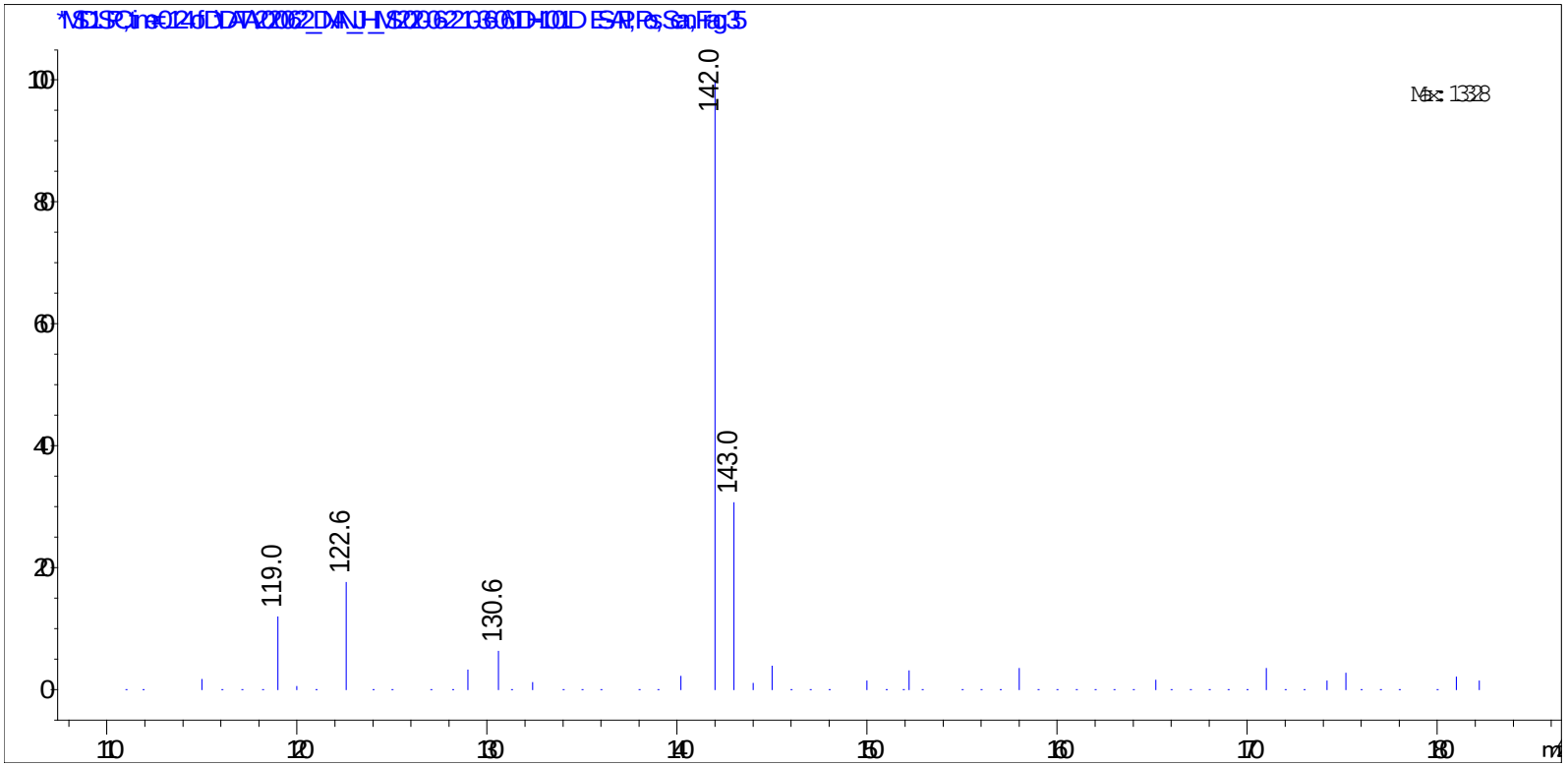

250:1 Trial

Sequence Name	Line	Vial	Sample Name	Region	RT	AMU
20200813_MS_DNAN_250-1_JH	2	P1-E-03	C3-H	H	0.376	192

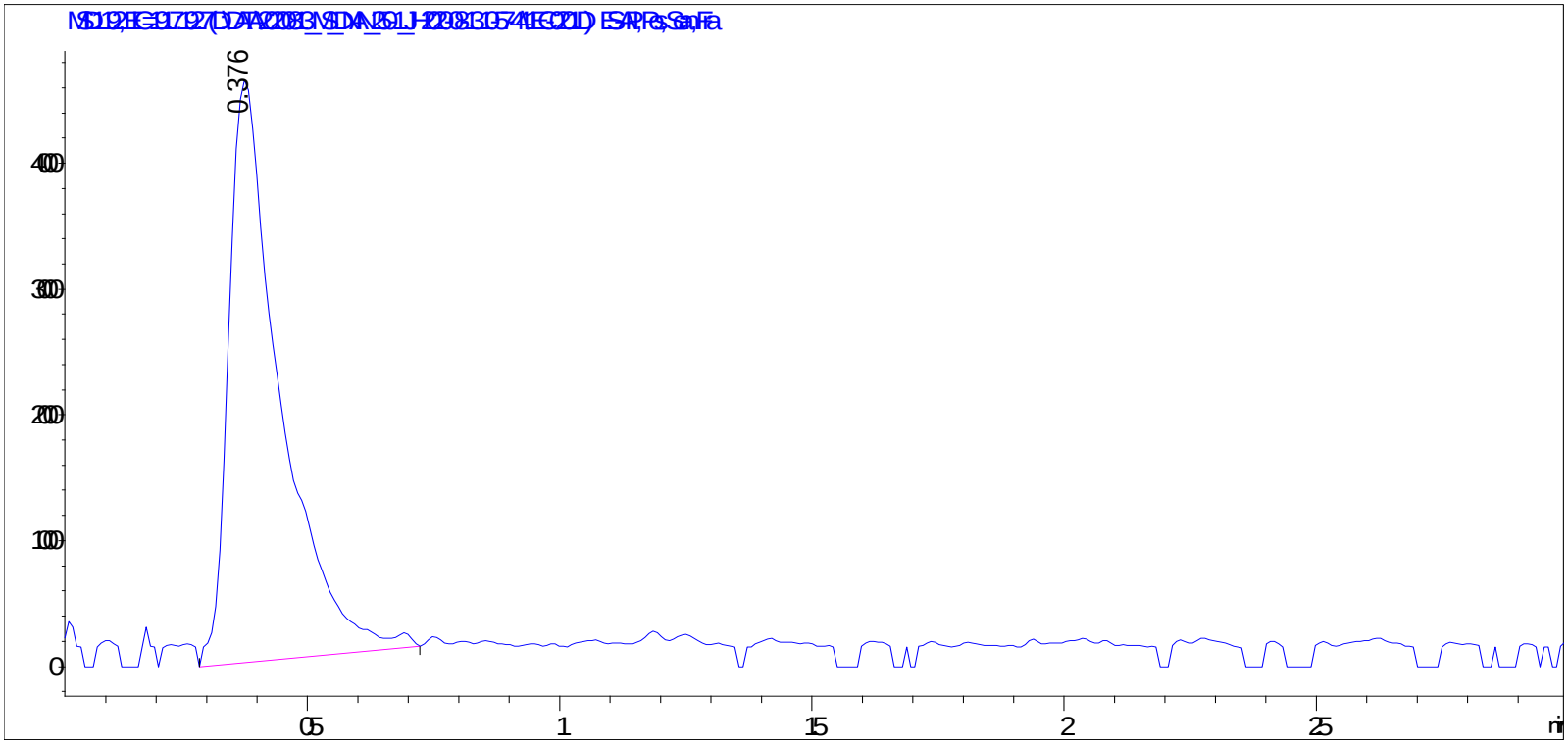

250:1 Trial

Sequence Name	Line	Vial	Sample Name	Region	RT	AMU
20200813_MS_DNAN_250-1_JH	2	P1-E-03	C3-H	H	0.376	192

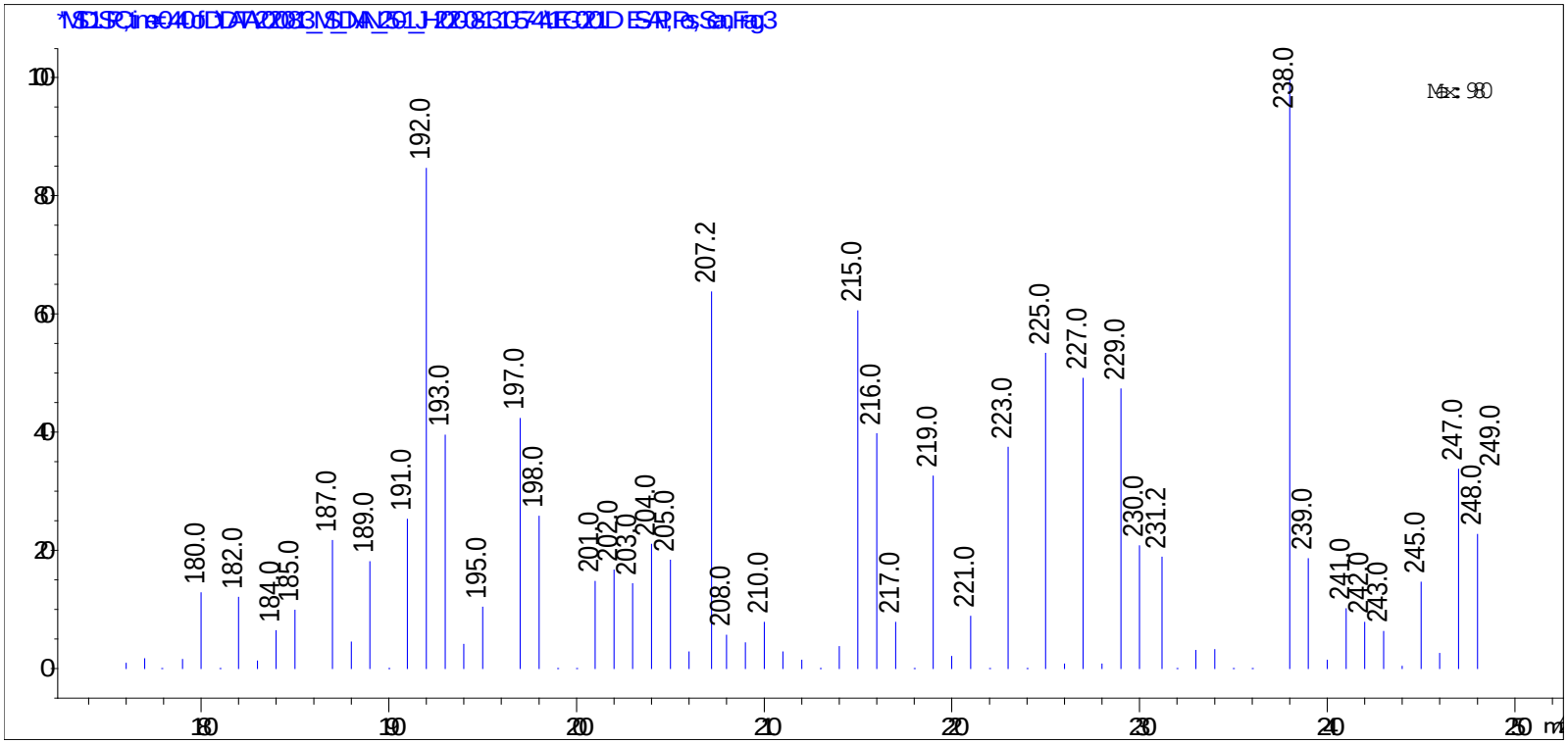

1000:1 Trial

Sequence Name	Line	Vial	Sample Name	Region	RT	AMU
20200723_MS_DNAN_B_JH	2	P1-E-03	C3-H	H	0.377	192

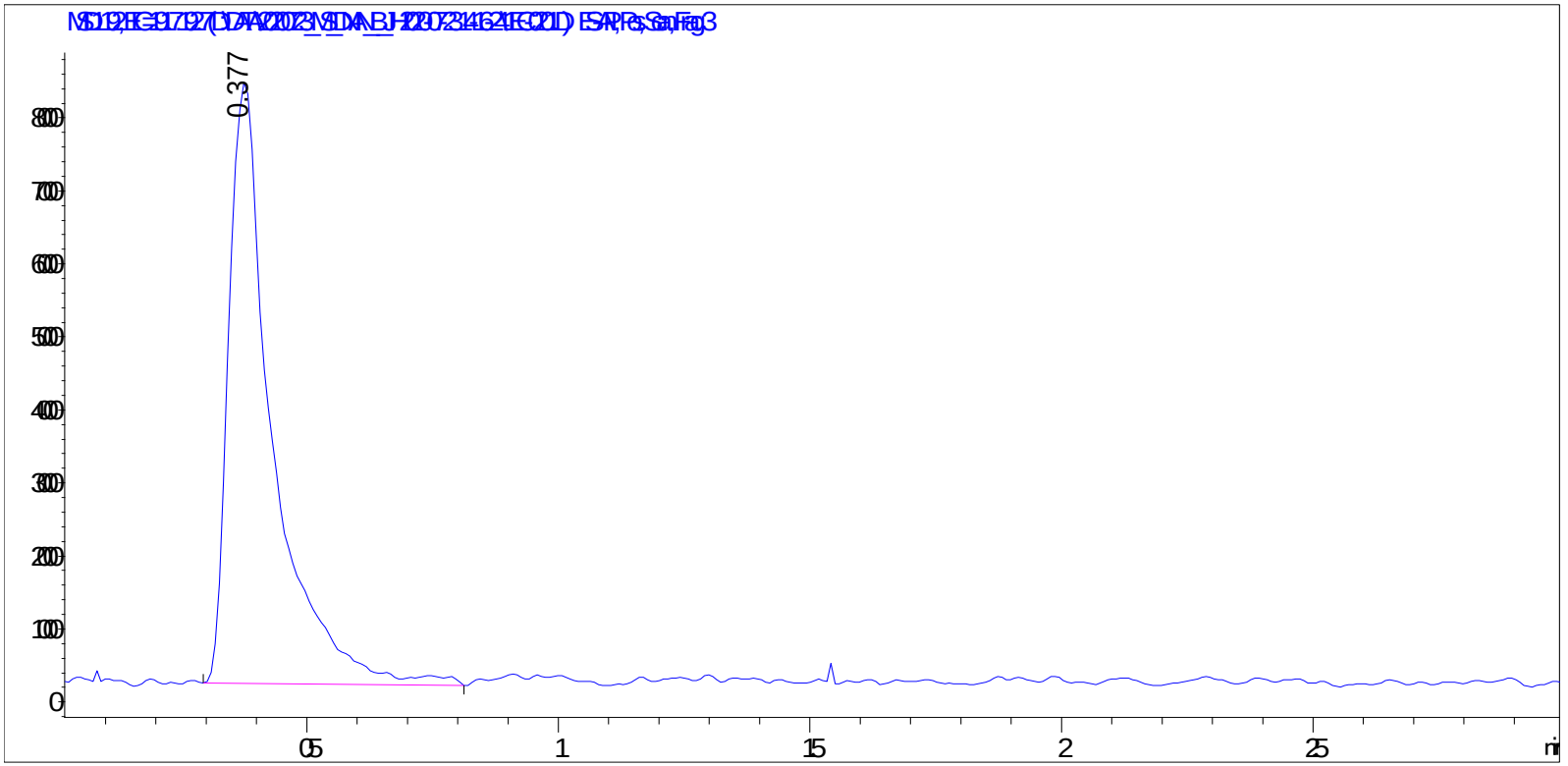

1000:1 Trial

Sequence Name	Line	Vial	Sample Name	Region	RT	AMU
20200723_MS_DNAN_B_JH	2	P1-E-03	C3-H	H	0.377	192

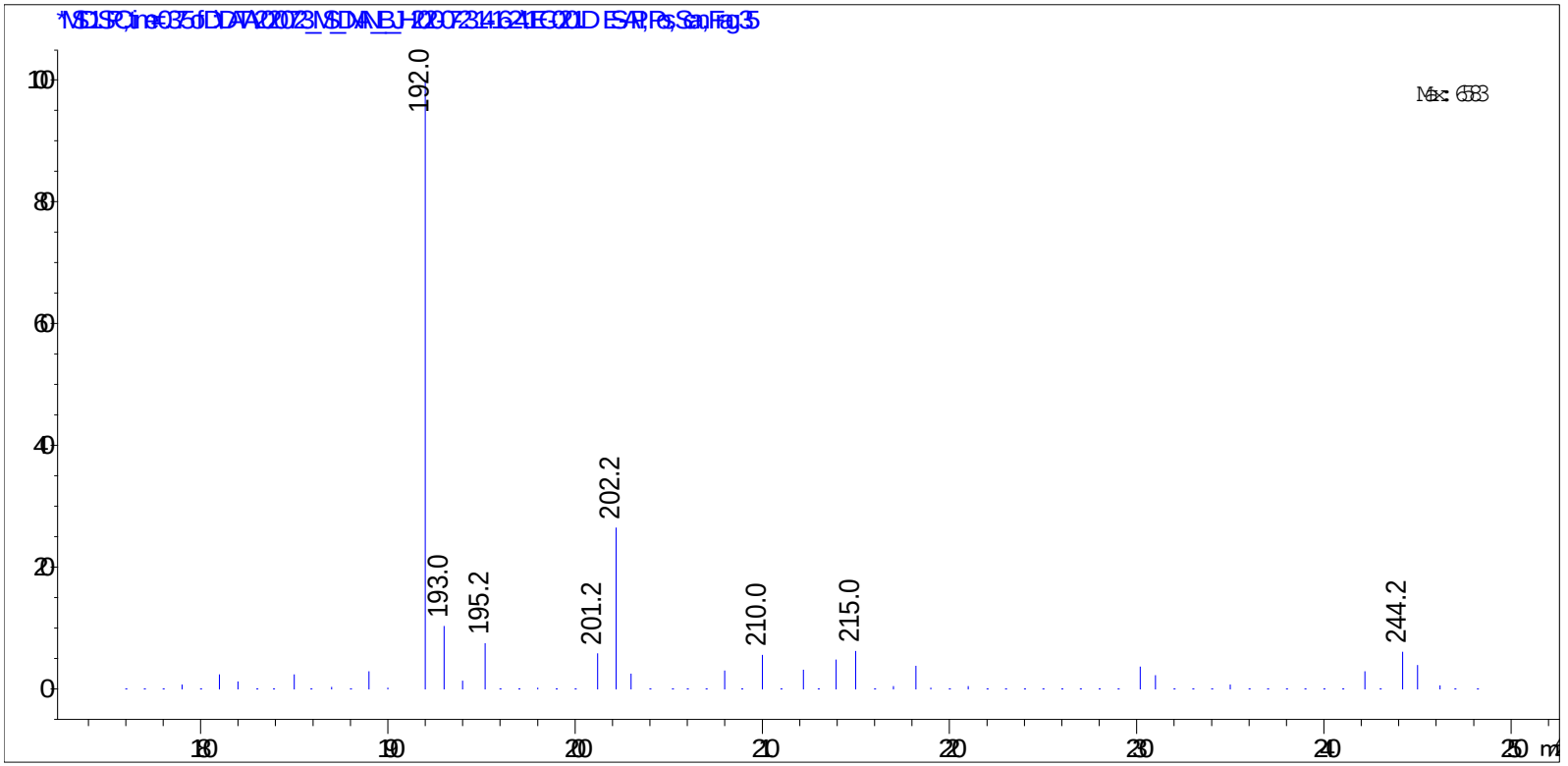

Bibliography

Azami, H., Sarrafzadeh, M. H., & Mehrnia, M. R. (2012). Soluble microbial products (SMPs) release in activated sludge systems : a review. *Iranian Journal of Environmental Health Sciences & Engineering*, *9*(1), 1. https://doi.org/10.1186/1735-2746-9-30

Barry, J. A. (2012). *Characterization of DoD Installation Wastewater Treatment*. (November). Retrieved from https://apps.dtic.mil/sti/pdfs/ADA575151.pdf

Beers, R., & Sizer, I. (1951). Spectrophometric Method for Measuring the Breakdown of Hydrogen Peroxide by Catalase. *J Biol. Chem*, *195*, 133–140.

Buxton, G., Greenstock, C. L., Helman, P., W, & Ross, A. (1988). Critical Review of rate constants for reactions of hydrated electrons, hydrogen atoms and hydroxyl radicals. *Journal of Physical Reference Data*, 513–886.

Chang, P. B. L., & Young, T. M. (2000). Kinetics of methyl tert-butyl ether Degradation and By-Product Formation During UV/Hydrogen Peroxide Water Treatment. *Water Research*, *34*(8), 2233–2240. https://doi.org/10.1016/S0043-1354(99)00392-9

Crittenden, J., Trussell, R., Hand, D., Howe, K., & Tchobanoglous, G. (2014). MWH Water Treatment Principles and Design. *GPSA 12 Ed 2004 - FPS*. https://doi.org/10.1016/B978-0-12-382092-1.00019-1

Deng, Y., & Zhao, R. (2015). *Advanced Oxidation Processes (AOPs) in Wastewater Treatment*. 167–176. https://doi.org/10.1007/s40726-015-0015-z

Dodard, S. G., Sarrazin, M., Hawari, J., Paquet, L., Ampleman, G., Thiboutot, S., & Sunahara, G. I. (2013). Ecotoxicological assessment of a high energetic and insensitive munitions compound: 2,4-Dinitroanisole (DNAN). *Journal of Hazardous*

Materials, *262*, 143–150. https://doi.org/10.1016/j.jhazmat.2013.08.043

Duckworth, K., Spencer, M., Bates, C., Miller, M. E., Almquist, C., Grimaila, M., … Racz, L. A. (2015). Advanced oxidation degradation kinetics as a function of ultraviolet LED duty cycle. *Water Science and Technology*, *71*(9), 1375–1381. https://doi.org/10.2166/wst.2015.108

Gallucci, D. D. (2016). *Material and Design Considerations for a Portable Ultra-Violet (UV) Light Emitting Diode (LED) Water Purification Device*.

Hawari, J., Monteil-Rivera, F., Perreault, N. N., Halasz, A., Paquet, L., Radovic-Hrapovic, Z., … Ampleman, G. (2015). Environmental fate of 2,4-dinitroanisole (DNAN) and its reduced products. *Chemosphere*, *119*, 16–23. https://doi.org/10.1016/j.chemosphere.2014.05.047

Ho, P. C. (1986). Photooxidation of 2,4-dinitrotoluene in Aqueous Solution in the Presence of Hydrogen Peroxide. *Environmental Science and Technology*, *20*(3), 260–267. Retrieved from https://pubs.acs.org/action/showCitFormats?doi=10.1021%2Fes00145a007&href=/doi/10.1021%2Fes00145a007

Hoigné, J. (1998). *Chemistry of Aqueous Ozone and Transformation of Pollutants by Ozonation and Advanced Oxidation Processes*. *5*, 83–141. https://doi.org/10.1007/978-3-540-68089-5_5

Huang, C., Dong, C., & Tang, Z. (1993). Advanced Chemical Oxidation: Its Present Role and Potential Future In Hazardous Waste Treatment. *Waste Management*, *13*, 361–377.

Jarusutthirak, C., & Amy, G. (2006). Role of Soluble Microbial Products (SMP) in

Membrane Fouling and Flux Decline. *Environmental Science & Technology*, *40*(3), 969–974.

Lenk, R., & Lenk, C. (2017). Practical Lighting Design With LEDs. *Practical Lighting Design With LEDs*, 57–64. https://doi.org/10.1002/9781118008218

Levsen, K., Preiss, A., & Berger-Preiss, E. (1995). <title>Analysis of organic compounds in aqueous samples of former ammunition plants</title>. *Environmental Monitoring and Hazardous Waste Site Remediation*, *2504*(October 1995), 350–361. https://doi.org/10.1117/12.224120

Li, Z. M., Comfort, S. D., & Shea, P. J. (1997). Destruction of 2,4,6-trinitrotoluene by Fenton oxidation. *Journal of Environmental Quality*, *26*(2). Retrieved from https://www.osti.gov/biblio/530779

Li, Z. M., Shea, P. J., & Comfort, S. D. (1998). Nitrotoluene destruction by UV-catalyzed Fenton oxidation. *Chemosphere*, *36*(8), 1849–1865. https://doi.org/10.1016/S0045-6535(97)10073-X

McDonald, K. F., Curry, R. D., Clevenger, T. E., Unklesbay, K., Eisenstark, A., Golden, J., & Morgan, R. D. (2000). A comparison of pulsed and continuous ultraviolet light sources for the decontamination of surfaces. *IEEE Transactions on Plasma Science*, *28*(5), 1576–1580. https://doi.org/10.1109/27.901236

Mitchell, D., & Ensley, R. (2019). Army water purification systems can leave units running dry |. Retrieved October 15, 2020, from https://www.army.mil/article/218519/army_water_purification_systems_can_leave_units_running_dry

Munter, R. (2001). Advanced Oxidation Processes. *Proc. Estonian Acad. Sci. Chem.*,

377–408. https://doi.org/10.1016/B978-0-444-53199-5.00093-2

Muruganandham, M., & Swaminathan, M. (2004). *Photochemical oxidation of reactive azo dye with UV – H 2 O 2 process*. *62*, 269–275. https://doi.org/10.1016/j.dyepig.2003.12.006

Ni, B. J., Rittmann, B. E., & Yu, H. Q. (2011). Soluble microbial products and their implications in mixed culture biotechnology. *Trends in Biotechnology*, *29*(9), 454–463. https://doi.org/10.1016/j.tibtech.2011.04.006

Noss, C. I., & Chyrek, R. H. (1984). *Tertiary Treatment of Effluent from Holston AAP Industrial Liquid Waste Treatment Facility: IV. Ultraviolet Radiation and Hydrogen Peroxide Studies: TNT, RDX, HMX, TAX, and SEX*. Fort Detrick.

Oancea, P., & Meltzer, V. (2014). Kinetics of tartrazine photodegradation by UV/H2O2 in aqueous solution. *Chemical Papers*, *68*(1), 105–111. https://doi.org/10.2478/s11696-013-0426-5

Platten III, W. (2011). *Anaerobic Treatment of Wastewaters Containing 2,4-dinitroanisole and N- methyl paranitro aniline from Munitions Handling and Production*.

Scott, R., Mudimbi, P., Miller, M. E., Magnuson, M., Willison, S., Phillips, R., & Harper, W. F. (2017). Advanced Oxidation of Tartrazine and Brilliant Blue with Pulsed Ultraviolet Light Emitting Diodes. *Water Environment Research*, *89*(1), 24–31. https://doi.org/10.2175/106143016x14733681696167

Searcy, T. (2020). *The Effect of Molar Stoichiometry on the Oxidation of 2,4 Dinitroanisole in an Ultraviolet Light Emitting Diode Advanced Oxidation Process [Unpublished Masters Thesis]*. Air Force Institute of Technology.

Sharma, S. (2015). *Green Chemistry for Dyes Removal from Wastewater*. Hoboken: Wiley.

Shen, J., Ou, C., Zhou, Z., Chen, J., Fang, K., Sun, X., … Wang, L. (2013). Pretreatment of 2,4-dinitroanisole (DNAN) producing wastewater using a combined zero-valent iron (ZVI) reduction and Fenton oxidation process. *Journal of Hazardous Materials*, *260*, 993–1000. https://doi.org/10.1016/j.jhazmat.2013.07.003

Sheng, G. P., Yu, H. Q., & Li, X. Y. (2010). Extracellular polymeric substances (EPS) of microbial aggregates in biological wastewater treatment systems: A review. *Biotechnology Advances*, *28*(6), 882–894. https://doi.org/10.1016/j.biotechadv.2010.08.001

Sincich, T., Mcclave, J., & Benson, G. (2018). *Statistics for Business and Economics*.

Stewart, B. M. (2016). *AFIT Scholar The Effect of pH and Pulsed Ultraviolet Light Emitting Diode Duty Cycles on the First Order Rate Constant and Byproduct Profile of the Advanced Oxidation of Tartrazine Recommended Citation*. Retrieved from https://scholar.afit.edu/etd/414

Stewart, B. M., Miller, M. E., Kempisty, D. M., Stubbs, J., & Harper, W. F. (2018). Oxidation of tartrazine with ultraviolet light emitting diodes: PH and duty cycles effects. *Water Science and Technology*, *77*(6), 1651–1659. https://doi.org/10.2166/wst.2018.045

Stocking, A., Rodriguez, R., & Browne, T. (2000). *Advanced Oxidation Processes: Literature Review, Removal of Methyl Tertiary Butyl Ether (MTBE) from Drinking Water: Air Stripping, Advanced Oxidation Process, Granular Activated Carbon, Synthetic Resin Sorbents*.

Stubbs, J. (2017). *Dynamics of Chemical Degradation in Water Using Photcatalytic Reactions in an Ultraviolet Light Emitting Diode Reactor*.

Su, H., Christodoulatos, C., Smolinski, B., Arienti, P., O'Connor, G., & Meng, X. (2019). Advanced Oxidation Process for DNAN Using UV/H2O2. *Engineering*, *5*(5), 849–854. https://doi.org/10.1016/j.eng.2019.08.003

Terracciano, A., Christodoulatos, C., Koutsospyros, A., Zheng, Z., Su, T. L., Smolinski, B., … Meng, X. (2018). Degradation of 3-nitro-1,2,4-trizole-5-one (NTO) in Wastewater With UV/H2O2 Oxidation. *Chemical Engineering Journal*, *354*(July), 481–491. https://doi.org/10.1016/j.cej.2018.07.216

Tran, T., Racz, L., Grimaila, M., Miller, M., & Harper Jr., W. (2014). Comparison of Continuous Versus Pulsed Ultraviolet LED Use For The Inactivation of Bacillus Globigii Spores. *Water Science & Technology*, *70*(9), 1473–1480.

US EPA. (1999). *Alternative Disinfectants and Oxidants Guidance Manual*. Washington, D.C.

US EPA. (2010). *National Pollutant Discharge Elimination System (NPDES) Permit Writers' Manual*.

Westgate, P. J. (2009). *Characterization of Proteins in Effluents from Three Wastewater Treatment Plants that Discharge to the Connecticut River*.

Wols, B. A., Hofman, J. A. M. H., Uijttewaal, W. S. J., Rietveld, L. C., & van Dijk, J. C. (2010). Evaluation of different disinfection calculation methods using CFD. *Environmental Modelling and Software*, *25*(4), 573–582. https://doi.org/10.1016/j.envsoft.2009.09.007

Yang, Y., Ji, Y., Yang, P., Wang, L., Lu, J., Ferronato, C., & Chovelon, J. (2018). Journal

of Photochemistry & Photobiology A : Chemistry UV-activated persulfate oxidation of the insensitive munitions compound 2 , 4-dinitroanisole in water : Kinetics , products , and in fl uence of natural photoinducers. *Journal of Photochemistry & Photobiology, A: Chemistry*, *360*(March), 188–195. https://doi.org/10.1016/j.jphotochem.2018.04.044

Zhang, D., Zhou, Y., Bugge, T. V., Mayanti, B., Yang, A., Poh, L. S., … Ng, W. J. (2017). Soluble microbial products (SMPs) in a sequencing batch reactor with novel cake filtration system. *Chemosphere*, *184*, 1286–1297. https://doi.org/10.1016/j.chemosphere.2017.06.110

REPORT DOCUMENTATION PAGE

Form Approved
OMB No. 074-0188

1. REPORT DATE *(DD-MM-YYYY)*	2. REPORT TYPE	3. DATES COVERED *(From – To)*
25-03-2021	Master's Thesis	October 2019 – March 2021

TITLE AND SUBTITLE

The Effect of Amino Acids and Molar Peroxide Ratio on the Oxidation of 2,4 Dinitroanisole in an Ultraviolet Light Emitting Diode/H2O2 Advanced Oxidation Process

5a. CONTRACT NUMBER

5b. GRANT NUMBER

5c. PROGRAM ELEMENT NUMBER

6. AUTHOR(S)

Hart, Jeffry P., Major, USMC

5d. PROJECT NUMBER

5e. TASK NUMBER

5f. WORK UNIT NUMBER

7. PERFORMING ORGANIZATION NAMES(S) AND ADDRESS(S)
Air Force Institute of Technology
Graduate School of Engineering and Management (AFIT/ENY)
2950 Hobson Way, Building 640
WPAFB OH 45433-8865

8. PERFORMING ORGANIZATION REPORT NUMBER

AFIT-ENV-MS-21-M-232

9. SPONSORING/MONITORING AGENCY NAME(S) AND ADDRESS(ES)
Defense Environmental Restoration Account
Air Force Civil Engineer Center
Lackland AFB, TX
DSN: 969-0625
ATTN: Richard Anderson

10. SPONSOR/MONITOR'S ACRONYM(S)

11. SPONSOR/MONITOR'S REPORT NUMBER(S)

12. DISTRIBUTION/AVAILABILITY STATEMENT
Distribution Statement A. Approved for Public Release; Distribution Unlimited.

13. SUPPLEMENTARY NOTES
This material is declared a work of the U.S. Government and is not subject to copyright protection in the United States.

14. ABSTRACT
2,4 Dinitroanisole (DNAN) is an organic insensitive munition that is a likely candidate to replace trinitrotoluene (TNT) for a variety of purposes. Advanced Oxidation Processes (AOPs) are a promising method that have the potential to reduce a variety of persistent chemicals, however, the performance of these systems may be degraded by co-contaminants in the influent. In this contribution, DNAN, with casamino acids as a co-contaminant, was oxidized with Ultraviolet (UV) Light Emitting Diodes (LEDs) with hydrogen peroxide (H2O2) in an AOP in a laboratory. The UV/ H2O2 AOP was capable of degrading DNAN with casamino acids present, from a relative concentration (C/C0) of 1.0 – 0.63 over a molar peroxide ratio (H2O2: DNAN) range of 50:1 to 1000:1. An increase in the degradation rate of DNAN was observed with increased concentrations of H2O2. The pseudo first order rate constant for DNAN removal was typically greatest at 250:1 and 500:1. The presence of casamino acids had minimal effects on the effectiveness of the AOP, possibly due to light screening.

15. SUBJECT TERMS
Advanced Oxidation Process, Insensitive Munition, 2,4-Dinitroanisole, Water Treatment, UV LED

16. SECURITY CLASSIFICATION OF:			17. LIMITATION OF ABSTRACT	18. NUMBER OF PAGES	19a. NAME OF RESPONSIBLE PERSON
a. REPORT	b. ABSTRACT	c. THIS PAGE			Dr. Willie Harper Jr., AFIT/ENV
U	U	U	UU	173	19b. TELEPHONE NUMBER *(Include area code)* (937) 255-6565, ext 4528 Willie.harper@afit.edu

Standard Form 298 (Rev. 8-98)
Prescribed by ANSI Std. Z39-18